Fakultät für Medizin

III. Medizinische Klinik und Poliklinik
Hämatologische Forschung

Dissertation

The role of Secreted frizzled-related protein 2 *(Sfrp2)* in haematopoiesis

Franziska Christina Ruf

Fakultät für Medizin

III. Medizinische Klinik und Poliklinik – Hämatologische Forschung

The role of Secreted frizzled-related protein 2 *(Sfrp2)* in haematopoiesis

Franziska Christina Ruf

Vollständiger Abdruck der von der Fakultät für Medizin der Technischen Universität München zur Erlangung des akademischen Grades eines

Doktors der Naturwissenschaften (Dr. rer. nat.)

genehmigten Dissertation.

Vorsitzender:	Univ.-Prof. Dr. J. Ruland
Prüfer der Dissertation:	1. apl. Prof. dr R. A. J. Oostendorp
	2. Univ.-Prof. Dr. B. Küster

Die Dissertation wurde am 14.08.2014 bei der Technischen Universität München eingereicht und durch die Fakultät für Medizin am 19.11.2014 angenommen.

Table of contents

Summary

Haematopoietic stem cells (HSCs) reside within the bone marrow microenvironment, which is crucial for the regulation of HSC self-renewal, activation and differentiation. Previous studies showed an enhanced expression of sFRP-2 in HSC-supporting stromal cell lines.

In this thesis, the role of Secreted frizzled-related protein 2 (*Sfrp2*) was studied in steady state haematopoiesis and under stress conditions.

In steady state, loss of *Sfrp2* resulted in a decreased number of very primitive haematopoietic cells, the $CD34^{-}$ $CD150^{+}$ LSKs as analysed in *Sfrp2* knockout mice, (KO, $Sfrp2^{-/-}$). These cells contain the bulk of HSCs, which exhibited an enhanced myeloid progenitor potential in $Sfrp2^{-/-}$ mice. Furthermore, $Sfrp2^{-/-}$ LSKs showed a decreased cell cycling behaviour, measured by Ki-67 expression (designating G1, S and G2/M phases of cell cycle) and the protein level of canonical Wnt signalling target Cyclin-D1. However, BrdU incorporation (indicating actively cycling cells) was increased in these cells. This suggests a stress-induced activation of $Sfrp2^{-/-}$ HSCs.

Dormant HSCs are activated in response to environmental stress. Therefore haematopoiesis was challenged in $Sfrp2^{-/-}$ mice and their wild type (WT) controls. Interestingly, after genotoxic stress induction via 5-FU, a strong increase in number of LSKs was identified as well as in aged twelve to 16 months old, naturally stressed $Sfrp2^{-/-}$ mice. Moreover in serial transplantation experiments it could be demonstrated that the self-renewal ability of WT HSCs was negatively affected after exposure to *Sfrp2* deficient microenvironment. In contrast, no intrinsic, HSC-dependent alterations were observed by transplanting *Sfrp2* deficient HSCs, indicating that sFRP-2 regulates HSC behaviour extrinsically. On the molecular level, the WT LSKs which engrafted into $Sfrp2^{-/-}$ mice demonstrated an enhanced protein level of canonical Wnt target Cyclin-D1 and of non-canonical Wnt members NF-ATc, NLK and C/EPB-alpha indicating an activation of the WT HSCs.

In summary, this study shows that sFRP-2 is required for the maintenance of $CD34^{-}$ $CD150^{+}$ LSKs in steady state haematopoiesis through activation of canonical and non-canonical Wnt signalling. Moreover, during haematopoietic stress, microenvironmental sFRP-2 regulates the activation of HSCs and thus is an important factor that regulates HSC homeostasis extrinsically.

Zusammenfassung

Hämatopoetische Stammzellen (HSZ) verbleiben in der Knochenmark-Nische, die einen wichtigen Beitrag zur Regulation der HSZ-Selbsterneuerung, deren Aktivierung und Differenzierung leistet.

In vorangehenden Studien wurde bereits die Überexprimierung von sFRP-2 in Stomazelllinien gezeigt.

In dieser Doktorarbeit wurde die Rolle des „Secreted frizzled-related protein 2“ *Sfrp2* in der Hämatopoese im unbehandelten Zustand und nach Stress-Induktion untersucht.

Im unbehandelten Zustand führte das Fehlen von sFRP-2 zu einer verringerten Anzahl von primitiven hämatopoetischen Zellen, ($CD34^-$ $CD150^+$ LSK Zellen). Diese primitiven HSZ weisen in *Sfrp2*$^{-/-}$ Mäusen ein erhöhtes Potential auf, myeloide Vorläufer zu bilden. Darüber hinaus zeigten die *Sfrp2*$^{-/-}$ LSK Zellen reduzierte Zellzyklusaktivität, was an Hand der Expression von Ki-67 (das ein Indikator für Zellen in der G1, S und G2/M Phase des Zellzyklus ist) und des Proteingehalts von Cyclin-D1 (Zielgen des kanonischen Wnt Signalweges) bestimmt wurde. Der Einbau von BrdU, das aktive Zellen im Zellzyklus markiert war allerdings erhöht. Dieses Ergebnis deutet auf eine Stress-abhängige Aktivierung von *Sfrp2*$^{-/-}$ HSZ hin.

Ruhende HSZ werden durch umweltbedingten Stress aktiviert. Um den Vorgang zu untersuchen, wurde das hämatopoetische System der *Sfrp2*$^{-/-}$ und der Kontroll-Mäuse in Stress versetzt. Interessanterweise wurde, nach Induktion von genotoxischem Stress und auch in gealterten, zwölf bis 16 Monate alten Mäusen (natürlicher Stress), eine stark erhöhte Anzahl an *Sfrp2*$^{-/-}$ LSK Zellen gefunden. Des Weiteren konnte in seriellen Transplantations-Experimenten gezeigt werden, dass die Fähigkeit zur Selbsterneuerung von Wild Typ (WT) HSZ durch eine *Sfrp2*-defiziente Mikroumgebung negativ beeinflusst wird.

In Gegensatz dazu wurden keine intrinsischen, HSZ-abhängigen Veränderungen in Transplantations-Experimenten gefunden. Das zeigt, dass sFRP-2 das HSZ-Verhalten extrinsisch reguliert. Auf molekularer Ebene hatten WT LSK Zellen, die sich in der *Sfrp2*-defizienten Nische aufgehalten haben, einen erhöhten Cyclin-D1-Proteingehalt und auch der Proteingehalt der Kandidaten des nicht-kanonischen Wnt Signalweges, NF-ATc, NLK und C/EBP-alpha war erhöht. Dies spricht für eine Aktivierung der WT HSZ.

Zusammengefasst beweist diese Studie, dass sFRP-2 für den Erhalt der $CD34^{-}$ $CD150^{+}$ LSK Zellen benötigt wird (unbehandelte Hämatopoese). Dies wird durch die sFRP-2-abhängige Aktivierung des kanonischen und des nicht-kanonischen Wnt Signalweges gewährleistet. Darüber hinaus reguliert das Nischen-sFRP-2 die Aktivierung der HSZ, während hämatopoetischem Stress. Daher ist sFRP-2 ein unverzichtbarer Faktor, der die Homöostase von hämatopoetischen Stammzellen extrinsisch reguliert.

1. Introduction

Somatic stem cells maintain and regenerate adult tissues by slow turn-over and rapid reactions to environmental stimuli. Haematopoietic stem cells (HSCs) are the best-understood example of somatic stem cells. HSCs are able to self-renew for long-term reconstitution and to regenerate the whole blood cell system in response to damage. Thus, the progeny of HSCs perform their biological activities like protection against infections, response to other microorganisms and the transport of vital molecules, like oxygen. HSCs are a rare population of relatively quiescent cells, which reside within the bone marrow in adult mammals. Details about the critical role of the surrounding bone marrow microenvironment, the so-called haematopoietic niche, for maintaining the HSC pool are slowly being elucidated. The niche is described as the collective concept of cell types and structures that comprise HSCs and which controls stem cell fate through direct and indirect interactions. One of the main functions of the HSC niche is to maintain the balance between quiescence and activation of HSCs to self-renew, proliferate or differentiate in response to damage signals. Disruption of the cellular composition, the structure, or signalling components of the niche may disturb this balance and promote chronic HSC activation, which, in turn, may be involved in accumulation of severe mutations with the possibility of the development of different types of leukaemia.

1.1. Haematopoietic stem cells

1.1.1. Early haematopoiesis

In vertebrates the haematopoietic system is derived from mesodermal germ layer. One of the main questions in developmental research concerns the origin of the first repopulating definitive haematopoietic stem cells. In murine embryonic development, haematopoiesis takes place in distinct anatomical compartments. As far back as 1970 Moore and Metcalf detected early haematopoietic stem cells in the yolk sac (Moore and Metcalf 1970), were the haematopoietic cells are organized in “blood islands”, which also contain blood vessels originating from primitive haemangioblasts. The circulation of the

blood cells starts at embryonic day 8.5 (E8.5) (Palis and Yoder 2001).The first definitive long-term multilineage HSCs, that were detected to be able to repopulate adult recipients are autonomously generated in the aorta-gonad-mesonephros (AGM) region at E10.5 and are also located in the vitelline and umbilical arteries (Muller *et al.* 1994, Medvinsky and Dzierzak 1996, de Bruijn *et al.* 2000). Thereafter, HSCs can also be isolated from other tissues like placenta and fetal liver (E11.5) (Muller *et al.* 1994, Gekas *et al.* 2005, Ottersbach and Dzierzak 2005). Haematopoietic cells start migration to fetal liver which is colonized but does not generate HSCs *de novo*. In the fetal liver, the number of HSCs expands tremendously within a few days (Takeuchi *et al.* 2002, Dzierzak and Speck 2008). Further haematopoietic cells are also found in thymus and spleen. At this stage HSCs expand by self-renewal and also start differentiation to increase the number of haematopoietic progenitors (Mikkola and Orkin 2006). At embryonic day 16.5, HSCs migrate to bone marrow and a few weeks after birth HSCs switch from an active, proliferative state to quiescence. Throughout lifetime the main function of HSCs is to maintain haemostasis by rapidly responding to environmental issues (Wilson *et al.* 2008).

1.1.2. Activation of adult HSCs and the haematopoietic hierarchy

A distinctive feature of HSCs is that they have the capability to undergo self-renewing cell divisions, as well as produce progeny which can differentiate in all blood cell types. As such, the HSC is at the top of a hierarchical system in which each layer of progeny cells gains specific functions and the defining stem cell features are gradually lost as the cells mature. Description and characterization of haematopoietic subsets of cells helps to understand the complex process of proliferation, differentiation as well as regeneration. The standard manner to follow this process of differentiation from HSCs throughout the hierarchy uses the technique of flow cytometry and fluorescently labelled antibodies.

The earliest long-term repopulating HSCs, known as LSKs, do not express markers of mature blood cell lineages (Lin^-), but both Ly-6A/E, (SCA^-1) and (KIT) (Lin^- $SCA\text{-}1^+$ KIT^+

(LSK)) (Ikuta and Weissman 1992). Further, this functionally rare population of cells does not express haematopoietic progenitor cell antigens CD34, FLK-2/FLT-3 or CD48 but express CD150 (Ikuta and Weissman 1992, Osawa *et al.* 1996, Christensen and Weissman 2001, Kiel *et al.* 2005, Balazs *et al.* 2006, Kent *et al.* 2009). Amongst the $CD34^-$ LSK cells only $CD150^{high}$, known as long-term (LT) HSCs but not $CD150^{medium/low}$ have the potential of multilineage reconstitution in secondary recipient mice (Morita *et al.* 2010). Thus, it is now possible to isolate single HSCs and interrogate their repopulating ability. Such studies have revealed a remarkable heterogeneity amongst the ability of single HSCs and several subtypes of HSCs were identified, which distinguish between lymphoid deficient α-HSCs and balanced (lymphoid and myeloid biased) β-HSCs as well as self-renewal lacking, myeloid-deficient γ+δ-HSCs (Dykstra *et al.* 2007, Benz *et al.* 2012). This is probably linked to the ability of HSCs to commit to myeloid progenitors (MPs) or common lymphoid progenitors (CLPs) that are defined as KIT^+ $SCA\text{-}1^-$ (MPs) and KIT^+ $IL7\text{-}R^+$ (CLPs) respectively (Kondo *et al.* 1997, Akashi *et al.* 1998, Renstrom *et al.* 2010).

The description of markers identifying single HSCs also facilitated more detailed studies concerning the balance between dormancy and activation of HSCs. Thus, it has become clear that quiescent (dormant) HSCs can rapidly and effectively be activated or “awakened” in stress situations, like wounding, toxic insult, chemotherapy, or single agents like IFN alpha, G-CSF and arsenic trioxide (As(2)O(3)) (Essers and Trumpp 2010, Trumpp *et al.* 2010). Further, all cells are permanently affected by genotoxic stress - endogenous processes causing DNA damage. HSCs are mostly in a quiescent state and reside caved within the haematopoietic niche in the bone marrow in order to protect their genomic integrity. Events of DNA damage in association with reactive oxygen species (ROS), cellular respiration and cell division are reduced to minimum (Rossi *et al.* 2007, Orford and Scadden 2008). Also in Drosophila system haematopoietic progenitor cells are capable to respond to stress like oxygen stress, infection or hypoxia, although the mechanism of sensing has not been elucidated in detail. Recently it was shown, that

haematopoietic progenitors are directly sensing systemic and nutritional signals which in turn maintain haematopoietic progenitors over Wingless signalling, which corresponds to Wnt signalling in mammals (Shim *et al.* 2012). Although constant genotoxic stress might cause severe damage (Cho *et al.* 2013). Mohrin *et al.* demonstrated that proliferating HSCs are as radioresistent as quiescent HSCs. In contrast to proliferating HSCs using the high-fidelity HR pathway to repair double strand breaks, quiescent HSCs use the DNA repair mechanism of non-homologous end joining (NHEJ), which makes them susceptible to genomic rearrangements and consequently may cause haematopoietic abnormalities (Mohrin *et al.* 2010). An example of natural genotoxic stress is aging which results in a decrease of functional HSCs (Beerman *et al.* 2010). The groups of Weismann and Rossi define mice as “middle aged” at the age of twelve months and “old” mice at the age of 22-24 month (Morrison *et al.* 1996, Beerman *et al.* 2010). Moreover, it was shown that DNA damage accumulates with age in HSCs. Aged mice deficient in pathways regulating genomic integrity (NHEJ, telomere maintenance, nucleotide excision repair) exhibited a strongly reduced stem cell function under stress (Rossi *et al.* 2007). Aged HSCs also show a reduced capability to regenerate the blood system after transplantation in the mouse model (Morrison *et al.* 1996).

As a response to diverse kinds of haematopoietic stress, LT-HSCs do self-renew and also produce cells with a shorter life time (eight to twelve weeks) called short-term HSCs (ST-HSCs), a population which is phenotypically distinguished from LT-HSCs by the expression of CD34 and FLK-2/FLT-3 (Morrison and Weissman 1994, Christensen and Weissman 2001, Adolfsson *et al.* 2005, Passegue *et al.* 2005). Further downstream in the haematopoietic hierarchy, progeny cells gain CD48 (SLAMF-2), commit to certain lineages, and haematopoietic cells progressively mature to lymphoid and myeloid lineages (Seita and Weissman 2010). However, the path down the hierarchy is by no means linear. For instance, Yamamoto *et al.* found long-term repopulating myeloid restricted progenitors within the phenotypically defined LT-HSC compartment (Yamamoto *et al.* 2013).

In addition to CD48, the more mature progenitors also start slowly up-regulating transcription factors important for lineage commitment. Following the hierarchy, the multipotent progenitor (MP) fraction cells were found expressing either the transcription factor GATA1 or PU1. GATA expressing MPs exhibit myeloerythroid potential (MEP, CMP) while PU.1-expressing progenitors differentiate into granulocyte/ monocyte/lymphoid lineages (CLP). Interaction of PU.1 with GATA-1 inhibits transcription of erythroid master regulator GATA-1. The other way around, GATA-1 prevents the interaction of PU.1 with its co-activator c-JUN (Rekhtman *et al.* 1999, Zhang *et al.* 1999, Zhang *et al.* 2000, Burda *et al.* 2009). This suggests that down-regulation of PU.1 is essential for normal red blood cell production (Mak *et al.* 2011). Taken together although the hierarchical system flows from the HSCs, the function of each single haematopoietic progenitor cell seems not to be fixed. The differential expression of transcription factors involved in lineage commitment leaves room for heterogeneity and variability. The environmental component of stem and progenitor differentiation is still in an early stage of investigation and it is likely to gain insights in the near future.

1.2. The haematopoietic stem cell niche

Schofield first proposed the anatomical compartment termed “niche” (Schofield 1978). This microenvironment regulates maintenance of HSCs and controls their self-renewal, survival, differentiation and proliferation (Fuchs *et al.* 2004, Morrison and Spradling 2008, Garrett and Emerson 2009, Nagasawa *et al.* 2011). Many investigators currently describe two possible categories of niches: the endosteal niche, where HSCs reside close to osteoblasts (OBs) of trabecular bone and the vascular niche were stem cells remain closer to sinusoid endothelium (Frassoni *et al.* 1982, Calvi *et al.* 2003, Zhang *et al.* 2003) (Figure 1). Using real-time live imaging it was observed that a small fraction of HSCs was localized close to OBs in endosteal surface shortly after intravenous injection (Lo Celso *et al.* 2009, Xie *et al.* 2009), demonstrating the endosteal niche as dominantly chemo-attractive.

1.2.1. Compartments and cell types of the niche

Several groups described cell types which are thought to be involved in niche formation and that are localized to the endosteal or vascular regions. The Spindle-shaped N-cadherin$^+$ CD45$^-$ osteoblasts (SNO) (Zhang *et al.* 2003), immature early B-cell factor 2$^+$ (EBF-2$^+$) osteoblasts (IEO) (Kieslinger *et al.* 2010) and Nestin$^+$ MSCs (Mendez-Ferrer *et al.* 2010) are found in endosteal region. The perivasculsar niche in the mouse so far comprises CXCL-12 abundant reticular cells (CAR) (Sugiyama *et al.* 2006) leptin receptor (LEP-R$^+$) stromal cells (Ding *et al.* 2012), non-myelinating Schwann cells (Yamazaki *et al.* 2011) and also Nestin$^+$ multipotent stromal cells (MSCs) (Frenette *et al.* 2013). Recently, several groups have described further combinations of surface markers, enabling the isolation of possible mesenchymal subpopulations. Nakamura *et al.* elucidated the influence of CD31$^-$, TER119$^-$, CD45$^-$, ALCAM$^+$, SCA-1$^+$ MSCs which reconstitute LT-status of HSC by up-regulation of homing and cytokine related genes. Osteoblastic cells expressing ALCAM but not SCA-1 were suggested to regulate HSCs through cell adhesive mechanisms (Nakamura *et al.* 2010). Chan *et al.* recently described three different subpopulations of stromal cells expressing THY-1 (CD90), endoglin (CD105) or Enpep (CD249). While *in vitro* THY-1+ or endoglin$^+$ cells promote differentiation, Enpep$^+$ cells exhibited the potential to maintain HSCs self-renewal (Chan *et al.* 2013). Morikawa *et al.* isolated PDGFRA$^+$, SCA-1$^+$, CD45$^-$, TER119$^-$ MSCs that exhibited osteogenic and adipogenic differentiation potential and also differentiation into haematopoietic niche cells (Morikawa *et al.* 2009). In Frenette`s group PDGFRA and CD51 were shown as markers of haematopoiesis-supporting Nestin$^+$ MSCs in the human system (Pinho *et al.* 2013).

Whether the endosteal and vascular niches are truly different still needs to be established. Despite the dominant chemotactic activity of the endosteal region, the majority of HSCs appear to reside within the vascular niche (Kiel and Morrison 2008). OB-deficient mouse models did not show any changes in LT-HSC G0/G1 state or function (Ma *et al.* 2009), suggesting different roles for niche subpopulations in

maintaining HSC dormancy. Also, loss of N-cadherin, a molecule described specifically on endosteal cells, does not influence HSC maintenance and haematopoiesis (Kiel *et al.* 2007). Endothelial cells expressing CD31 are able to restore haematopoiesis after lethal irradiation and positively influence long-term reconstitution (Salter *et al.* 2009, Li *et al.* 2010). These findings show that both niche types function as niches for HSC maintenance. The initial view that the endosteal region preferably houses dormant cells, still holds true, since only endothelial cells of vascular niche express the adhesion molecule E-selectin and loss of E-selectin results in increased HSC quiescence. This points to the role of vascular niche in ensuring the regulation of proliferation and differentiation (Kiel *et al.* 2007, Kiel *et al.* 2009, Winkler *et al.* 2012). Thus, cells isolated from both endosteal and vascular regions of the marrow may support LT-HSC activity in culture and localize to the same areas as HSCs and it is well possible that different niche cells maintain different HSC subpopulations.

Dormant HSCs remain quiescent and divide about five times per lifetime (Wilson *et al.* 2008). This population comprises the majority of multilineage long-term self-renewal activity. The dormant HSC is activated by response to haematopoietic stress and returns to dormancy after re-establishment of homeostasis (Wilson *et al.* 2008). Previous studies identified members of the Wnt signalling pathway as critical regulators of HSC behaviour by analysing gene manipulated models. Changes in the level of these proteins seem to generally affect the proportion of HSCs residing in the G0 phase of the cell cycle (dormant HSCs) confirming the view that the main function of the niche is to maintain HSCs in a quiescent state.

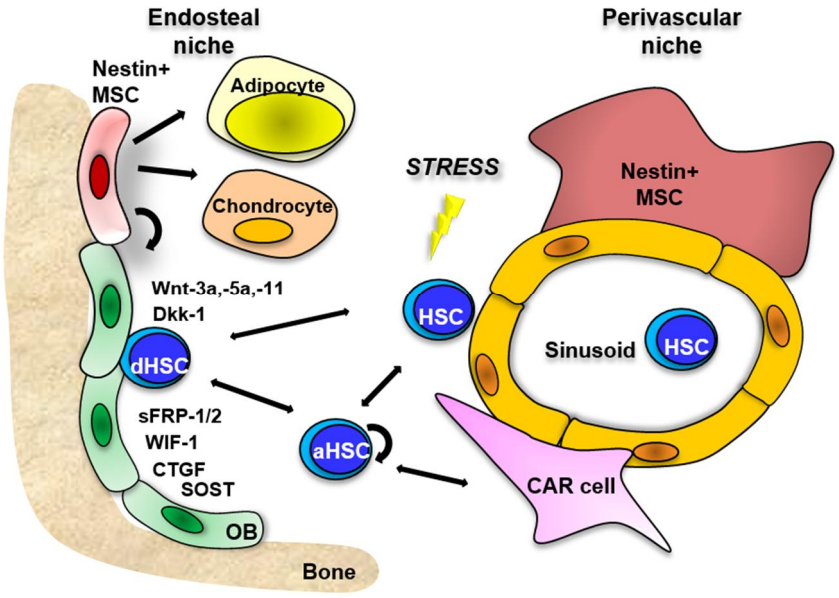

Figure 1. Members of Wnt signalling pathway in a model of endosteal and perivascular niche. *Mesenchymal stem cells (MSCs) can differentiate into osteoblasts (OBs), adipocytes and chondrocytes. In endosteal region OBs and Nestin^{+} MSCs maintain HSCs in a dormant state (dHSC). Factors of Wnt signalling, including Wnt ligands Wnt-3a, -5a, -11 and Wnt inhibitors Dkk-1, sFRP-1, -2, CTGF, SOST and WIF-1 regulate HSC quiescence. Dormant HSCs are activated (aHSC) by response to haematopoietic stress like wounding, infection, irradiation or leukaemia. CAR cells are components of perivascular niche promoting self-renewal of active HSCs. Model adapted from Ehninger et al., 2011 (Ehninger and Trumpp 2011) and recently published by Schreck, C. and Bock, F., 2014 (Schreck et al. 2014).*

1.2.2. The haematopoietic niche in leukaemia

With the increasing knowledge about the normal haematopoietic stem cell niche, it becomes more and more important to analyse the niche in leukaemic conditions, how the possible change in composition of niche cells can change cell signalling. A disrupted homeostasis in haematopoiesis is expected. Malignant transformed leukaemic stem cells (LSCs) share the characteristics of renewal and proliferation to normal HSCs, but in contrast LSCs do not differentiate (Reya *et al.* 2001). As some of the LSCs, like normal HSCs, remain in a quiescent state within the niche, it is very important for therapeutic issues to get a detailed knowledge of how the niche regulates and influences HSCs and vice versa. Recent evidence showed that leukaemic cells (CLL cells) can hijack the niche through direct cell-cell interaction inducing severe changes in stromal cell gene expression. Here PKC-beta II improved CLL cell survival over stromal NF-kappa-b

signalling (Lutzny *et al.* 2013). The other way around, perturbation of niche stromal cells causes severe HSC transformation. The first niche-dependent defects were seen in *Ikbα*$^{-/-}$ mice, where increasing Notch signalling was demonstrated in myelocytes (Rupec *et al.* 2005). Niche-dependent alterations can result in an increased risk of secondary oncogenic mutations which leads to malignant diseases assuming niche-induced oncogenesis. Interestingly recent investigations showed that a knockout of niche expressed genes like *Dicer1* or *Sbds* leads to myelodysplasia and possibly to leukaemic development (Raaijmakers *et al.* 2010).

Serial transplantation studies showed defects of homing mechanisms of HSCs to endosteal niche in CD44 (Jin *et al.* 2006, Krause *et al.* 2006) as well as in the interaction of CXCR4 and CXCL12 (Rombouts *et al.* 2004, Sipkins *et al.* 2005, Neering *et al.* 2007). In AML mouse model the reduced number and function of osteoblasts and osteoprogenitors as well as severe loss of bone mineralization strengthened the idea of leukaemic cells interacting with a malignant transformed niche (Frisch *et al.* 2012). This is confirmed as Schepers *et al.* elegantly showed that in myeloproliferative neoplasia (MPN) the endosteal BM niche was remodelled to a leukaemic LSC-supporting niche. Myeloid leukaemic cells stimulate MSCs to an increased production of transformed osteoblastic cells (OBCs). The group could also show alterations of the two critical pathways Notch and TGF-beta (Schepers *et al.* 2013).

1.3. Wnt signalling in haematopoietic niche

A central class of mediators shown by several investigators to modulate HSC number and quality are members of Wnt signalling. The nuclear factor of activated T-cells (NF-AT), which is involved in non-canonical signalling (further described below), was found to negatively regulate osteoblast differentiation and bone formation. OB-specific NF-AT activity mediates early B lymphopoiesis, possibly by regulating VCAM-1 expression on osteoblasts (Sesler and Zayzafoon 2013). Moreover, the well characterized Wnt molecule Wnt-5a is reported to function as mesenchymal regulatory

factor by influencing recruitment, maintenance, and differentiation of MSCs and enhancing osteogenesis *ex vivo* (Baksh *et al.* 2007). Furthermore, Wnt-3a induces proliferation and inhibits differentiation in co-cultures of marrow cells only in the presence of stromal cells, indicating the requirement of niche cells in canonical Wnt signalling in haematopoiesis (Yamane *et al.* 2001).

The Wnt genes encode a large family of secreted molecules, which are known to play an important role in embryonic development. Wnts have local effects on multiple cell types by transducing signals through their receptors, Frizzled and Dishevelled expressed on the target cells (Wodarz and Nusse 1998, Yamane *et al.* 2001). Wnt signalling was reported to be essential for blood cell production (Austin *et al.* 1997, Van Den Berg *et al.* 1998) and its deregulation may promote the development of leukaemia. The regulation of haematopoiesis by activators and inhibitors of Wnt signalling from the niche is reviewed in our previous publication (Schreck *et al.* 2014).

1.3.1. Canonical and non-canonical Wnt signalling

Wnt signalling is roughly separated into canonical and non-canonical pathways as it is presented in Figure 2. The canonical pathway mainly signals through Catenin beta-1 (Beta-catenin) via activation of Beta-catenin-transcription complex. Non-canonical Wnt signalling is diverse and involves calcium-dependent and -independent pathways as well as Rho-type GTPases, MAP kinases and nuclear factors like NF-AT. The non-canonical pathway in particular is involved in shaping the niche architecture through its involvement in skeletogenesis and mesenchymal differentiation.

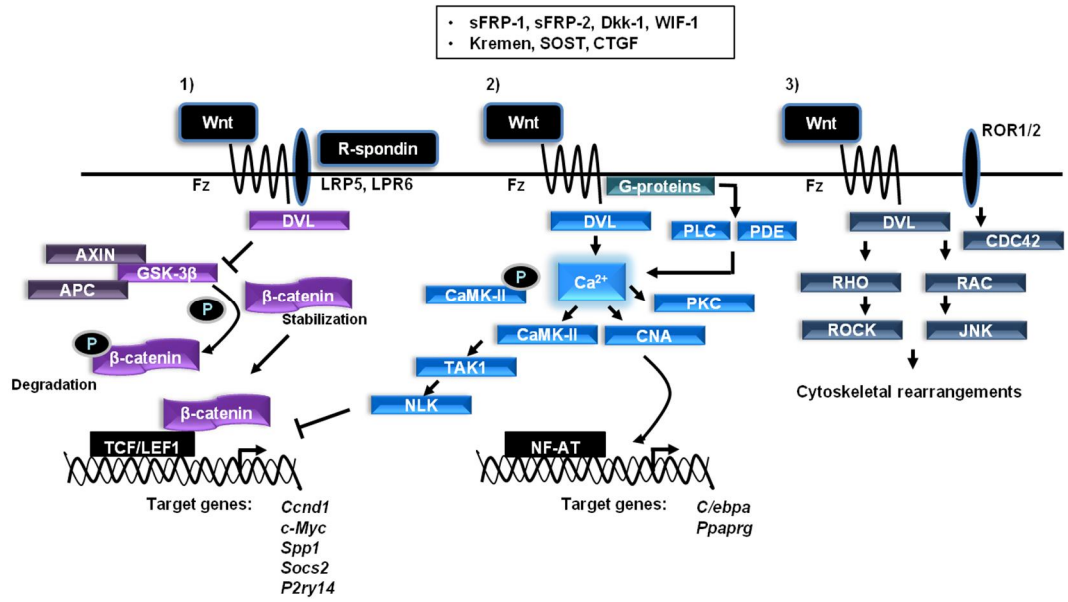

Figure 2. Wnt signalling pathways. *1) Beta-catenin-dependent (canonical Wnt signalling. 2) Ca^{2+}-dependent (non-canonical) Wnt signalling. 3) Planar cell polarity (PCP) pathway.*

Canonical Wnt signalling

Wnt-1 and Wnt-3a are so-called “classical” canonical stimulators. In absence of canonical Wnt ligands, Beta-catenin is linked to Axin-APC complex. Further, the upstream protein kinase GSK-3 beta target Beta-catenin for ubiquitination which leads to proteasomal degradation. Binding of Wnt ligands to Frizzled (Fz) receptors and its co-receptors low-density lipoprotein receptor-related protein 5 and 6 (LRP-5 and LRP-6) causes Dishevelled (DVL) activation and disruption of the AXIN complex. Subsequently Beta-catenin translocates to the nucleus and binds to TCF/LEF transcription complex, resulting in transcriptional activation of several genes (Figure 2 left) like *Myc*, osteopontin (*Spp1*), suppressor of cytokine signalling 2 (*Socs2*), P2Y purinoreceptor 14 (*P2ry14*) and Cyclin-D1 (*CcnD1*) (Logan and Nusse 2004, Nygren *et al.* 2007). Recently, a new protein family has been linked to Wnt/canonical signalling activation and regulation. The R-spondin (Rspo1-4) proteins can also bind to LRP-6, and therefore, activate the Beta-catenin-dependent pathway (Boudin *et al.* 2013).

The role of Beta-catenin as a regulator of canonical Wnt signalling is controversial in haematopoiesis. Mx-Cre-mediated deletion of Beta-catenin (Cobas *et al.* 2004) or Beta-

and Gamma-catenin simultaneously did not affect haematopoiesis (Jeannet *et al.* 2008, Koch *et al.* 2008). Kirstetter *et al.* investigated, by using a transgenic approach, that overexpression of activated Beta-catenin led to multilineage differentiation, and a transient expansion of the HSC pool, followed by the exhaustion of LT-HSCs (Kirstetter *et al.* 2006). In a further transgenic approach it was shown that the amount of Beta-catenin is crucial for the regulation of HSC behaviour and different, lineage-specific Wnt dosages regulate HSCs and progenitors (Luis *et al.* 2011).

Non-canonical Wnt signalling

Wnt-5a and Wnt-11 activate non-canonical Wnt pathways, which are involved in diverse processes such as embryogenesis, cell movement, cell division, and skeletogenesis (Veeman *et al.* 2003). The non-canonical Wnt pathway is a required component of the planar cell polarity (PCP) pathway, which governs asymmetric cell division and asymmetric distribution of proteins within the cell. As such, the PCP could be involved in asymmetric cell divisions of HSCs. This pathway is stimulated through Frizzled and Dishevelled and downstream activation of Jun-N-terminal kinase (JNK) and small G-proteins, like RAC and RHO and the Rock1 RHO-associated kinase (Figure 2 right) (Veeman *et al.* 2003). A second pathway activated through non-canonical Wnt signalling involves heterotrimeric GTP-binding proteins, which mobilize phospholipase C (PLC) and phosphodiesterase (PDE), with further release of Ca^{2+} ions from intracellular sources. Besides the Fz receptors, ROR1/2 receptors can also bind some Wnt factors and activate non-canonical signalling through release of Ca^{2+}. Calcium release activates calcium/calmodulin-dependent kinase-II (CamK-II) and protein kinase C (PKC). This pathway diverges and NF-AT can be dephosphorylated by calcineurin (CNA), or the TAK1/NLK pathway which both lead to transcriptional activation (Figure 2 middle). Interestingly, there is cross-talk between canonical and non-canonical Wnt pathways. Many Wnt activators and inhibitors may stimulate or inhibit both pathways, depending on the constellation of receptors present. Intrinsically, both pathways are also connected. For instance, NLK negatively regulates Beta-catenin-dependent Wnt signalling by

phosphorylating TCF/LEF, and thus inhibiting the building of Beta-catenin/TCF/LEF complex and its DNA binding for transcriptional activation of target genes (Yamada *et al.* 2006, Lv *et al.* 2014). In neurons, the overexpression of NLK supressed the Beta-catenin/LEF binding (Xu *et al.* 2014). Further, GSK-3 beta was shown to phosphorylate NF-AT promoting its nuclear export, demonstrating that non-canonical Wnt stimulation may inhibit canonical signalling (Beals *et al.* 1997, Beals *et al.* 1997)

1.3.2. Regulators and inhibitors of Wnt signalling

Wnt signalling members also include a complex network of Wnt regulators, that bind the Wnt mediators themselves (sFRP-1 sFRP-2, Dkks), and some of which disrupt the assembly of the Frizzled signalosome (Kremen, connective tissue growth factor (CTGF), and Sclerostin (SOST)). Direct binding of soluble factors with Wnt ligands, like the Secreted frizzled-related protein 1 (sFRP-1) can also modulate Wnt signalling (Kawano and Kypta 2003).

The Secreted frizzled-related proteins sFRP-1 and sFRP-2 directly bind Wnt molecules and, thus, regulate the interaction of Wnts with canonical and non-canonical Fz receptors (Suzuki *et al.* 2004). *Sfrp1* and *Sfrp2* double mutants have been shown to activate the non-canonical Wnt/PCP pathway in embryonic stem cells and interestingly the phenotype of these double mutants is closely related to phenotype of Wnt-5a$^{-/-}$ mice (Kele *et al.* 2012). Nakajima *et al.* revealed the expression of sFRP-1 and sFRP-2 in osteoblasts and their differential regulation of HSC homeostasis (Nakajima *et al.* 2009). For sFRP-1 it was previously shown, that sFRP-1 is required for HSC self-renewal and HSC maintenance in an extrinsic manner (Renstrom *et al.* 2009).

Dkk-1, a member of the Dickkopf (Dkk) family of Wnt inhibitors, binds to the Wnt co-receptor LRP-5/6 in combination with a Kremen receptor leading to the internalization of the complex. While Dkk-1 is expressed in LT-HSCs (Renstrom *et al.* 2009) it is also expressed in osteoblasts and thus can extrinsically influence Wnt signalling and regulate number and function of HSCs (Mao *et al.* 2001, Mao *et al.* 2002, Fleming *et al.* 2008).

WIF-1 is a member of Wnt inhibitory factor (WIF) family that, like sFRP-1, binds to Wnt ligands directly and can block both canonical and non-canonical Wnt signalling (Surmann-Schmitt *et al.* 2009). Schaniel *et al.* analysed *Col2.3-Wif1* transgenic (*Wif1Tg*) mice in which WIF-1 is overexpressed in osteoblasts. While there is no effect in the bone architecture, the overexpression of WIF-1 resulted in the unexpected activation of the canonical Wnt signalling with an impact on quiescence and self-renewal potential of HSCs (Schaniel *et al.* 2011), suggesting that WIF-1 may interact with both canonical and non-canonical Wnt signalling pathways.

1.3.3. Wnt signalling in leukaemia

Dysregulation of Wnt signalling in the niche was demonstrated to impair HSC function (Fleming *et al.* 2008, Renstrom *et al.* 2009) and in acute myeloid leukaemia (AML) the Wnt/Beta-catenin pathway seems to be required for LSC self-renewal. LSC develops from HSC or GMP while in the latter the normally inactive Wnt/Beta-catenin signalling has to be reactivated by oncogenes (Wang *et al.* 2010). Additionally, an activating mutation of Beta-catenin in murine osteoblasts leads to alterations in the differentiation potential of myeloid and lymphoid progenitors and consequently results in the development of AML (Kode *et al.* 2014). The molecules are involved in skeletal development and are expressed by stromal cells. SFRP-1 is known to regulate extrinsically the cycling activity and maintenance of haematopoietic stem cells (Renstrom *et al.* 2009). Furthermore, *Dicer1* deletion in osteoblastic cells leads a reduced expression of SBDS, the gene mutated in Schwachman-Bodian-Diamond syndrome. *Sbds* deletion in osteoprogenitors induced even bone marrow dysfunction with myeloplasia (Raaijmakers *et al.* 2010). These findings suggest a possible extrinsic mechanism and a niche-induced oncogenesis.

Surprisingly little is known about the state of Wnt signalling in niche cells in the presence of leukaemic cells. Whether expression of Wnt inhibitors is affected, or if signal transduction through this pathway is altered in cells of the leukaemic niche is not clear.

Since Wnt ligand expression is increased in leukaemic cells, it seems likely that Wnt signalling is increased in niche cells through local interactions. Wnt signalling is critically involved in the maintenance and differentiation of mesenchymal niche cells. Thus, it is possible that the observed effects of leukaemic cells on the cellular composition of the niche (Frisch *et al.* 2012, Schepers *et al.* 2013) and altered differentiation behaviour of niche cells in MDS (Geyh *et al.* 2013), are caused at least in part by local Wnt signals emitted by the dysplastic or leukaemic cells. Taken together, the up-regulation of Wnt signalling in haematopoietic cells has been shown to be required for the development of both AML and for progression of CML into blast crisis. Although the niche is a critical regulator of LSCs in AML and CML, dissecting alterations of Wnt signalling in cells of the leukaemic niche or how Wnt signalling is coupled to alterations in other signalling pathways as for instance the TGF pathway (Krause *et al.* 2013) has so far, only scratched the surface.

1.4. Secreted frizzled-related protein 2 *(Sfrp2)*

As described above, Secreted frizzled-related protein 2 (*Sfrp2*) is a regulator of Wnt signalling. SFPR-2 belongs to a family of five secreted glycoproteins (sFRP-1, -2, -3, -4 and -5) which have been detected to modulate Wnt signalling (Jones and Jomary 2002). SFRP-2 is a 33 kDa secreted protein type I and it is also called SDF5 or SARP-1 (Secreted apoptosis related protein 1). It was primary identified in signal sequence gene trap screen in 1996 (Shirozu *et al.* 1996). Mouse *Sfrp2* gene is located on chromosome 3 (37.37cM) and consists of three exons. The structure of sFRP-2 was clarified, revealing that sFRP-2 contains two functional domains, an N-terminal domain homologous to a cysteine rich frizzled domain and a netrin like domain. In contrast to Fz receptors, sFRP-2 is lacking a transmembrane domain and is thus not able to transduce signals directly into the cell. It modulates Wnt signalling by competitive binding to Wnt ligands or direct binding to Fz receptors (Jones and Jomary 2002). Mice homozygous for a null allele exhibit background-sensitive syndactyly. About 95 % of *Sfrp2* knockout mice bred on 129/SvJ inbred strain or 129/SvJxCBA/N background exhibit polydactyly.

129/SvJxC57Bl/6 mice showed a lower rate of syndactyly (15 %), but exclusively in 129/SvJxC57BL/6 mice preaxial synpolydactyly was observed (15 %) (Ikegawa *et al.* 2008). Additionally, brachy-syndactyly was detected in homozygous *Sfrp2* KO mice bred on Sv129EvxC57BL/6 (Morello *et al.* 2008). *Sfrp2* homologs were identified in different vertebrate species like human, rat, chimpanzee, rhesus macaque, cattle, dog, chicken and zebrafish.

1.4.1. The role of sFPR-2 during mouse embryonic development

SFRP-2 is differentially expressed during embryogenesis in developing tissues (Leimeister *et al.* 1998, Blackshaw *et al.* 2004): During kidney development sFRP-2 is expressed at E10.5 to E14.5. From E8.0 onwards, expression is detected in the nervous system and sFRP-2 was found to be regulated in the developing CNS (Kim *et al.* 2001). In the developing eye sFRP-2 expression was identified at E9.0. Additionally, a role of sFRP-2 during lens development by regulation of Wnt/Beta-catenin signalling in lens epithelial cells was shown (Esteve *et al.* 2011, Sugiyama *et al.* 2013). SFRP-2 plays a critical role during limb development (E11.5 to E14.5). Expression was found during cartilaginous condensation of the shoulder, food and hand paddle extending along the digital ray as well as in forelimb and hind limb where the interphalangeal joints are developing. Additionally, sFRP-2 expression was detected between the sternal bands and at the contact point of ribs and sternum.

In embryonic system the knockout of *Sfrp2* affects axis elongation and somite segmentation as well as early trunk formation (Satoh *et al.* 2006, Satoh *et al.* 2008, Warr *et al.* 2009). Regarding *Sfrp1* and *Sfrp2* double mutants in embryonic stem cells, Wnt/planar cell polarity pathway (PCP) was shown to be activated (Kele *et al.* 2012).

1.4.2. SFRP-2 in the bone marrow niche

It was demonstrated that there is redundancy between the function of sFRP-1 and sFRP-2 during mouse embryogenesis (Satoh *et al.* 2006, Satoh *et al.* 2008, Warr *et al.* 2009). Nakajima *et al.* revealed the expression of sFRP-1 and sFRP-2 in osteoblasts

and their differential regulation of HSC homeostasis. For sFRP-1, it was previously shown, that sFRP-1 is required for HSC self-renewal and HSC maintenance in an extrinsic manner (Renstrom *et al.* 2009). Whether sFRP-2 has a similar role and significance in the regulation of haematopoietic cells within the niche has not been published so far. SFRP-2 is highly secreted by mineralized osteoblasts in the endosteal niche (Roux 2010) and sFRP-2 has been suggested to inhibit differentiation of HSCs by enhancing self-renewal (Nakajima *et al.* 2009). SFRP-2 is strongly expressed in stromal cells which maintain HSCs in culture (Oostendorp *et al.* 2005). The notion that sFRP-2 might be important for this maintenance was shown in experiments where $CD34^-$ LSKs were treated with sFRP-2 *in vitro,* which results in an increased HSC engraftment in serial transplantation experiments. The role of sFRP-2 seemed to be unique in this respect, since treatment with sFRP-1 did not show similar results. In addition, the different activity of sFRP-1 and sFRP-2 is hinting to an important and non sFRP-1-redundant role of sFRP-2 in steady state haematopoiesis or possibly under haematopoietic stress conditions (Nakajima *et al.* 2009).

1.4.3. SFRP-2 - a regulator in disease processes, cancer and leukaemia

Secreted frizzled-related proteins have been shown to be important regulators of developmental and disease processes by antagonizing Wnt signalling. SFRP-2 is expressed in the heart and could be shown to influence fibrosis associated with myocardial infarction and it is a key regulating factor for myocardial repair and survival (Mirotsou *et al.* 2007, Kobayashi *et al.* 2009).

Epigenetic regulations or down-regulation of *Sfrps*, including *Sfrp2* were identified in various types of cancers. Methylation of the *Sfrp2* promoter region was found in bladder cancer (Stoehr *et al.* 2004), prostate cancer (Lodygin *et al.* 2005), endometrial cancer (Risinger *et al.* 2005) and breast cancer (Veeck *et al.* 2006). *Sfrp2* methylation was further found in colorectal and gastric cancer (Suzuki *et al.* 2004, Nojima *et al.* 2007). Although these studies suggest that a down-regulation of the *Sfrp2* gene is a contributing

factor to tumorigenesis, sFRP-2 was also shown to promote apoptotic resistance in mammary tumorigenesis (Lee *et al.* 2004). Thus, the possible role of sFRP-2 in tumorigenesis is controversial and both up- and down-regulations have been reported.

In haematopoiesis, epigenetic alterations of Wnt signalling inhibitors is thought to be an important mechanism in developing myeloproliferative disease and leukaemia. *Sfrp2* promoter methylation results in down-regulation of *Sfrp2* in AML (Jost *et al.* 2008) and in ALL (Roman-Gomez *et al.* 2007, Valencia *et al.* 2009) and it affects the clinical outcome of Philadelphia positive ALL (Martin *et al.* 2008, Martin *et al.* 2010). *Sfrp2* methylation status also influences childhood ALL (Roman-Gomez *et al.* 2006). In a large scale analysis of DNA methylation of *Sfrp2* methylation was detected in CLL (Rahmatpanah *et al.* 2009). But, sFRP-2 does not seem to be suppressed in all types of haematopoietic malignancies. In multiple myeloma cells for instance, bone formation is suppressed by secretion of sFRP-2 (Oshima *et al.* 2005).

So far, sFRP-2 has not directly been linked to respond to genotoxic stress, although sFRP-2 might be targeted for suppression by p53 (Yam *et al.* 1999), which is a universal sensor for gentoxic stress regulating the expression of genes involved in cell cycling and apoptosis. To elucidate the extent of the absence of sFRP-2 in stress situations in the haematopoietic system was one of the aims of this thesis.

1.5. Aim of this study and overview of the experimental approach

Haematopoietic stem cells (HSCs) are mostly in a dormant state residing within the bone marrow niche. The interplay as well as niche-dependent regulation of HSCs is only slowly elucidated.

In this thesis the communication of HSCs with their microenvironment was studied and the extent of the involvement of Secreted frizzled-related protein 2, sFRP-2, was investigated. There are several methods to gain further knowledge of the interaction and regulation of HSCs and their environment. Here, a *Sfrp2* homozygous knockout mouse model (*Sfrp2*$^{-/-}$) was used, which allows to study steady state haematopoiesis and the niche cell phenotype in the absence of sFRP-2 *in vivo*. Morover an *in vivo* mouse model facilitates the induction of stress via 5-FU for instance, or more importantly to analyse the effect of aging, which is a natural stress factor for HSCs. My goal was to study how HSCs deal with such challenges in the absence of sFRP-2. SFPR-2 is highly secreted by osteoblasts, one type of endosteal niche cells (Nakajima *et al.* 2009). A technique to investigate the niche-dependent effect on HSCs and niche cells separately in *Sfrp2*$^{-/-}$ mice, is the transplantation assay. A disturbed regulation might have severe effects on HSC quality and function. Consequently, this can cause malignant mutations, which influence leukaemogenesis. Therefore, in a second transplantation model, BCR-ABL-induced development of leukaemia in *Sfrp2*$^{-/-}$ mice was investigated.

The regulation of HSC self-renewal and differentiation is controlled by combined internal HSC signals, extrinsic environmental signals and also secreted molecules. In 2002, Oostendorp and colleagues published a multitude of embryo derived stromal cell lines to investigate the niche-dependent regulation of HSC behaviour (Oostendorp *et al.* 2002). Two of these, EL08-1D2 and UG26-1B6 turned out to support HSCs in a non-contact manner (Oostendorp *et al.* 2005, Buckley *et al.* 2011). Analysing the gene expression profile of this HSC maintaining cells, several secreted molecules were overrepresented compared to non-supportive stromal cell lines. SFRP-2 expression was one of the highest differentially expressed factors (Oostendorp *et al.* 2005). Thus, I set up *in vitro*

co-culture assays with lineage depleted haematopoietic cells (Lin^-) on *Sfrp2* knockdown stromal cells (*shSfrp2,* UG26-1B6) in order to analyse HSC maintenance and quality. In former studies sFRP-2 itself was shown to enhance HSC engraftment after serial transplantations, which supports the hypothesis that sFRP-2 extrinsically maintains HSCs (Nakajima *et al.* 2009). Interestingly, the knockout of family member *Sfrp1* extrinsically regulates haematopoiesis through cell cycle regulation by altered Wnt signalling (Renstrom *et al.* 2009). However, the effect of *Sfrp2* deficiency has never been studied before, regarding HSC behaviour and function. Here, HSC proliferation and cell cycle regulation was analysed with different techniques including Ki-67 staining and BrdU incorporation. In addition, I examined Cyclin-D1 expression level, a target of canonical Wnt signalling pathway. During embryonic development sFRP-2 activates Wnt/planar cell polarity pathway (PCP) in embryonic stem cells (Kele *et al.* 2012) and Beta-catenin-dependent canonical Wnt pathway is regulated during lens development dependent on sFRP-2 (Esteve *et al.* 2011, Sugiyama *et al.* 2013). In the thesis, the Wnt signalling profile of HSCs of adult *Sfrp2*$^{-/-}$ mice and in extrinsically modified WT HSCs after transplantation in *Sfrp2* deficient microenvironment was illuminated.

There is clear evidence of the importance of the niche in regulation of HSC behaviour and function, and sFRP-2 is highly overrepresented in stromal cell lines maintaining HSC (Oostendorp *et al.* 2005). The aim of the thesis was, to analyse functional and molecular effects, both intrinsic and extrinsic, of *Sfrp2* deficiency in steady state (pathogen-free) haematopoiesis and under challenging conditions like regenerative stress and leukaemia. For this purpose, I analysed the regulation of HSC maintenance, activation and self-renewal *in vivo,* also considering the underlying molecular mechanisms. I investigated the proliferative activity of HSCs also with regard to sFRP-2-dependent changes in canonical and non-canonical Wnt signalling.

2. Materials

2.1. General materials

Table 1: Materials

Materials	Manufacturers
Blood lancets Supra	megro GmbH & Co KG, Wesel, Germany
Cell Culture Flasks Cellstar125 ml/250 ml/550 ml	Greiner Bio-One GmbH, Frickenhausen, Germany
Cell Culture Dish, 10 mm, growth enhanced treated	Corning Inc., Corning, U.S.A.
Cell Culture Dish, 10 cm, growth-enhanced treated	TPP Techno Plastic Products AG, Trasadlingen, Schweiz
Cell Culture Plates Cellstar 6/12/24/48/96 Well	Greiner Bio-One GmbH, Frickenhausen, Germany
Cryogenic vial, 2 ml	Corning Inc., Corning, U.S.A.
Disposable bags	Carl Roth, Karlsruhe, Germany
Disposable UV cuvettes	Brand GmbH & Co KG, Wertheim, Germany
Filter Vacuum driven disposable bottle top filter Steritop	Millipore Co., Billerica, U.S.A.
Filters 0.45/30/70/100 µm	BD FalconTM, BD Biosciences, Heidelberg, Germany
Filter tips TipOne 10/100/200/1000 µm	Starlab, Hamburg, Germany
MACS LS cell separation columns	Miltenyi Biotec, Bergisch Gladbach, Germany
MicroAmp® Fast 96-Well Reaction Plate with Barcode	Applied Biosystems, Foster City, U.S.A.
Microcentrifuge safe-lock tubes, 1.5/2 ml	Eppendorf AG, Hamburg, Germany
Monoject, blunt cannula needles	Kendall Healthcare, Mansfield, U.S.A.
Needles, 100 Sterican, 27 Gauge	B. Braun Melsungen AG, Melsungen, Germany
Petri dish with vants 10 mm	Greiner Bio-One GmbH, Frickenhausen, Germany
Poly-L-lysine-coated glass slides	Thermo Fisher Scientific Inc., Waltham, U.S.A.
Polypropylene centrifuge tubes 15/50 ml	Greiner Bio-One GmbH, Frickenhausen, Germany

Serological pipettes	BD FalconTM, BD Biosciences, Heidelberg, Germany
S-Monovette Blood Collection System	Sarstedt AG & Co., Nümbrecht, Germany
Syringes, U-40 Insulin, Omnifix, 1 ml	B. Braun Melsungen AG, Melsungen, Germany
Syringes with Needle, Sub-Q, 1 ml	BD, Franklin Lakes, U.S.A.
Syringes single-use Omnifix 3/5/10/20/30 ml	B. Braun Melsungen AG, Melsungen, Germany

2.2. Instruments and equipment

Table 2: Instruments and equipment

Type of device	Name	Manufacturer
Animal Blood Counter	Counter Scil Vet AbcTM	Scil vet academy, Viernheim, Germany
Cell incubator	Hera Cell 240	Heraeus Instruments, Hanau, Germany
Cell sorter	MoFlo High Speed	Beckman Coulter, US
Centrifuge	Megafuge 3.0 RS, Multifuge 3S	Heraeus Instruments, Hanau, Germany
Counting chamber	Neubauer-improved	Paul Marienfeld GmbH, Lauda Königshofen, Germany
DNA gel electrophoresis chamber	Sub Cell ® GT	Bio-Rad, U.S.A.
DNA gel electrophoresis chamber-power supply	Power Pac 300	Bio-Rad, U.S.A.
Flow cytometer	CyAn ADP LxP8, CyAn ADP 9C	Beckman Coulter Inc., U.S.A.
Fluorescent microscope	Leica DM RBE	Leica, Wetzlar, Germany
Gel-/Chemi-Doc	Gel-/Chemi-Doc, Universal Hood	Bio-Rad, U.S.A.
Ice machine	S.-No:061244	Ziegra Eismaschinen, Isernhagen, Germany
Laminar flow hood	ANTAES 48/72	BIOHIT, Germany
Linear accelerator	Mevatron KD2	Siemens, Erlangen, Germany
Microscope	Axiovert 25	Carl Zeiss, Jena, Germany

NanoDrop	ND-1000 UV/Vis-spectrophotometer	NanoDrop Technologies, Wilmington, DE, U.S.A.
Precision scales	PLJ 2100-2M	Kern & Sohn GmbH, Balingen, Germany
QuadroMACS Separator	MACS	Miltenyi Biotec, Bergisch Gladbach, Germany
Real-Time PCR System	StepOne	Applied Biosystems, Foster City, U.S.A.
Spectrophotometer	SmartSpec Plus	Bio-Rad, U.S.A.
Thermal Cycler	PTC 100 Peltier	Bio-Rad, U.S.A.
Thermomixer	comfort	Eppendorf AG, Hamburg, Germany
Vortex	IKA MS1 minishaker	Werke & Co., Staufen im Breisgau, Germany
Water bath	SUB	Grant Instruments Ltd., Cambridgeshire, UK
Radiation Unit	Gulmay	Gulmay, Suwanee, U.S.A.

2.3. Chemical and biological reagents

Table 3: Reagents

Reagents	Manufacturer
Agar	Sigma-Aldrich, Taufkirchen, Germany
Albumin Fraction V; ≥ 98 %, bovine (BSA)	Carl Roth, Karlsruhe, Germany
Ampicillin	Sigma-Aldrich, Taufkirchen, Germany
AnnexinV-FITC	BD Pharmingen, San Diego, CA, U.S.A.
Beta-Mercaptoethanol	Invitrogen, Darmstadt, Germany
Borgal ® solution 24 %	Virbac GmbH,Bad Oldesloe, Germany
Ciprofloxacin	Fresenius Kabi, Bad Homburg, Germany
Collagenase Type 1	Worthington Biochemical Corp, Lakewood, NY, U.S.A.
Cycloheximide	Sigma-Aldrich, Taufkirchen, Germany
Dimethyl sulfoxid (DMSO)	SERVA Electrophoresis GmbH, Heidelberg, Germany

Diphteria toxin	Sigma-Aldrich, Taufkirchen, Germany
Ethanol, 99.8 %	AppliChem, Darmstadt, Germany
Ethidium bromide, 1 % solution	Carl Roth, Karlsruhe, Germany
Fetal calf serum (FCS)	PAA, Cölbe, Germany
Formalin solution, 10 %	Sigma-Aldrich, Taufkirchen, Germany
Gelatine	Sigma-Aldrich, Taufkirchen, Germany
HBSS	Invitrogen, Darmstadt, Germany
HEPES	Invitrogen, Darmstadt, Germany
Horse serum (HS)	BioWhittaker, Vallensbaek, Denmark
Hygromycin B	Life technology, Darmstadt, Germany
Isolfluran 100 %	Abbott Laboratories, Abbott Park, Illinois, U.S.A.
Isopropanol	Sigma-Aldrich, Taufkirchen, Germany
Lipofectamine 2000	Invitrogen, Darmstadt, Germany
mIL3, mIL6, mSCF	R&D Systems, Wiesbaden, Germany
Penicillin/Streptomycin (Pen/Strep)	Invitrogen, Darmstadt, Germany
Peptone	Carl Roth, Karlsruhe, Germany
Polybrene	Sigma-Aldrich, Taufkirchen, Germany
Propidium-Iodide (PI)	Invitrogen, Darmstadt, Germany
Triton X-100	Carl Roth, Karlsruhe, Germany
Trypan blue	Invitrogen, Darmstadt, Germany
Trypsin 10x	Invitrogen, Darmstadt, Germany
Türk’s solution	Merck KGaA, Darmstadt, Germany

UltraPure DNase/RNase-Free Distilled Water	Invitrogen, Darmstadt, Germany
5-FU, 5-Fluoruracil	Medac GmbH, Hamburg, Germany

2.4. Buffers and media

Table 4: Home-made buffers, solutions and media

Name	Ingredients
Adipogenic induction medium	alpha-MEM plus GlutaMAX Human recombinant insulin (10 µg/ml) 3-Isobutyl-1-Methylxanthine (IBMX) (0.5 mM) Dexamethasone (1 µM) 20 % FCS Ciprofloxacin antibiotic (1:200)
Adipogenic maintenance medium	alpha-MEM plus GlutaMAX Human recombinant insulin (10 µg/ml) 20 % FCS Ciprofloxacin antibiotic (1:200)
Annexin buffer (10x)	Hepes (0.1 M) NaCl (1.4 M) $CaCl_2$ (25 mM)
BBMM (500 ml)	325 ml IMDM (1x) 150 ml FCS 25 ml BSA 5 ml L-Glutamine 2.5 ml Pen/Strep (100x) 1 ml beta-Mercaptoethanol (50 mM)
Blocking Buffer (30 ml)	29 ml PBS 10 % FCS 0.1 % Triton X-100
FACS buffer (500 ml)	500 ml DPBS 0.5 % BSA
Gelatin solution (1 %, 500 ml)	5 g Gelatin powder 500 ml deionized H_2O
HF2+ buffer (1000 ml)	100 ml HBSS 10x 20 ml FCS 10 ml HEPES 10 ml Pen/Strep 860 ml deionized H_2O
LB medium	6 g Peptone 3 g Yeast extract

	1.5 g NaCl Ampicillin (50 µg/ml) 300 ml deionized H_2O
MSC medium (500 ml)	444.5 ml alpha-MEM 50 ml FCS 5 ml Pen/Strep (1:100) 0.5 ml beta-Mercaptoethanol (1:1000)
Oil Red O Stock solution	0.5 g Oil Red O 100 ml Isopropanol
Osteogenic differentiation medium	alpha-MEM plus GlutaMAX Ascorbic acid-2-phosphat (0.05 mM) beta-Glycerolphosphate (10 mM) Dexamethasone (100 nM) Human recombinant insulin (10 µg/ml) 20 % heat-inactivated FCS Ciprofloxacin antibiotic (1:200)
Phoenix Eco culture medium	500 ml DMEM 50 ml FCS
Silver Nitrate solution	1 g $AgNO_3$ 20 ml deionized H_2O
Sodium Carbonate solution	5 g Na_2CO_3 200 µl Formaldehyde (37 %) 100 ml deionized H_2O
Stroma medium (500 ml)	400 ml alpha-MEM 75 ml FCS 25 ml Horse Serum (HS) 5 ml Pen/Strep (1:100) 0.5 ml beta-Mercaptoethanol (1:1000)

Table 5: Commercial buffers and media

Name	Ingredients
ACK Lysing buffer	Invitrogen, Darmstadt, Germany
Alpha-MEM	Invitrogen, Darmstadt, Germany
DMEM	Invitrogen, Darmstadt, Germany
Dulbecco´s PBS (DPBS)	PAA, Cölbe, Germany
MethoCult M3434	Stemcell Technologies, Vancouver, Canada
Opti-MEM	Invitrogen, Darmstadt, Germany
0.5 % Trypsin-EDTA (10x)	Invitrogen, Darmstadt, Germany

Table 6: Kits

Name	Ingredients
APC/FITC BrdU Flow Kit	BD Pharmingen, San Diego, CA, U.S.A.
DNA extraction Kit	Quiagen Inc, Hilden, Germany
Lineage cell depletion Kit	Miltenyi Biotec, Bergisch Gladbach, Germany
MaxiPrep Kit	Quiagen Inc, Hilden, Germany
Power SYBR Green PCR Master Mix	Applied Biosystems, Foster City, CA, U.S.A.
QuantiTect Reverse Transcription Kit	Quiagen Inc, Hilden, Germany
RNeasy Micro Kit	Quiagen Inc, Hilden, Germany

2.5. Antibodies

Table 7: Primary antibodies for Flow cytometry

Antigen	Clone	Fluorochrome	Volume/ $1x10^6$cells.	Manufacturer
CD4	GK1.5	PE-Cy5	1 µl	ebioscience, San Diego, CA, U.S.A.
CD8a	53-6.7	PE-Cy5	1 µl	ebioscience, San Diego, CA, U.S.A.
CD11b	M1/70	APC-eFluor®780	1 µl	ebioscience, San Diego, CA, U.S.A.
CD16/32	93	PE	2 µl	ebioscience, San Diego, CA, U.S.A.
CD31 (PECAM-1)	390	FITC APC	2 µl	ebioscience, San Diego, CA, U.S.A.
CD34	RAM34	FITC eFluor®647	2 µl	ebioscience, San Diego, CA, U.S.A.
CD45	30-F11	FITC PE PE-Cy5 PE-Cy5.5 PE-Cy7 eFluor450® APC APC-eFluor®780	1 µl	ebioscience, San Diego, CA, U.S.A.
CD45.1	A20	PE FITC eFluor450®	1 µl	ebioscience, San Diego, CA, U.S.A.

CD45.2	104	FITC PE	1 µl	ebioscience, San Diego, CA, U.S.A.
CD45r (B220)	RA3-6B2	PE-Cy7	1 µl	ebioscience, San Diego, CA, U.S.A.
CD117 (KIT)	2B8	PE APC APC-eFluor®780	3 µl	ebioscience, San Diego, CA, U.S.A.
CD127 (IL7-R)	A7R34	APC PE	3 µl	ebioscience, San Diego, CA, U.S.A.
CD150	9D1	APC PE	2.5 µl	ebioscience, San Diego, CA, U.S.A.
CD166 (ALCAM)	ebioALC 48		2 µl	ebioscience, San Diego, CA, U.S.A.
Gr-1	RB6-8C5	eFluor450®	1 µl	ebioscience, San Diego, CA, U.S.A.
Ki-67	SolA15	FITC	1 µl	ebioscience, San Diego, CA, U.S.A.
Sca-1	D7	PE-Cy7	3 µl	ebioscience, San Diego, CA, U.S.A.
TER119	TER119	eFluor450®	1 µl	ebioscience, San Diego, CA, U.S.A.
Biotinylated anti-mouse Gr-1/Ly-6G	RB6-8C5		0.5 µl	ebioscience, San Diego, CA, U.S.A.
Biotinylated anti-mouse B220	RA3-6B2		0.5 µl	ebioscience, San Diego, CA, U.S.A.
Biotinylated anti-mouse CD3e	145-2C11		0.5 µl	ebioscience, San Diego, CA, U.S.A.
Biotinylated anti-mouse TER119	TER119		0.5 µl	ebioscience, San Diego, CA, U.S.A.
Biotinylated anti-mouse CD11b	M1/70		0.5 µl	ebioscience, San Diego, CA, U.S.A.

Table 8: Secondary antibodies for flow cytometry

Reagent	Conjugate	Volume/ $1x10^6$cells	Manufacturer
Streptavidin	eFluor450® PE-Cy5.5	0.5 µl	Invitrogen, Darmstadt, Germany

Table 9: Antibodies for immunofluorescence (IF)

Product	Species	Dilution	Manufacturer
Anti-Cyclin-D1	rabbit	1:25	Cell Sign. Techn., U.S.A.
Anti-Beta-catenin	rabbit	1:50	Cell Sign. Techn., U.S.A.
Anti-CaMK-II	rabbit	1:100	Cell Sign. Techn., U.S.A.
Anti-C/EBP-alpha	rabbit	1:50	Cell Sign. Techn., U.S.A.
Anti-DVL-2	rabbit	1:100	Cell Sign. Techn., U.S.A.
Anti-GSK-3-beta (Ser9)	rabbit	1:100	Cell Sign. Techn., U.S.A.
Anti-NF-ATcc1	mouse	1:50	Santa Cruz Biotechnology, Inc., U.S.A.
Anti-NLK	rabbit	1:50	Santa Cruz Biotechnology, Inc., U.S.A.
Anti-Phospho-Beta-catenin (Ser33/37/Thr41)	rabbit	1:50	Cell Sign. Techn., U.S.A.
Anti-Phospho-CamK-II (Thr286)	rabbit	1:100	Cell Sign. Techn., U.S.A.
Anti-PPAR-gamma	rabbit	1:200	Cell Sign. Techn., U.S.A.

Table 10: Secondary antibodies for immunofluorescence (IF)

Reagent	Conjugate	Manufacturer
Anti-Alexa Fluor®488	rabbit	Invitrogen, Darmstadt, Germany
Anti-mouse IgG (Alexa Fluor®488 Conjugate)	goat	Invitrogen, Darmstadt, Germany
Anti-rabbit IgG (FITC labelled)	goat	ebioscience, San Diego, CA, U.S.A.
Anti-rabbit IgG (Alexa Fluor®488 Conjugate)	goat	Invitrogen, Darmstadt, Germany

2.6. Primers for PCR and qRT-PCR

Table 11: Primers for qRT-PCR (SYBR Green-based detection) and PCR

Name	Sequence (5'-3')
Rpl13a-F	CCCTCCACCCTATGACAAGA
Rpl13a-R	TTCTCCTCCAGAGTGGCTGT
Rpl39-F	ATTCCTCCGCCATCGTGCGCG
Rpl39-R	TCCGGATCCACTGAGGAATAGGGCG
qPCR *Sfrp2*-F	AGGGACCTGAAGAAATCCGT

qPCR *Sfrp2*-R	GGAGATGCGCTTGAACTCTC
m*Sfrp2* (g)-F (25 nmole)	CACGAGTAGTGAATACCTGAG
m*Sfrp2* (g)-R (25 nmole)	GACACATTGTTGCTGCTTCCT
m*Sfrp2* bfA-F (25 nmole)	GATCAATTCTCTAGAGCTCGC

2.7. Expression vectors

Table 12: Expression vectors

Name	Factory
pMIG	Kindly provided by Bubnoff group (Miething *et al.* 2003)
pMIG-p185 (BCR-ABL)	Kindly provided by Bubnoff group (Miething *et al.* 2003)
pLKO.1	Open Biosystems, Huntsville, LA, U.S.A
sh*Sfrp2*-pLKO.1; sequence: TTGATGTACGTTATCTCCTTC	Open Biosystems, Huntsville, LA, U.S.A

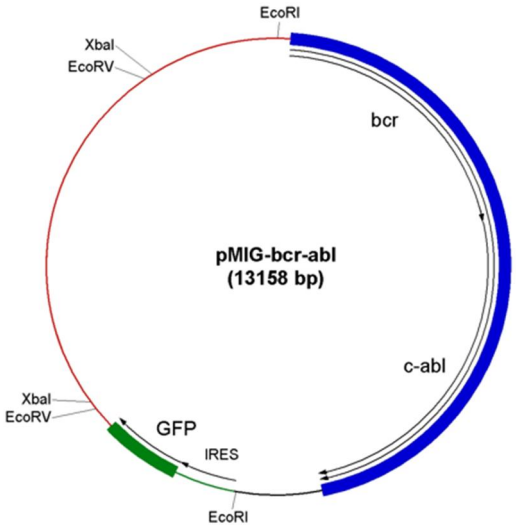

Figure 3. Vector map of pMIG-p185 BCR-ABL plasmid. *The MIG vector is derived from murine stem cell virus (MSCV) and contains the genes encoding the green fluorescent protein (GFP), Ampicillin resistance (AMP), internal ribosomal entry side (IRES) and the fusion oncogene p185 BCR-ABL (Miething et al. 2003); The control vector MIG contains GFP, AMP and IRES.*

2.8. Cell lines

Table 13: Cell lines

Name	Factory
Phoenix™ ecotropic helper-free retroviral producer cells	G. Nolan, Stanford, USA
UG26-1B6	(Oostendorp *et al.* 2002)

2.9. Mice

Table 14: Mice strains

Name	Factory
C57BL/6.J	Harlan Laboratories, Rossdorf, Germany
BL/6/SJL (Ly5.1)	Taconic Europe, Ry, Denmark
129S2/SvHsd	Harlan Laboratories, Rossdorf, Germany
129xBL/6	Breeding in ZPF*: 129S2/SvHsd x C57BL6.J
129xLy5.1	Breeding in ZPF: 129S2/SvHsd x B6/SJL (Ly5.1)
129xBL/6 *Sfrp2*$^{+/+}$	Laboratory of Akihiko Shimono (Satoh *et al.* 2006), Breeding in ZPF
129xBL/6 *Sfrp2*$^{-/-}$	Laboratory of Akihiko Shimono (Satoh *et al.* 2006), Breeding in ZPF

ZPF: Zentrum für präklinische Forschung

3. Methods

3.1. Mice and genotyping

Sfrp2$^{-/-}$ mice were bred on 129S2xBL/6(129xBL/6) background. Age- and sex-matched *Sfrp2*$^{+/+}$ wild type (WT) littermates or 129xBL/6 WT mice were used as controls in the experiments. Mice were kept in micro isolators in individually ventilated cages (IVC) under specific-pathogen-free (SPF) conditions according to FELASA recommendations in centre for preclinical research (Zentrum für präklinische Forschung (ZPF)).

Sfrp2 homozygous knockout (KO) and WT mice were distinguished from each another via polymerase chain reaction (PCR). Either small pieces of the ear (from ear clipping) or the tail were used as samples. The tissue samples were incubated overnight in lysis buffer (100 mM Tris/HCl), 1 % Tween 20, with freshly added 200 µg/ml Proteinase K at 50 °C with constantly shaking in order to decompose the tissue. The next day, the Proteinase K was inactivated by incubation of the samples at 95 °C for 5 min. After that, the samples were centrifuged at 15,000 g for 2 min and the supernatant or 0.5 µl of purified DNA were used for PCR analysis. DNA purification was performed following manufacuture's descriptions (DNA extraction Kit, Quiagen). For PCR the peqGOLD PCR Master Mix Y (Peqlab) was used

10 µl peqGOLD PCR Master Mix Y (Peqlab)
1 µl Primer
1 µl Primer
1 µl Primer
1 µl DMSO
1 µl $MgCl_2$
0.5 µl gDNA template
4.5 µl H_2O
20 µl final volume

The samples were run in a PTC 100 Peltier Thermal Cycler.

Program:

94 °C	4 min	
94 °C	20 s	35 cycles
58.5 °C	20 s	
72 °C	2 min	
72 °C	10 min	
4 °C	hold	

Afterwards, 5 µl of loading buffer (30 % glycerol with Orange G) were added to the samples. After loading the samples on a 1.5 % agarose gel made with NaB buffer (0.01 M di-sodium tetra-borate) and ethidium bromide (0.5 µg/ml), the gel was run with 150 V and analysed with Bio-Rad Gel-Doc XR Imaging System. Wild type DNA displays a 480 bp fragment, *Sfrp2*$^{-/-}$ DNA shows a 350 bp mutant band. DNA of heterozygous mice results in both bands (Figure 4).

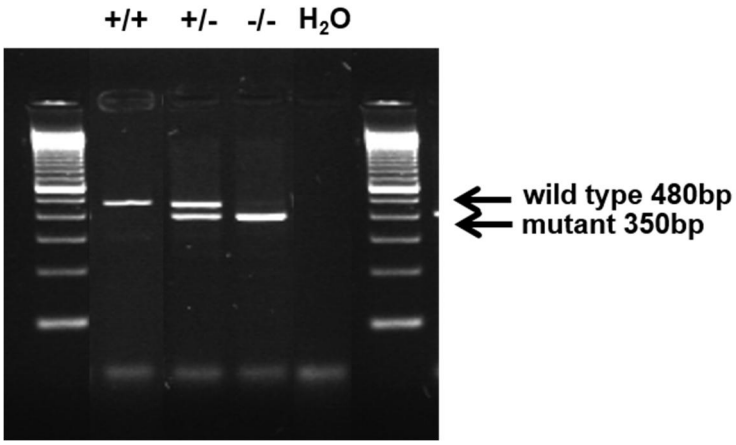

Figure 4. Genotyping of Sfrp2 knockout mice. *Mouse DNA loaded on a 1.5 % agarose gel. 100 bp ladder was used to distinguish the size of the bands. WT (Sfrp2*$^{+/+}$*) DNA shows a 480 bp fragment, Sfrp2*$^{-/-}$ *DNA shows a 350 bp mutant band. DNA of heterozygous Sfrp2*$^{+/-}$ *mice displays both bands.*

3.2. Preparation of murine tissues

In this project fetal liver (FL), bone marrow (BM), stromal niche cells, spleen (Sp) and peripheral blood (PB) were analysed.

To obtain embryonic tissues for the analysis of haematopoietic cells, adult male mice were mated with two females in the late afternoon. On the following morning the females

were checked for the presence of a vaginal plug. The time point of plug existence is considered embryonic day zero (E0). Pregnant females were sacrificed on E14.5 for isolation of fetal liver. The uteri were removed and by using fine forceps and scissors, the embryo was transferred out of the uterus into culture dishes containing HF2+ buffer. The dissection needles are used to cut the trunk of the embryo from tail and head. The tail was used for genotyping. The ventral dermis was removed and the liver can be dissected cleanly and transferred to culture dishes containing HF2+ buffer at 4° C. Fetal liver was squeezed and subsequently filtered through 70 µm cell strainers, digested with DNase and further analysed for haematopoietic cell population by flow cytometry.

For the BM analysis, the four long bones (tibia and femur) of both hind legs were dissected and BM was flushed with a total of 10 ml HF2+ buffer. The cell suspension was homogenized and filtered through a 30 µm filter and used for analysis.

For stromal niche cell isolation the whole bone marrow was flushed and the remaining bone was fragmented with mortar and pestle. Bone fragments were washed once in HF2+ buffer to release the loosely adherent BM cells and several times in PBS until the fragments were white. Endosteal stromal cells were released from the haematopoietic-depleted bone fragments by digestion with 3 mg/ml type I collagenase and 15 µg/ml DNAse dissolved in PBS for one hour at 37 °C at 110 rpm. This stromal fraction was used in all subsequent analyses of endosteal populations.

For the analysis of spleen, the organs were squeezed, filtered through 100 µm filter, homogenized, filtered through a 30 µm filter and used for analysis.

Murine peripheral blood was obtained by punctuating the facial vein (during experiment) or was directly sampled from the heart (end of experiment). The blood was collected in EDTA-coated vials. Blood samples were mixed with 5 ml ACK lysing buffer and incubated on ice for 15 min in order to lyse the erythrocytes. The samples were centrifuged at 500 g for 5 min and the pellet was resuspended in HF2+ buffer.

3.3. Flow cytometry staining

For staining of surface markers, the cells were resuspended in 100 µl staining buffer with primary antibodies. For bone marrow staining, $2x10^6$ cells were used for mature population stains, and $6x10^6$ for staining of progenitors and HSCs. Used antibodies are listed in Table 7 and Table 8. The cells were incubated with the antibodies for 15 min at 4 °C and after that, washed with staining buffer. In some stainings, a secondary antibody was added (diluted in FACS buffer, Table 4). Finally the stained cells were resuspendend in FACS buffer with 1 µg/ml propidium iodide and analysed on CyAn ADP LxP8 or CyAn ADP 9C.

For sorting of several cell population, the cells were stained as described above, and sorted on MoFlo cell sorter.

3.4. Single cell staining

For immunofluorescence staining, LSK, MP, and CLP populations were sorted and a total amount of 500-1000 cells was spotted on poly L-Lysin coated slides. After incubation for 30 min at 4 °C, the cells were fixed with 4 % paraformaldehyde for 5 min and subsequently blocked with blocking buffer (10 % FCS and 0.1 % Triton-X in PBS) for 30 min at room temperature (RT). Cells were stained overnight at 4° C in humid chamber with primary antibody diluted in blocking buffer. The next day, the cells were washed with blocking buffer and stained overnight at 4 °C in humid chamber with secondary antibody. Afterwards, the cells were washed twice with blocking buffer and once with PBS. The cells were counterstained with slow fade Gold with DAPI (4.6-diamino-2-phenylindole dihydrochloride) at RT followed by one week desiccation at RT in the dark. Using constant settings, fluorescence digital images were taken on Leica DM RBE fluorescent microscope using Axio Vision software (Carl Zeiss). Afterwards, 20-30 cells were snapped with 100x magnification. Fluorescence intensities of stained cells were quantified in total pixel using ImageJ software (NIH), by circling the cells. The

background fluorescence was subtracted from specific signals caused by antibody staining.

3.5. Colony-forming assay

To quantify the multi-potential and lineage restricted progenitors, colony forming assay, a functional cellular assay was used. Burst-forming unit-erythroid progenitors (BFU-E), colony-forming unit-granulocyte/macrophage (CFU-GM) and CFU-granulocyte/ erythroid/macrophage/megakaryocyte progenitors (CFU-GEMM) were distinguished by colour and shape. For colony forming assay, BM cells ($2.5x10^4$) or one week co-cultures initiated with 5000 Lin^- cells were cultured in methylcellulose (MethoCult M3434) on 3.5 mm dishes ($1x10^4$ per dish) for ten days at 37 °C and 5 % CO_2. Colonies formed, were distinguished into GM, GEMM and BFU-E, and counted under the microscope following the manuals of Stemcell Technologies (Figure 5).

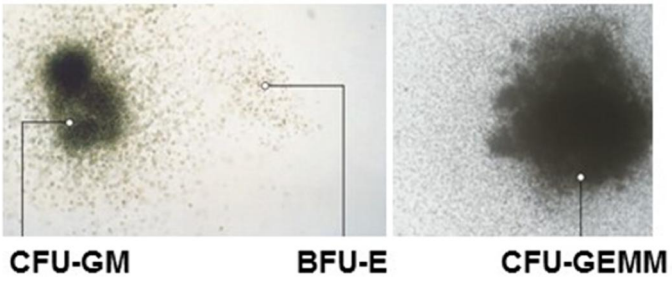

Figure 5. Examples of CFU-GM, BFU-E and CFU-GEMM. *Stemcell technologies' manuals serving as guidelines for experimental analysis. BFU-E, CFU-GM and CFU-CEMM are shown in 50x magnification.*

3.6. Gene expression analysis

In order to detect gene expression in haematopoietic tissues, analysis from different haematopoietic cell populations was performed. LSKs, MPs, CLPs, B-cells, T-cells, granulocytes and monocytes were isolated by cell sorting. UG26-1B6 stromal cell line was used as murine stromal tissue.

RNA isolation was performed using the RNeasy Micro-Kit according to the manufacturer´s instructions. Cell populations were sorted into HF2+ buffer, pelleted and

resuspended in RLT buffer containing guanidine-thiocyanate lysing the cells and inactivating RNase. Subsequently the samples are homogenized by QIAshredder spin columns. The homogenized samples are mixed with ethanol to optimize binding conditions and loaded on RNeasy Mini spin columns where the RNA binds to the silica-based membrane. Contaminants were washed away by the use of the wash buffers RW1 and RPE and finally, the total RNA was eluted under low-salt conditions.

Subsequently, reverse transcription was carried out. RNA was transcribed to cDNA using Quanti Tect Reverse Transcription Kit.

Genomic DNA elimination reaction:
1 µg RNA
1x DNA Wipeout buffer
RNase free water
The mixture was incubated for 2 min at 42 °C.

Reverse transcription master mix on ice
Quantiscript Reverse Transcriptase
1x Quantiscript RT Buffer
RT Primer Mix
+genomic DNA elimination reaction

After an incubation time of 15 min at 42 °C, the Quantiscript Reverse Transcriptase is inactivated by 3 min at 95 °C. The cDNA can be stored at -20 °C, or real time PCR was carried out.

Real time PCR was used to determine the expression levels of *Sfrp2* in haematopoietic cell population. Real time PCR allows monitoring the progress of PCR as it occurs and can therefore detect and quantify cDNA. In this study, the SYBR Green System was used to detect PCR products. After reverse transcription the samples were diluted (Stroma 1:8, mature haematopoietic cells 1:6, stem and progenitor cells 1:4). The standard was serially diluted and used for every primer to determine the amplification

rate per cycle. *Rpl13a* (Curtis *et al.* 2010) and *Rpl39* (Warrington *et al.* 2000, Maltseva *et al.* 2013) were used as housekeeping genes for normalization.

3.7. Stable Knockdown of *Sfrp2*

The stable knockdown of *Sfrp2* in UG26-1B6 stromal cell line was kindly provided by a colleague, Kerstin Gauthier. In brief, a lentiviral system with NX Phoenix Eco packaging cell line was used to infect the stromal cells with pLKO.1-*shSfrp2* or empty vector control pLKO.1 which stably integrated into the genome. Prior to experimental use, stromal cells containing pLKO.1-*shSfrp2* or empty vector were selected by 5 µg/ml puromycin for three days.

3.8. Co-cultures of Lin$^-$ BM cells on UG26-1B6 stromal cell

Stromal cell lines were cultured on 0.1 % gelatine coated dishes in stroma medium (alpha-MEM, 15 % FCS, 5 % HS, 100 U Penicillin, 100 µg streptomycin, 10 µM beta-Mercaptoethanol) and 20 % of conditioned medium from prior passage.

Lineage-depleted bone marrow cells (Lin$^-$) were co-cultured with 30 Gy irradiated confluently grown stromal cells. The lineage fraction was negatively selected from flushed bone marrow according to the manufacturer's instructions. In brief, bone marrow cells were first incubated with a mixture of primary biotinylated antibodies (CD3, B220, CD11b, Gr-1 and TER119) and subsequently with Streptavidin-conjugated magnetic Micro Beads. The labelled cells were run through columns in a magnetic field. Cells coated with Micro Beads were restrained in the column, the lineage negative, unlabelled cells run through the column. The 5000 Lin$^-$ cells were plated on confluent and irradiated stromal cells in a 10 cm dish. The cells were cultured in stroma medium for one week.

3.9. MSC differentiation

To test whether sorted mesenchymal populations show the capacity for multipotent differentiation *in vitro*, cultured non-haematopoietic cell populations were tested for their ability to differentiate into mesenchymal lineages. In previous work (Friedenstein *et al.*

1974, Friedenstein *et al.* 1987, Pittenger *et al.* 1999) three main differentiation pathways of the mesenchymal cells are determined *in vitro* and *in vivo*. *In vitro*, MSCs should have the potential to differentiate into adipogenic, chondrogenic and osteogenic lineage.

In this work, the differentiation potential of murine bone marrow MSCs was tested. Differences in adipogenic and osteogenic differentiation potential of *Sfrp2*$^{-/-}$ BM-MSCs and their WT littermate BM-MSCs were analysed. Endosteal niche cells were isolated as described in Chapter 3.2. and sorted corresponding to their surface markers (TER119^{-} CD45^{-}, PECAM-1 (CD31)$^{-}$, SCA-1^{+}), following the gating scheme of Nakamura *et al.* (Nakamura *et al.* 2010) (Figure 6). In 6-well plates 1000 to 2000 sorted MSCs were cultured in AlphaMEM medium, supplemented with 15 % FCS, 100 U Penicillin, 100 µg streptomycin, 10 µM beta-Mercaptoethanol. After ten days formed colonies were counted and afterwards MSCs were expanded up to passage two. Adipogenic and osteogenic differentiation was induced after the MSCs have grown to a confluent monolayer.

Adipogenic differentiation

Adipogenic differentiation was performed following the protocol of Pittenger *et al*. (Pittenger *et al.* 1999). The adipogenic differentiation procedure consists of a cycled process by changing induction medium with maintenance medium (Table 4). When cells were grown to confluent monolayer, the cell culture medium was removed and replaced by induction medium. After three days, the induction medium was removed and replaced by maintenance medium for two days. This process was repeated three times. Finally, the cells were incubated for one week in maintenance media.

Histological detection of adipogenic differentiation with Oil Red O staining:

After 20 days (three times induction/maintenance), adipogenic differentiation is visible by expansion of the cytoplasmatic lumen and appearance of fatty vesicles of different sizes. For coloration of the lipid vesicles, Oil Red O staining was performed. Oil Red O was incorporated in the fatty vesicles and appears red.

To prepare Oil Red O staining solution, six parts of Oil Red O stock solution were diluted with four parts distilled water. The solution should be mixed well and incubated for 24 h at RT. The next day, prior using, the solution was filtered to remove unsolved particles.

After removing the maintenance medium, the MSCs were washed carefully with 1xPBS and fixed with 2 % Paraformaldehyd (PFA) in 1x PBS for 30 min at 4 °C. After fixation, PFA was discarded and the cells were incubated with Oil Red O staining solution for 30 min at RT. Finally, the cells were washed several times with distilled water. The staining is stable for a few days (Figure 6).

Osteogenic differentiation

Osteogenic differentiated cells will change their morphological appearance into cuboidal phenotype and will deposit calcium, which can be detected by staining of mineralized osteogenic membrane. To detect this calcium deposition, the von Kossa procedure was used. The induction of the osteogenic differentiation is performed as described at Jaiswal *et al.* (Jaiswal *et al.* 1997).

After formation of a confluent monolayer culture, MSC culture medium was replaced by osteogenic differentiation medium (Table 4) and renewed every third day for a total of three weeks. Calcium accumulations will appear which are visible as dense brown-coloured areas in the culture. The mineralized matrix of osteogenic differentiated cells was visualized by von Kossa staining.

Histological detection of osteogenic differentiated cells with von Kossa staining:

Calcium deposits at the membrane of osteogenic differentiated cells could be detected by von Kossa staining. Here, calcium salts (phosphate, carbonate) of the mineralized matrix are revealed by substitution to metallic cations from silver nitrate. The silver nitrate is visualized after reduction to metallic silver (black). This black staining indicates the mineralization of the bone matrix.

After removing the medium, the MSCs were washed carefully with 1xPBS and fixed with ice-cold methanol for 20 min at 4 °C. After fixation, the cells were washed, covered with

silver nitrate and incubated for 30 min at room temperature in the dark. The silver nitrate binds to the calcium and marks the osteogenic differentiated cells. The reaction will be stopped by washing several times with 1xPBS after removing the silver nitrate. Finally, sodium carbonate was added. After 5-10 min, the silver nitrate will be reduced and black staining will appear. The cells can be stored in distilled water for photography (Figure 6).

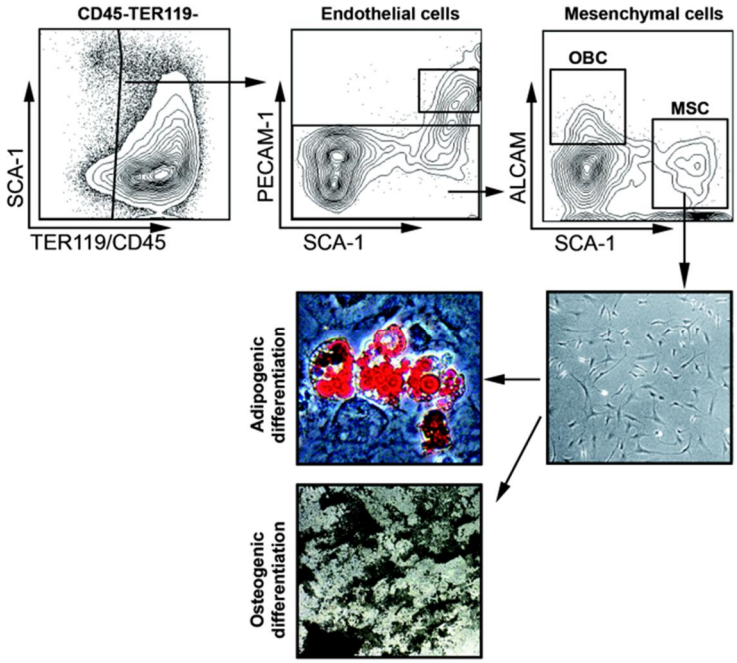

Figure 6. Bone marrow niche cell components and differentiation of MSCs. *Upper panel: Niche cells were stained as described in Nakamura et al., 2010 (Nakamura et al. 2010). CD45^{-}Ter119^{-}, PECAM-1^{+} cells represent endothelial cells, CD45^{-}TER119^{-}, PECAM-1^{-}, ALCAM^{+} define osteoblasts (OBCs), CD45^{-}Ter119^{-}, PECAM-1^{-}, SCA-1^{+}, ALCAM^{med} cells represent mesenchymal stromal cell populations (MSCs). Cells were analysed using flow cytometry Lower panel: For differentiation MSCs were sorted and osteogenic and adipogenic differentiation was induced. Figure recently published by Schreck, C. and Bock, F., 2014 (Schreck et al. 2014).*

3.10. Transplantation assays

Since regeneration of tissues *in vivo* is one of the required properties of somatic stem cells, transplantation assays were performed to determine donor-derived blood cell regeneration and to study HSCs functionally, *in vivo*. Throughout this thesis, the CD45 congenic system (CD45.1 and CD45.2) was used to distinguish donor-derived cells from recipient cells.

Transplantation assay was used for intrinsic/extrinsic analyses: Eight to twelve weeks old, lethally irradiated recipient mice (8.5 Gy) received $2x10^5$ donor cells via intravenous injection (i.v.) in the tail vein.

In the first five weeks after transplantation, all recipients received 1 mg/ml Borgal through drinking water. Peripheral blood was analysed five and ten weeks after transplantation by flow cytometry. Sixteen weeks after transplantation mice were sacrificed, bone marrow (BM), spleen, and peripheral blood (PB) were analysed by flow cytometry. BM cells were also used as donor cells for further transplantations. Mice were defined as engrafted with ≥ 1 % myeloid and 1 % lymphoid donor cells.

In leukaemia models, $1x10^5$ GFP^+ BM cells, carrying the oncogene of interest (BCR-ABL), were injected into adult recipients. Mice were sacrificed when severe disease pattern was discovered. The symptoms are for instance anaemia, loss of weight, arched back, ruffled fur and a reduced general state of health. An extended scoring protocol can also be found in Chapter 4.7. Mice were sacrificed when symptoms got worse and behaviour was characterized with slow or irregular moving, irregular breathing and thick stomach due to splenomegaly. The GFP expression system was used to detect injected oncogene-expressing cells.

3.11. Ki-67 staining

Ki-67 is a marker for active cell cycling of cells. It is present during G1, S and G2 and mitosis (M) phases.

In this case, *Sfrp2* knockout mice were compared to 129xBL/6 WT controls. Untreated ten weeks old mice were sacrificed and bone marrow was flushed as described before (Chapter 3.2.). After staining of surface markers, fixation and permeabilization were performed following the manufacturer's instructions of BrdU Flow Kit. In brief, for fixation and permeabilization of cells Cytofix/Cytoperm buffer was used, containing para-formaldehyde (fixation) and saponin (permeabilization). After that FITC-labelled anti

Ki-67 antibody was added to the cells and incubated at 4 °C for 16 h. Cells were washed and analysed by flow cytometry.

3.12. BrdU incorporation assay

For short-term assay, mice were injected intraperitoneally (i.p.) with 1 mg BrdU Bromodeoxyuridine (5-bromo-2'-deoxyuridine, BrdU, BD Bioscience) and were sacrificed 16 h after injection. For the long-term assay, mice were injected i.p. with 500 ng once, followed by ten days of oral gavage in drinking water in a concentration of 0.8 mg/ml. The mixture was made up fresh and changed daily. Seventy days after injection mice were sacrificed. To assess the incorporation of BrdU into DNA of different populations of replicating cells, in the S-phase of cell cycle, bone marrow cells were first stained for surface markers and the BrdU staining was performed following the manufacturer's instructions (FITC-BrdU/APC-BrdU Flow Kit, BD Bioscience). After fixation and permeabilization, the cells were treated with 30 µg DNase for 1 h at 37 °C. After that FITC- or APC-labelled anti- BrdU antibody was added to the cells and incubated at 4 °C for 16 h. Prior to FACS analysis, cells were washed and total DNA level was stained with 7-aminoactinomycin D (7-AAD) which allows to detect the distribution of cells in G0/G1, S and G2/M phase of cell cycle.

3.13. 5-FU- (BrdU) incorporation assay

For stress induction, mice were injected i.p. with 150 mg/kg (mouse bodyweight) 5-fluorouracil (5-FU). Peripheral blood, extracted from mouse cheek was analysed four days after injection, mice were sacrificed six days after injection and peripheral blood extracted from the heart as well as bone marrow were analysed as described above.

For proliferative analysis 50 mg/kg BrdU was injected i.p., five days after injection of 150 mg/kg mouse 5-FU. Mice were sacrificed and bone marrow was analysed 16 h after BrdU injection as described in Chapter 3.12.

3.14. Apoptosis assay

Proidium iodide (PI) in conjunction with AnnexinV is used to discriminate viable (PI^- $AnnexinV^-$) apoptotic (PI^- $AnnexinV^+$) and necrotic (PI^+ $AnnexinV^-$) cells. For apoptosis assay $1x10^7$ bone marrow cells were cultured for 16 h with growth factors (mIL-3 10 ng/ml, IL-6 10 ng/ml, SCF 50 ng/ml) and with cycloheximide (50 µg/ml, Sigma-Aldrich) at 37°C. Cells were stained corresponding to their surface markers with FACS-buffer (1x PBS + % BSA) and apoptosis marker AnnexinV-FITC with 1x Annexin buffer (10x Annexin buffer: 0.1 M Hepes, 1.4 M NaCl and 25 mM $CaCl_2$). Propidium iodide was added prior to flow cytometry analysis.

3.15. Phoenix™ helper-free retrovirus producer cell line culturing

The cell line is based on the 293T cell line (a human embryonic kidney line transformed with adenovirus E1a and carrying a temperature sensitive T-antigen co-selected with neomycin). The Phoenix cell line was created by placing constructs capable of producing gag-pol and envelope (env) proteins for ecotropic viruses into 293T cells. The cell line is highly transfectable (Figure 7).

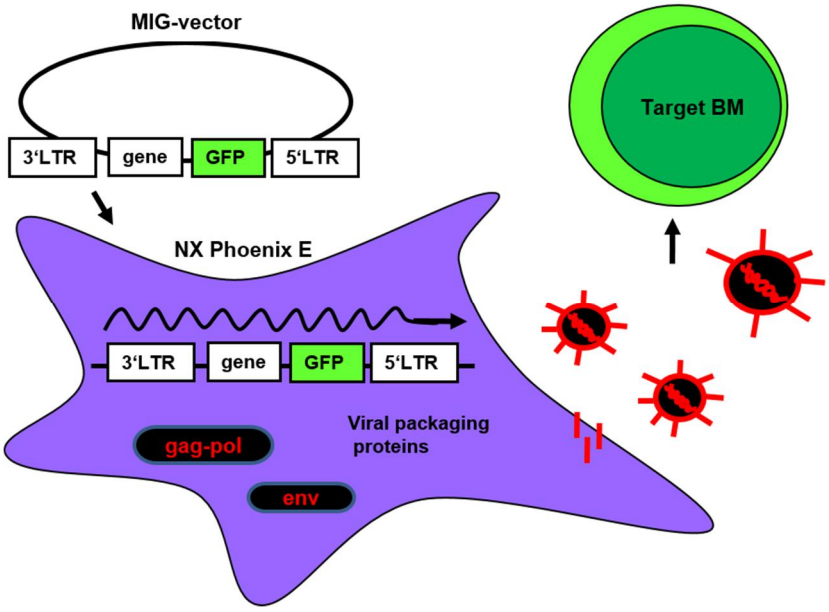

Figure 7. Retroviral transfection of NX Phoenix E cells and infection of bone marrow. *Phoenix E cells (G. Nolan, Stanford, USA), containing gag-pol and env protein for production of retroviruses are transfected with MIG vector. The vector stably expresses the marker gene GFP. The produced virus is used for stable infection of bone marrow target cells.*

Prior to transfection, Phoenix cells were selected with selective medium, DMEM+10 % FCS+ 0.3 mg/ml hygromycin for gag-pol selection and 2 µg/ml diphtheria toxin for envelope selection. Daily, supernatant was discarded (removing dead cells) and cells were maintained in a concentration of 0.5-1x10^6 cells per ml fresh selective medium. Selection was continued until no more cells died due to Gag-pol env deficiency (five to six days). After that passage zero (p0) phoenix cells were rescued with Phoenix medium (DMEM+10 % FCS), maintained in a concentration of 0.5-1x10^6 cells/ml and expanded to p5 to p10 which are the appropriate passages for transfection.

3.16. Retroviral transfection of phoenix producer cells with p185 BCR-ABL and infection of bone marrow cells

MIG empty vector control and MIG-p185 BCR-ABL vector were kindly provided by Prof. Dr. Nikolas von Bubnoff's group. To isolate high quantities of plasmid DNA, competent Escherichia coli bacteria were transformed by heat-shock with MIG empty vector control and MIG-p185BCR-ABL vector containing an ampicillin resistance gene (Amp) and a gene encoding green fluorescence protein (GFP) and cultured 16 h in liquid LB- medium with 100 µg/ml ampicillin. After that, Maxiprep was performed following manufacturer's instructions (Quiagen Inc, Hilden, Germany).

Phoenix™ NX ecotropic helper-free retroviral producer cells were grown in Phoenix medium (DMEM+10 % FCS). Retroviruses were generated by transient transfection of Phoenix producer cells with p185 BCR-ABL and MIG control retroviral construct using Lipofectamine 2000 according to the manufacturer's recommendations.

The target bone marrow cells from male BL/6 donor mice were isolated four days after treatment with 150 mg/kg 5-FU. After ACK-lysis, cells were resuspended in BBMM (Table 4) containing growth factors (mIL-3 10 ng/ml, mIL-6 10 ng/ml, mSCF 50 ng/ml) and prestimulated for 24 h. BM cells were transduced with viral supernatants by spin infection four times every 12 h (90 min, 32 °C, 2400 rpm). The cells were harvested 12 h after the last spin infection, washed with PBS, resuspended in HF2+ buffer and MIG

control as well as MIG-BCR-ABL infected cells were tested for GFP expression by FACS analysis. Lethally irradiated mice were transplanted with $1x10^5$ GFP^+ BM cells via tail vein injection.

3.17. Statistics

For statistical analysis unpaired and paired Student's t-test was used where appropriate.

4. Results

4.1. Co-cultures of Lin$^-$ BM cells on *shSfrp2* knockdown stroma

The basis of the current studies was the establishment of stromal cell lines, two of which EL08-1D2 and UG26-1B6, supported the maintenance of haematopoietic stem cells (HSCs) under contact (Oostendorp *et al.* 2002) and non-contact (Oostendorp *et al.* 2005, Buckley *et al.* 2011) conditions. Several secreted molecules that are overexpressed in these stromal cell lines were identified and sFRP-2 was one of the highest overexpressed molecules (Oostendorp *et al.* 2005) (Figure 8). In a later study, these results were confirmed and, in addition, the closely related sFRP-1 was also found to be overrepresented by these cell lines (Oostendorp *et al.* 2005, Ledran *et al.* 2008).

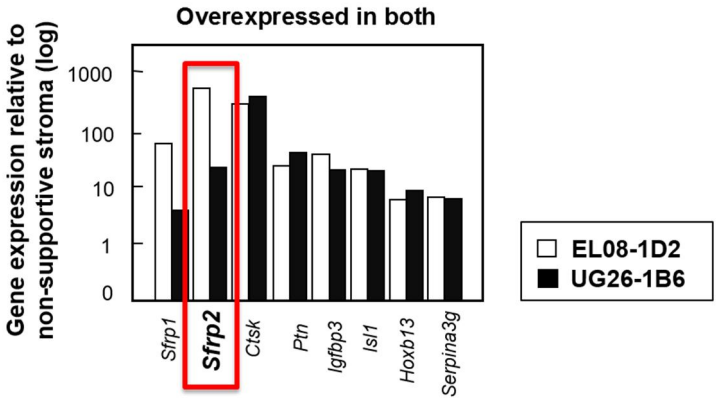

Figure 8. Gene expression in haematopoietic stem cell-supporting stromal cells. *The expression of Sfrp1, Sfrp2, Ctsk, Ptn, Igfbp3, Isl1, Hoxb13 and Serpina3g is shown in EL08-1D2 and UG26-1B6 relative to non-supportive stroma, measured by real time PCR. Values were calculated on 2^delta CT x100 % values relative to housekeeping gene Rpl13a (Oostendorp et al. 2005).*

4.1.1. Increased expression of LSKs co-cultured on *shSfrp2* knockdown stroma

To analyse the role of the sFRP-1-related sFRP-2 in HSC regulation, stable knockdown of *Sfrp2* in UG26-1B6 stromal cells was established by our group by lentiviral transfection. The lentiviral vector pLKO.1 encoded puromycin resistance as well as a shRNA targeting *Sfrp2*. The puromycin-selection resulted in the establishment of UG26-1B6 cells expressing the pLKO.1 empty vector (control stroma), or UG26-1B6

cells in which expression of *Sfrp2* was knocked down. Expression of *Sfrp2* mRNA in these cells was determined by qPCR and the efficient knockdown to 85 % levels of the pLKO.1 control is shown in Figure 9.

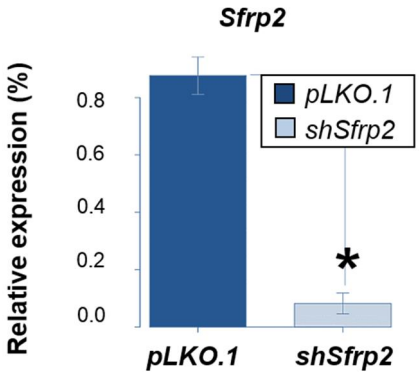

Figure 9. Knockdown of Sfrp2 in UG26-1B6 stromal cells. *The expression of Sfrp2 in knockdown (shSfrp2) and control stromal cells (pLKO.1) is shown. Values were calculated on 2^delta CT x100 % values relative to housekeeping gene Rpl13a.*

To study the influence of reduced sFRP-2 expression by the stromal cells on HSCs, 5000 lineage negative (Lin^-, excluding mature erythroid (TER119) lymphoid (B220, CD3e) and myeloid (Gr-1, CD11b populations)) bone marrow cells of wild type (WT) BL/6 mice were co-cultured on 80 % confluent, irradiated (30 Gy) *shSfrp2* knockdown and pLKO.1 control UG26-1B6 cells (Chapter 3.8. and Figure 10 A). After one week of co-culture haematopoietic stem and progenitor cell population's phenotypes were analysed by flow cytometry. Surface antigen CD45 was used to distinguish stromal cells and haematopoietic cells. As it is also described in our latest review (Schreck *et al.* 2014), to define stem and progenitor cell populations, the well-established surface antigens Ly-6A/E (originally described as SCA-1) and KIT was used to visualize LSKs (Lin^- $SCA\text{-}1^+$ KIT^+) (Ikuta and Weissman 1992), which includes HSCs, and myeloid progenitors (MPs: Lin^- $SCA\text{-}1^-$ KIT^+). IL7-R was used for common lymphoid progenitors (CLPs: Lin^- KIT^{med} $IL7\text{-}R^+$, Figure 10 B) (Kondo *et al.* 1997, Renstrom *et al.* 2010).

Flow cytometric analysis exhibited a fourfold increased percentage of LSK cell population after one week of co-culture using *Sfrp2* knockdown stromal cells, which suggests an enhanced potential to either maintain or generate cells with the LSK phenotype. In contrast, the total number of myeloid and lymphoid progenitors (MPs, CLPs) showed no

significant alterations in co-cultures. The cell number of these cell populations remained unchanged after one week of co-culture (Figure 10 C).

4.1.2. Increased clonogenic activity of progenitor cells co-cultured on *shSfrp2* knockdown stroma

A small number of haematopoietic stem cells (HSCs) produce heterogeneous populations of actively dividing haematopoietic progenitors. To further determine the number of cells with clonogenic progenitor activity from Lin^- cells co-cultured on pLKO.1 control versus *Sfrp2* knockdown stroma, colony forming (CFU) assay was performed (Chapter 3.5.). Counting the colonies ten days after start of clonogenic culture revealed a 1.6-fold higher number of granulocyte/macrophage (GM) colonies formed from cells isolated from co-cultures with *Sfrp2* knockdown stroma. The increase in number of colonies was almost entirely due to granulocyte/macrophage colonies (CFU-GM) as the number of erythroid (BFU-E) and mixed granulocyte/erythroid/macrophage/mega-karyocyte (GEMM) colonies was similar as in cultures on control stromal cells (Figure 10 D).

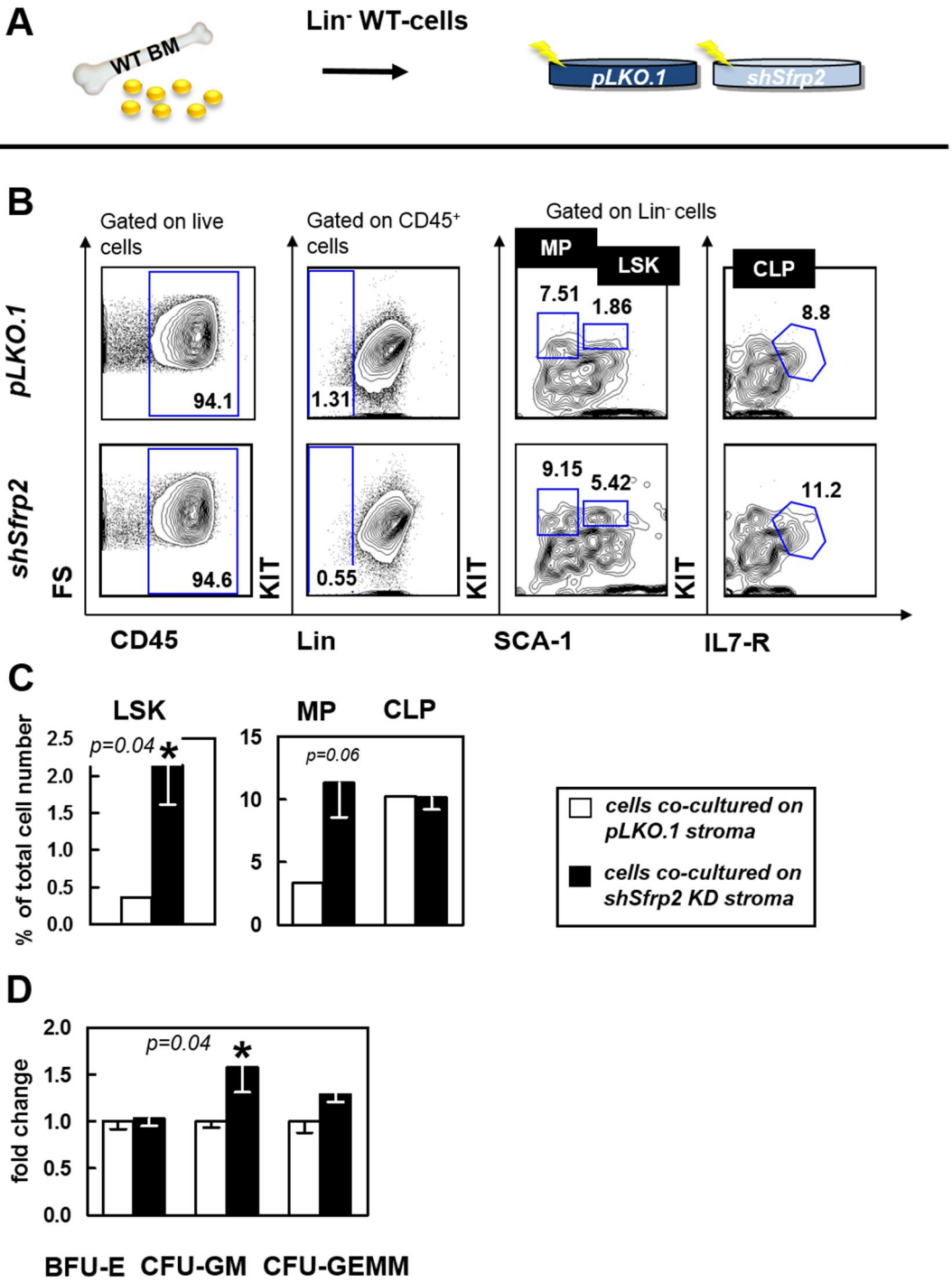

Figure 10. One week co-cultures of Lin- wild type bone marrow cells on UG26-1B6-pLKO.1 control and shSfrp2 knockdown stroma. *(A) Experimental design. (B) Representative FACS plots with gating strategy of CD45+ donor LSKs, myeloid progenitors (MPs) and lymphoid progenitors (CLPs). (C) Percentage of donor LSKs, MPs and CLPs analysed by flow cytometry. (D) Fold change of colonies formed by co-cultured Lin- cells. White bars represent cells co-cultured on UG26-1B6-pLKO.1 control stroma, cells co-cultured on shSfrp2 knockdown stroma are shown in black bars. Mean ± SEM, *p<0.05.*

4.2. Characterization of *Sfrp2* homozygous knockout mice

The *in vitro* data (Chapter 4.1.) together with published *in vivo* data suggest that sFRP-2 positively influences key HSC behaviour: Maintenance of LT-HSC (Nakajima *et al.* 2009) and production of progenitors (Figure 10). To further explore the role of *Sfrp2 in vivo* I studied haematopoiesis in *Sfrp2* knockout mice. *Sfrp2* knockout mice were established and kindly provided by the laboratory of Akihiko Shimono (Satoh *et al.* 2006). To establish this mouse strain, a 14 kb BamHI fragment containing the entire *Sfrp2* coding sequence served as *Sfrp2* targeting construct in the C57BL/6 BAC clone. The vector containing a 5' 2.0 kbAsp718-EcoRI fragment and a 3' 6.5 kb EcoRV-BamHI fragment of the subcloned fragment was electoporated into embryonic stem cells. The identification of homologous recombination events followed the strategy of Shimono and Behringer in 2003 and Satho *et al.,* 2006 (Shimono and Behringer 2003, Satoh *et al.* 2006).

For the studies performed for this thesis, homozygous *Sfrp2* knockout mice (*Sfrp2*$^{-/-}$) mice were bred on a 129S2xBL/6.J (129xBL/6) background. In experimental settings *Sfrp2*$^{-/-}$ were compared to age- and sex-matched wild type 129xBL/6 mice and littermate controls (WT). As it was shown in former studies that sFRP-2 family member sFRP-1 is estrogen inducible in BM stromal cells and influences haematopoiesis (Yokota *et al.* 2008) we decided to analyse male mice exclusively.

4.2.1. Altered distribution of haematopoietic cells in fetal liver

The phenotype of cell populations of HSCs and haematopoietic progenitor cells in E14.5 fetal liver and the bone marrow of adult (eight to ten weeks of age) and middle aged (twelve to 16 months of age) mice was analysed. The fetal liver (FL) is an important haematopoietic tissue. After embryonic day 11.5 (E11.5) haematopoietic stem cells colonize the fetal liver, starting to self-renew and differentiate to lay the foundation of the whole haematopoietic system.

To study the implication of *Sfrp2* deficiency on fetal liver haematopoietic populations, B220 (CD45RA) was used as a marker of B-cell fraction, CD4/CD8a for T-cells, while CD4 is a marker for helper T-cells, CD8a for cytotoxic T-cells. Myeloid populations were separated according to the surface markers Gr-1 and CD11b (Mac-1).

Fetal liver cells were isolated as described in Chapter 3.2. The total cell number of fetal liver was found to be significantly decreased in *Sfrp2*$^{-/-}$ mice compared to wild type controls (Figure 11 upper panel). As total number of mature, progenitor and stem cells is also decreased due to the decrease in total number of FL, alterations in percentage of haematopoietic cell fractions are shown. The percentage of Gr-1^{med} CD11b^{+} monocytes and Gr-1^{+} CD11b^{+} granulocytes gated on non-lymphoid cells (B220^{-}, CD4^{-} CD8a^{-}) was significantly decreased. The percentage of lymphoid fractions B220^{+} B-cells and CD4^{+} CD8a^{+} T-cells respectively, was detected to be unchanged (Figure 11 lower panel).

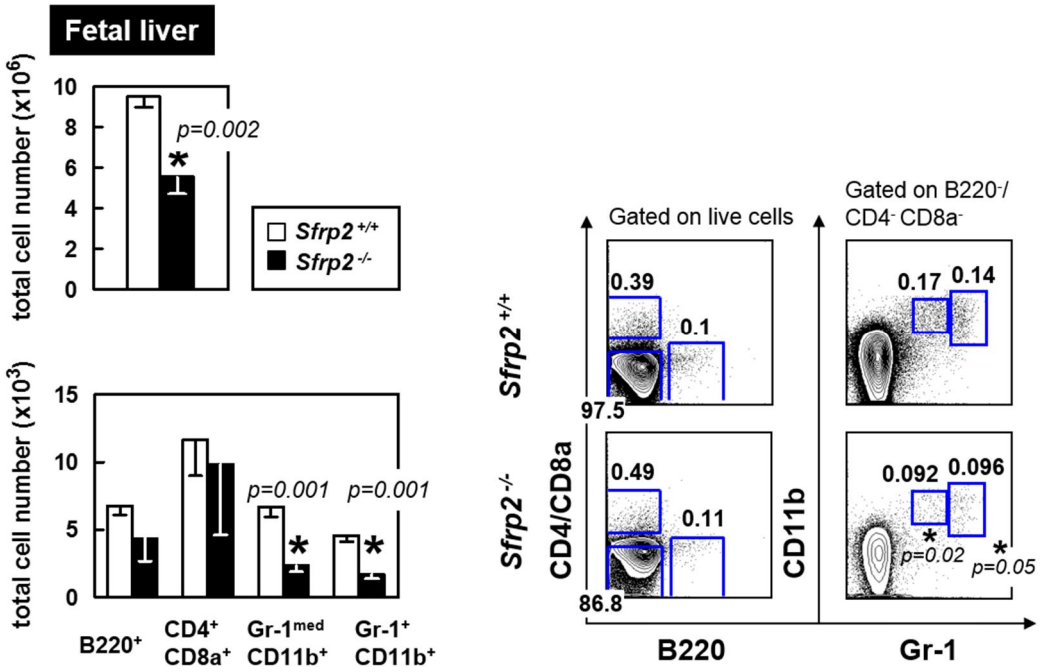

Figure 11. Characterization of haematopoietic cells in fetal liver. *Upper panel: Total cell number of fetal liver in wild type and Sfrp2 knockout mice. Lower panel: Total cell number of B220^{+}, CD4^{+} CD8a^{+}, Gr-1^{med} CD11b^{+}, and Gr-1^{+} CD11b^{+} cells in fetal liver analysed by flow cytometry. Representative FACS plots with gating strategy are shown. White bars represent Sfrp2$^{+/+}$ wild type (WT) littermates (n=6), black bars show Sfrp2$^{-/-}$ knockout (KO) mice (n=6), Mean ± SEM, *p<0.05.*

Alterations in myeloid cell populations might be due to changes in myeloid progenitors ($CD11b^{low}$ Lin^- $SCA\text{-}1^-$ KIT^+ cells) or stem cells ($CD11b^{low}$ Lin^- $SCA\text{-}1^+$ KIT^+ cells) (Figure 12 B). The data revealed a slight but not significant decrease in total LSK cells (Figure 12 A), however, LSKs were present in a significantly increased percentage in *Sfrp2*$^{-/-}$ FL (Figure 12 B). Further, the IL7-R^+ cells (CLPs, Figure 12 B) were found unchanged, myeloid progenitors (MPs) were significantly reduced in total number (Figure 12 A). To further analyse even more primitive cells, the CD34 surface marker was used. The expression of CD34 on HSCs changes during mouse development (Matsuoka *et al.* 2001). While it is expressed on fetal and neonatal HSCs in adult bone marrow and spleen, long-term HSCs in adult mice are characterized by the absence of CD34 on LSK cells (Osawa *et al.* 1996, Goodell *et al.* 1997). Analysing the primitive LSK populations of fetal liver of *Sfrp2*$^{-/-}$ mice compared to wild type controls, the $CD34^+$ LSK were identified to be slightly reduced in total cell number (Figure 12 A) but they were present in a significantly enhanced percentage (Figure 12 B). Taking a closer look at the more committed myeloid progenitor cell fractions, staining for CD16/CD32 (Fc gamma receptor (FcγR)) and CD34 were examined. The absolute cell number of common myeloid progenitors (CMP: $CD34^+$, $CD16/CD32^{low}$) and granulocyte/monocyte progenitors (GMP: $CD34^+$, $CD16/CD32^+$) was unchanged, compared to WT. However, CMPs were present in an increased percentage (Figure 12 C). Further, E14.5 fetal livers from *Sfrp2*$^{-/-}$ embryos showed less megakaryocytic/erythroid progenitors (MEP: $CD34^{low}$, $CD16/CD32^{med}$) in total number and percentage (Figure 12 C).

Thus, in the analysis of fetal liver haematopoiesis, a general decrease in cell number was detected, which is associated with an altered distribution of immature and mature cell populations, particularly of mature myeloid cells, MEPs and $CD34^+$ LSK cells. These results suggest a role of *Sfrp2* in the regulation of haematopoietic stem cells.

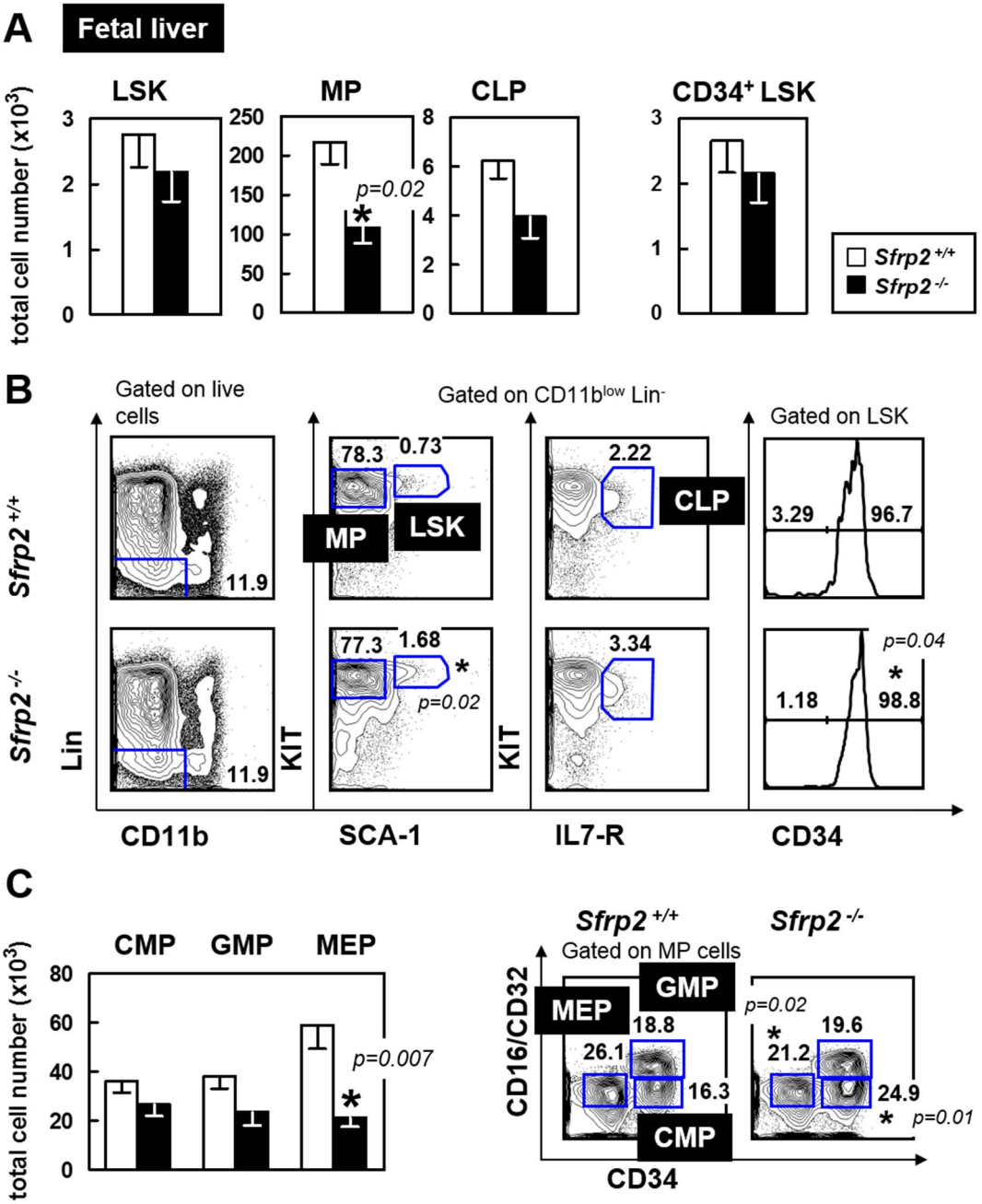

Figure 12. Alterations in early haematopoiesis in fetal liver. *(A) Total cell number of LSKs, MPs, CLPs and CD34⁺ LSK cell populations analysed by flow cytometry. (B) Representative FACS plots and gating strategy of LSKs and progenitors and histogram of CD34⁺ cells gated on LSKs. (C) Total cell number of committed progenitors CMPs, GMPs, MEPs analysed by flow cytometry and representative FACS plots with gating strategy on the right panel. White bars: Sfrp2$^{+/+}$ littermates (n=6), black bars: Sfrp2$^{-/-}$ mice (n=6), Mean ± SEM, *p<0.05.*

4.2.2. Haematopoiesis in adult mice (young): eight to ten weeks old

4.2.2.1. *Decreased number of mature myeloid populations in haematopoietic tissues of eight to ten weeks old Sfrp2$^{-/-}$ mice*

The findings with fetal liver prompted me to study post natal haematopoiesis in adult mice. The isolation of haematopoietic tissues peripheral blood (PB), bone marrow (BM) and spleen was performed as described in Chapter 3.2. A first finding was that in contrast to the above detected decreased number of fetal liver cells, the total cell number in adult haematopoietic organs was similar between WT and *Sfrp2*$^{-/-}$ mice (Figure 13 A). Analysis of PB using the Animal Blood Counter Scil Vet AbcTM showed unchanged results in red blood cells (RBC), haematocrit (HCT) and platelets (PLT) of *Sfrp2* KO mice but a significant decrease in monocytes (WT: 0.27x10^3/µl; *Sfrp2*$^{-/-}$: 0.11x10^3/µl) and granulocytes (WT: 1.59x10^3/µl; *Sfrp2*$^{-/-}$: 0.81x10^3/µl) (Table 15). FACS analysis of PB demonstrated that, in concordance with blood counter data, the percentage of Gr-1^{med} CD11b$^+$ monocytes was significantly decreased, whereas the percentage of Gr-1$^+$ CD11b$^+$ granulocytes and lymphoid fractions remained unchanged in *Sfrp2* knockout mice (Figure 13 C). Further analysis of haematopoietic tissues showed that in bone marrow of *Sfrp2*$^{-/-}$ mice, no alterations were found in myeloid and lymphoid cell populations, whereas in the spleen an increase in the number of CD4$^+$ CD8a$^+$ T-cells was notable (Figure 14 A, B).

B

Table 15: Standard blood count

Peripheral blood	*Sfrp2* $^{+/+}$ (n=18)	*Sfrp2* $^{-/-}$ (n=18)	p value	
WBC (10^3/µl)	4.86 ± 0.58	3.9 ± 0.42	0.225	ns
Lymph (10^3/µl)	3.26 ± 0.41	3.00 ± 0.38	0.651	ns
Mono (10^3/µl)	0.27 ± 0.05	0.11 ± 0.03	0.008	< 0.01
Gran (10^3/µl)	1.59 ± 0.24	0.81 ± 0.13	0.01	< 0.01
Eos (10^3/µl)	4.53 ± 1.45	3.84 ± 0.51	0.675	ns
RBC (10^6/µl)	8.923 ± 0.56	8.33 ± 0.51	0.457	ns
HCT (%)	46.79 ± 2.90	44.32 ±02.67	0.551	ns
PLT (10^3/µl)	1425 ± 98.62	1291.67 ± 156.75	0.486	ns

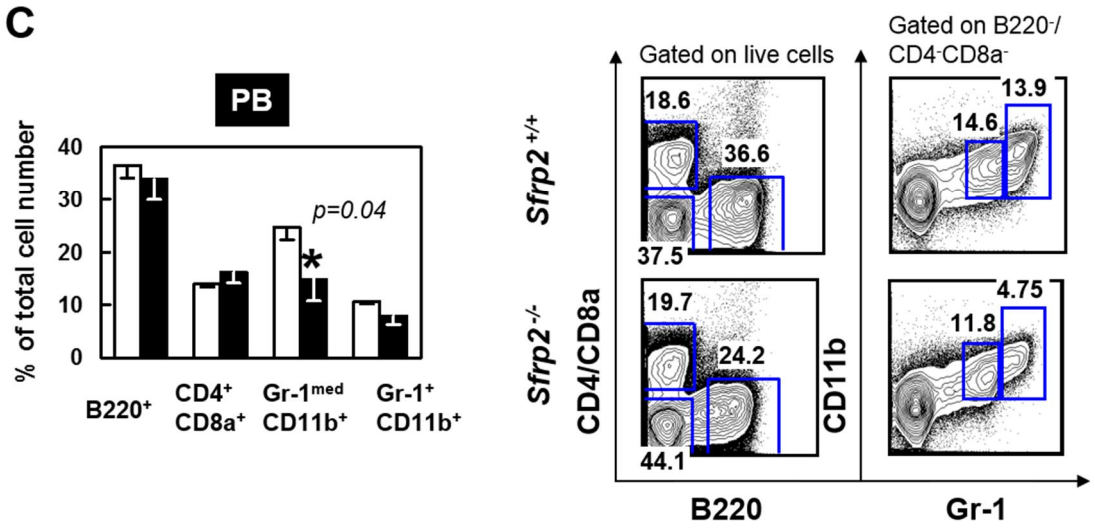

Figure 13. Alterations in steady state haematopoiesis of eight to ten weeks old, adult mice. *(A) Total cell number of peripheral blood (PB) bone marrow (BM), counted of four long bones and spleen. (B) See Table 15. (C) Percentage of total cell number of lymphoid (B220⁺, CD4⁺ CD8a⁺) and myeloid (Gr-1^{med} CD11b⁺, Gr-1⁺ CD11b⁺) cell populations in PB, analysed by flow cytometry, with representative FACS plots (right side). White bars: Sfrp2$^{+/+}$ littermates (n=18), black bars: Sfrp2$^{-/-}$ mice (n=18), Mean ± SEM, *p<0.05.*

Table 15: Standard blood count of *Sfrp2*$^{-/-}$ mice and WT controls.

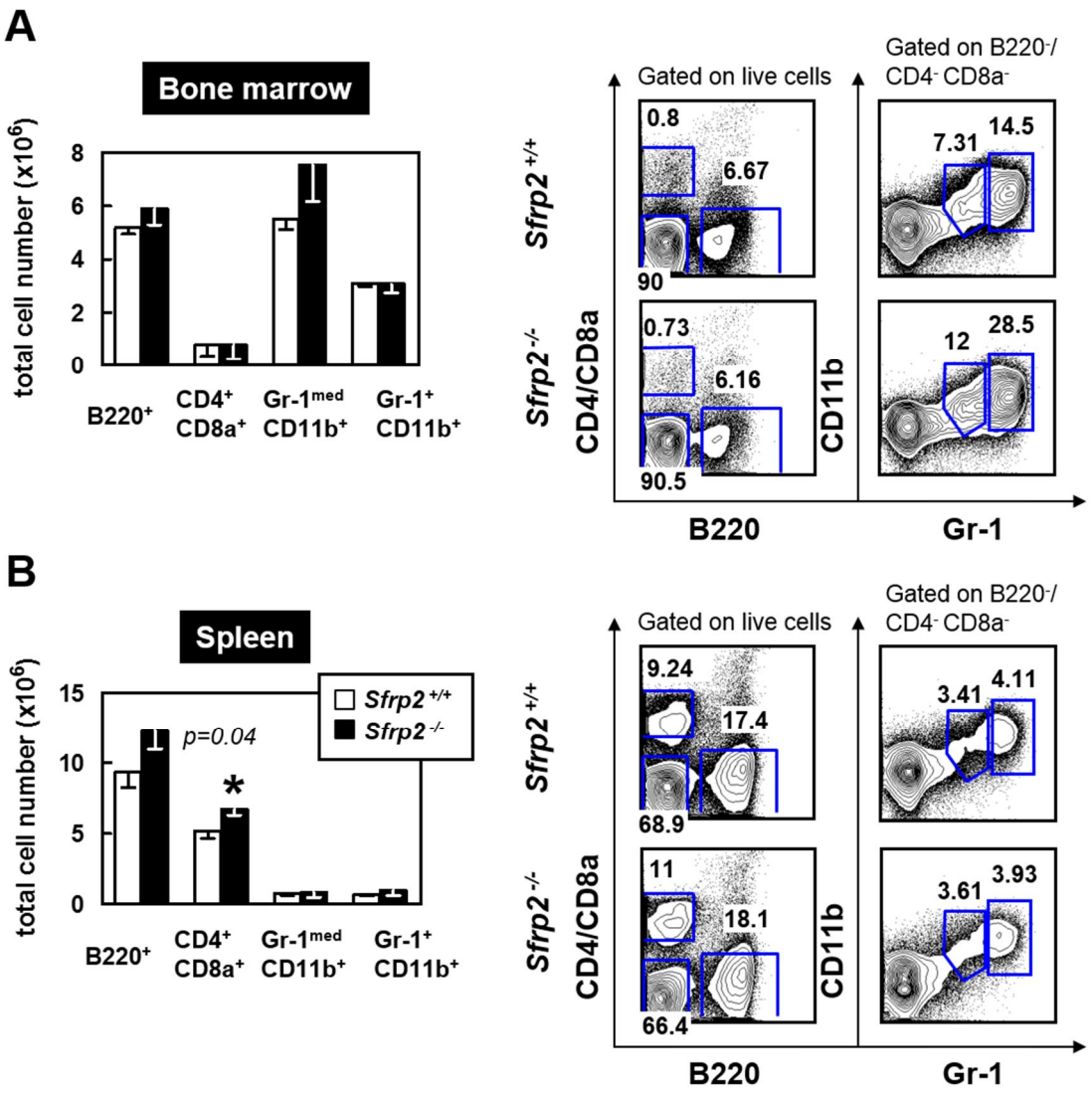

Figure 14. Alterations in steady state haematopoiesis in bone marrow and spleen of eight to ten weeks old, adult mice. *(A) Total cell number of lymphoid (B220$^+$, CD4$^+$ CD8a$^+$) and myeloid (Gr-1^{med} CD11b$^+$, Gr-1$^+$ CD11b$^+$) cell populations in (A) BM, counted of four long bones and (B) spleen, analysed by flow cytometry, with representative FACS plots (right side). White bars: Sfrp2$^{+/+}$ littermates (n=18), black bars: Sfrp2$^{-/-}$ mice (n=18), Mean ± SEM, *p<0.05.*

4.2.2.2. *Decreased number of primitive LSKs and increased clonogenic activity of progenitor cells in bone marrow of Sfrp2$^{-/-}$ mice*

To assess whether alterations in myeloid populations in PB and T-lymphoid populations in the spleen arise from changes in earlier haematopoietic stem and progenitor cells, the number of LSKs, MPs and CLPs was determined in BM and spleen of *Sfrp2$^{-/-}$* mice compared to WT controls. To exclude lymphoid progenitor cells LSK and MP cell populations were gated on Lin$^-$ IL7-R$^-$ fraction. The data exhibited unchanged total

numbers of LSKs and progenitor cells in BM and spleen of knockout mice (Figure 15 A, B and 16 A, B). Further, the more myeloid committed progenitors: CMP, GMP and MEP were unchanged (Figure 15 C and 16 C).

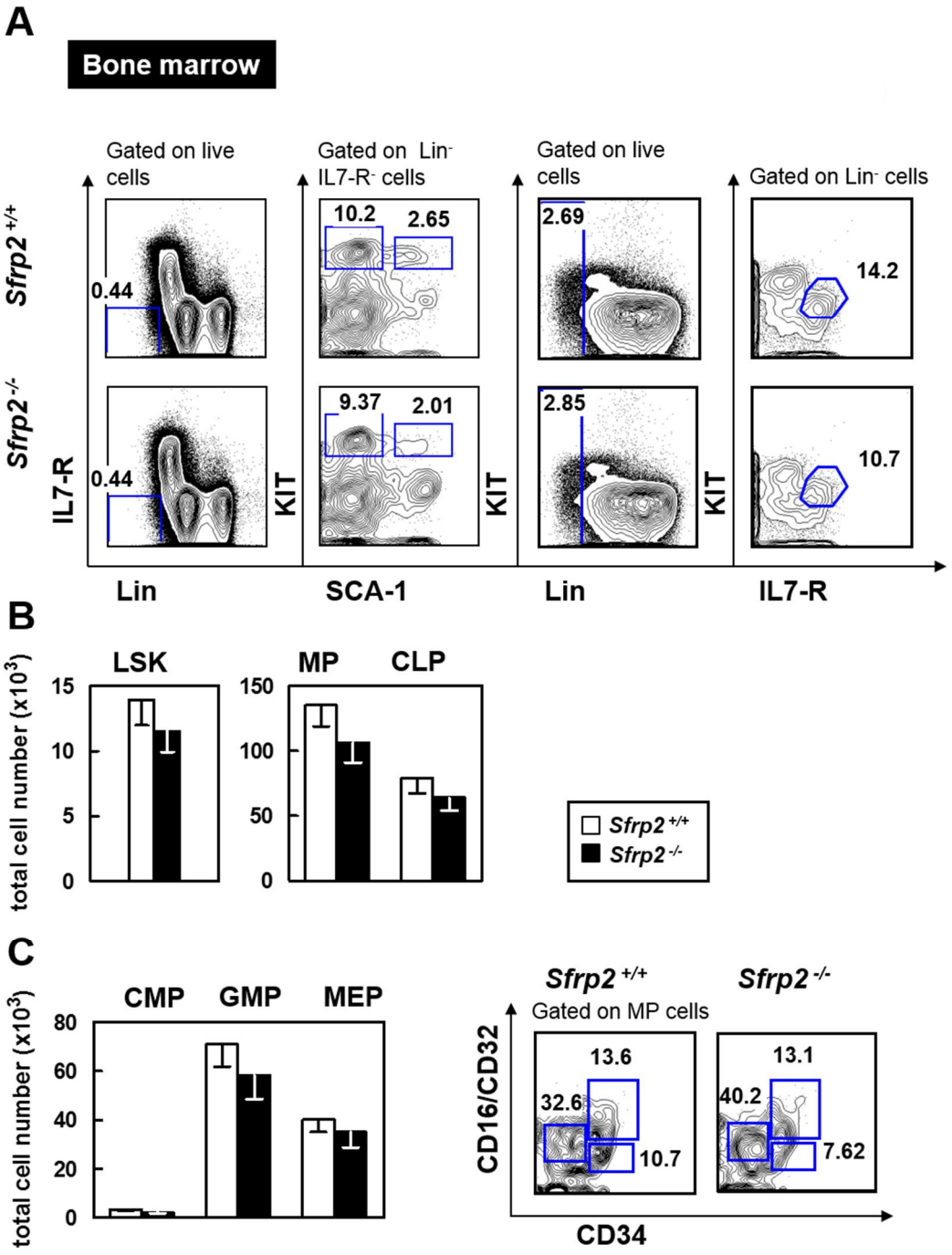

Figure 15. Stem and progenitor cell populations in bone marrow of Sfrp2 KO and WT mice. *(A) Representative FACS plots and gating strategy of LSK, MP and CLP cell populations. (B) Total cell number of LSKs, MPs and CLPs of Sfrp2$^{+/+}$ (n=18) and Sfrp2$^{-/-}$ (n=15). (C) Total cell number of committed CMPs, GMPs and MEPs, Sfrp2$^{+/+}$ (n=12) and Sfrp2$^{-/-}$ (n=8) with representative FACS plots on the right. White bars: Sfrp2$^{+/+}$ littermates, black bars: Sfrp2$^{-/-}$ mice, Mean ± SEM, *p<0.05.*

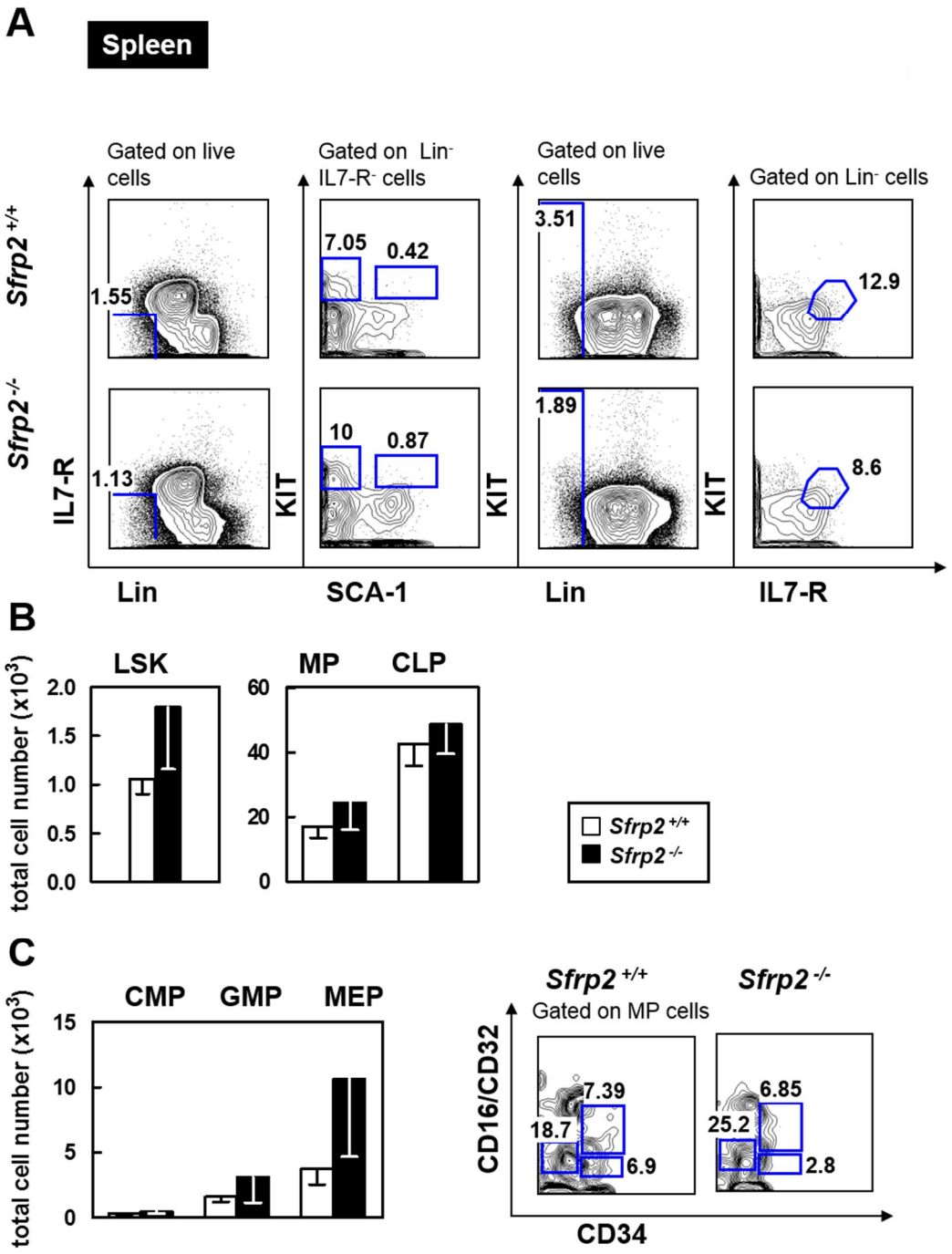

Figure 16. Stem and progenitor cell populations in spleen of Sfrp2 KO and WT mice. *(A) Representative FACS plots and gating strategy of LSK, MP and CLP cell populations. (B) Total cell number of LSKs, MPs and CLPs of Sfrp2$^{+/+}$ (n=13) and Sfrp2$^{-/-}$ (n=15). (C) Total cell number of committed CMPs, GMPs and MEPs, Sfrp2$^{+/+}$ (n=9) and Sfrp2$^{-/-}$ (n=11) with representative FACS plots on the right. White bars: Sfrp2$^{+/+}$ littermates, black bars: Sfrp2$^{-/-}$ mice, Mean ± SEM, *p<0.05.*

To study the earliest cells, the phenotypic population which contains long-term repopulating cells, CD34 and CD150 surface markers were used (Ikuta and Weissman 1992, Osawa *et al.* 1996, Morita *et al.* 2010). This analysis demonstrated a significant

decreased total number of CD34$^-$ CD150$^+$ LSKs in the bone marrow of *Sfrp2* deficient mice (Figure 17 A).

To extend these analyses of phenotype with functional analyses, I investigated the quality of stem and progenitor cells in bone marrow. Similar to the previous *in vitro* data (Chapter 4.1.2.), I observed an increased frequency, and as a result, number of GM colonies formed by haematopoietic progenitor cells of *Sfrp2*$^{-/-}$ mice. This suggests an enhanced progenitor cell activity of mice deficient in *Sfrp2*. As in the *in vitro* studies (Figure 10 D), the number of BFU-E and CFU-GEMM colonies was unchanged (Figure 17 B).

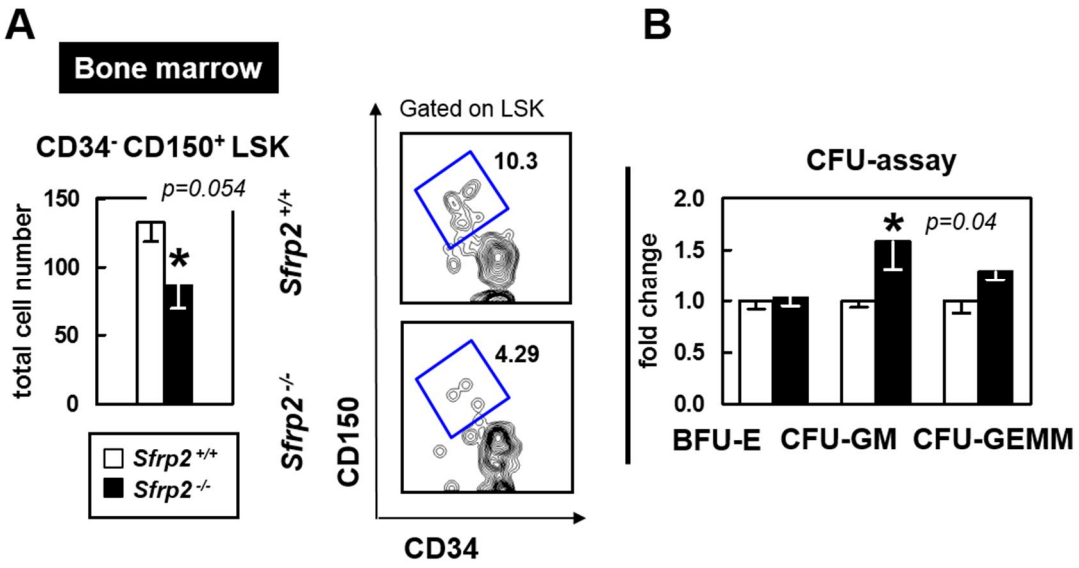

Figure 17. Alterations in primitive LSK cells in bone marrow of Sfrp2 KO and WT mice and clonogenic activity. *(A) Total cell number of long-term HSC-like CD34$^-$ CD150$^+$ LSKs of Sfrp2$^{+/+}$ (n=7) and Sfrp2$^{-/-}$ mice (n=7) with representative FACS plots. (B) Fold change of colonies formed by 25,000 BM cells of Sfrp2$^{+/+}$ littermates (n=6) and Sfrp2$^{-/-}$ mice (n=8). White bars: Sfrp2$^{+/+}$, black bars: Sfrp2$^{-/-}$ mice, Mean ± SEM, *p<0.05.*

4.2.3. Increased HSCs and progenitor cells in middle aged mice: twelve to 16 months old

In aging mice, HSCs undergo various changes affecting them quantitatively and qualitatively which is reviewed by Waterstrat and Van Zant (Waterstrat and Van Zant 2009). The number of phenotypical CD34$^-$ CD150$^+$ LSK cells increases, but at the same time, their functional repopulating activity decreases. In addition, with age, lymphoid

potential is lost, and the population of myeloid repopulating cells becomes dominant (Beerman *et al.* 2010). Dykstra and colleagues also observed a reduction in homing efficiency and long-term repopulation potential as well as a delayed proliferative activity in old HSCs (Dykstra *et al.* 2011).

As data suggested a decrease of primitive $CD34^{-}CD150^{+}$ LSKs in *Sfrp2* KO mice (Figure 17), it could be hypothesised that the number of functional long-term repopulating stem cells might be further reduced in aged mice.

In experiments with “middle aged” twelve to 16 months old mice an unchanged numbers of total BM cells, spleen cells and PB was observed in *Sfrp2* knockout mice compared to wild type controls (Figure 18 A). In additions, the results exhibited no alterations in mature cell number of PB and spleen. But, a striking increase in the number of BM monocytes and granulocytes could be detected, whereas, as in younger mice, B- and T-cells were unchanged (Figure 18 B-D).

Analysis of bone marrow progenitor cells in the middle aged mice showed a significantly increased number of myeloid progenitors (MPs) in *Sfrp2* knockout mice, which is in line with the developing myeloid dominance during aging, whereas lymphoid progenitors (CLPs) remained unchanged (Figure 19 A). To find out whether changes in mature and progenitor cells are due to stem cell alterations, subpopulations of LSKs were studied. Indeed, significantly increased numbers were found in LSKs as well as in long-term ($CD34^{-}CD150^{+}$ LSKs) stem cells (Figure 19 A, B). Figure 19 C describes the rise of LSKs from fetal liver to the adult system in both *Sfrp2* KO and WT mice. Interestingly, data suggests that the absolute number of LSKs in wild type mice is decreasing during the process of aging, while the total number of LSKs in $Sfrp2^{-/-}$ mice remains almost the same in the aged mice compared to young adult ones. This could be due to an enhanced maintenance or increased activation of stem cells in $Sfrp2^{-/-}$ mice (Figure 19 C).

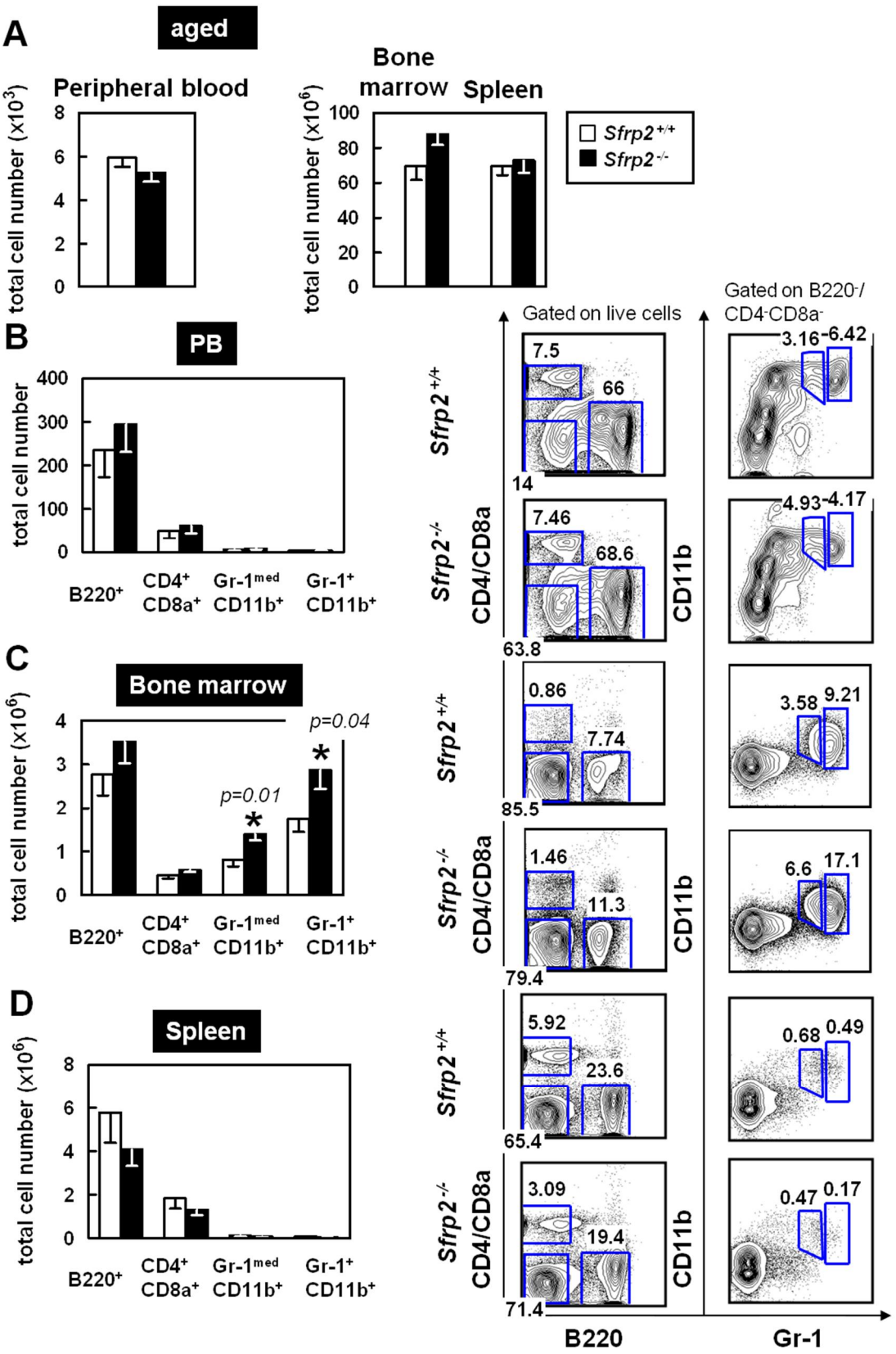

Figure 18. Alterations in haematopoiesis of twelve to 16 months old, middle aged mice. *(A) Total cell number of PB, BM and spleen. (B-D) Total cell number of lymphoid (B220⁺, CD4⁺ CD8a⁺) and myeloid (Gr-1^{med} CD11b⁺, Gr-1⁺ CD11b⁺) cell populations in (C) PB of Sfrp2$^{+/+}$ littermates (n-19) and Sfrp2$^{-/-}$ (n=18), (D) BM of Sfrp2$^{+/+}$ (n-11) and Sfrp2$^{-/-}$ (n=11) and (E) spleen of Sfrp2$^{+/+}$ (n-5) and Sfrp2$^{-/-}$ (n=6), analysed by flow cytometry. White bars: Sfrp2$^{+/+}$, black bars: Sfrp2$^{-/-}$ mice, Mean ± SEM, *p<0.05.*

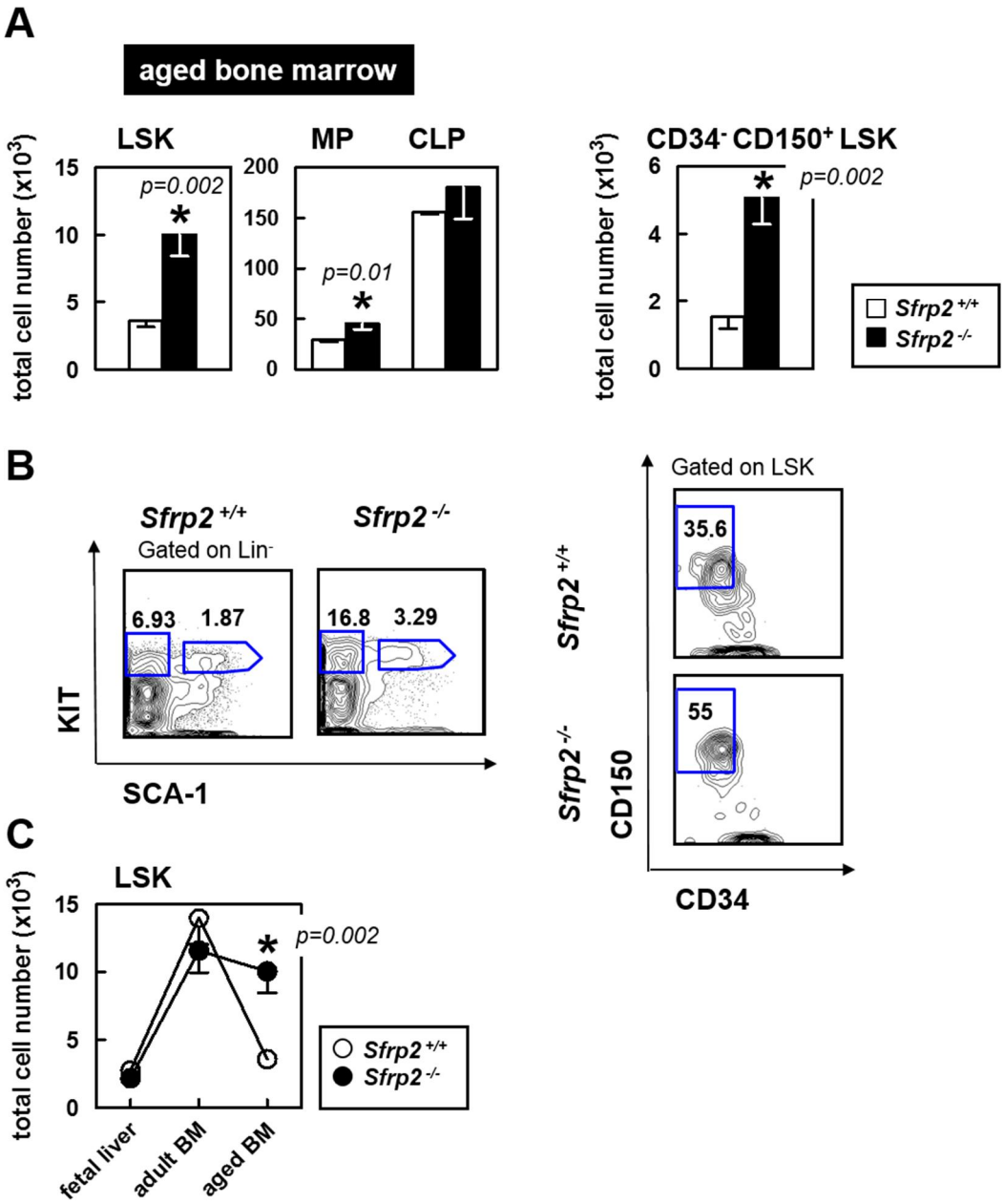

Figure 19. Alterations of stem and progenitor cell populations in bone marrow of aged Sfrp2 KO and WT mice and cellularity of fetal liver, adult BM and aged BM. *(A) Total cell number of LSKs, MPs, CLPs and CD34⁻ CD150⁺ LSK cell populations of Sfrp2$^{+/+}$ (n=13) and Sfrp2$^{-/-}$ (n=15) with (B) representative FACS plots. (C) Comparison of total LSK number of fetal liver, BM of adult and BM of aged mice. White bars: Sfrp2$^{+/+}$ littermates, black bars: Sfrp2$^{-/-}$ mice, Mean ± SEM, *p<0.05.*

4.2.4. Alterations of mesenchymal stromal/stem cells (MSCs) due to *Sfrp2* deficiency

Haematopoietic stem cells reside within an anatomical compartment, the haematopoietic niche. This microenvironment, a composition of different cell types, regulates the maintenance of HSCs and controls their self-renewal, survival, differentiation and

proliferation (Fuchs *et al.* 2004, Morrison and Spradling 2008, Garrett and Emerson 2009, Nagasawa *et al.* 2011). *Sfrp2* was shown to be expressed in osteoblasts and it plays an important role in maintenance and regulation of HSCs (Nakajima *et al.* 2009, Roux 2010).

So far, investigations of the thesis were focused on alterations of haematopoietic stem, progenitor and mature cells themselves in the absence of sFRP-2. To examine the influence of *Sfrp2* deficiency on the composition and cell number of niche cells (Figure 20 A), mesenchymal stromal/stem cells (MSCs) osteoblastic cells (OBCs) and sinusoidal endothelial cells were analysed according to a reported staining strategy which is shown in Figure 20 C. For this purpose, the four long bones (tibia and femur) of *Sfrp2*$^{-/-}$ and control mice were flushed and the bone fragments digested with collagenase to isolate the endosteal and perivascular cells of bone marrow niche. The procedure is described in detail in Chapter 3.2. In brief, the two fractions (flushed and digested) were then combined and MSCs, OBCs and endothelial cells were separated corresponding to their surface markers following the gating strategy of Nakamura *et al.* and analysed by flow cytomertry (Nakamura *et al.* 2010). CD45^{-} TER119^{-} PECAM-1^{+} SCA-1^{+} fraction represents endothelial cells. In PECAM-1^{-} fraction osteoblasts are defined as ALCAM^{+}, mesenchymal stromal/stem cells are SCA-1^{+} ALCAM^{med} (Figure 20 C).

The total number of MSCs, OBCs and endothelial cells were unchanged in *Sfrp2* knockout mice, although data suggested a trend of an enhanced MSC number in the knockouts (Figure B).

Further, the clonogenic activity of MSCs was analysed. Therefore CD45^{-} TER119^{-} PECAM-1^{-} SCA-1^{+} sorted MSCs of *Sfrp2*$^{-/-}$ and wild type mice were cultured for ten days (Figure 21 A). The formed colonies were counted and found unchanged, suggesting no alterations in the number of CFU-F, or their proliferation potential (Figure 21 B left side).

Interestingly, however, cultured *Sfrp2*$^{-/-}$ MSCs seemed to accelerate their proliferation from passage two to three (Figure 21 B right side), suggesting an increased growth rate.

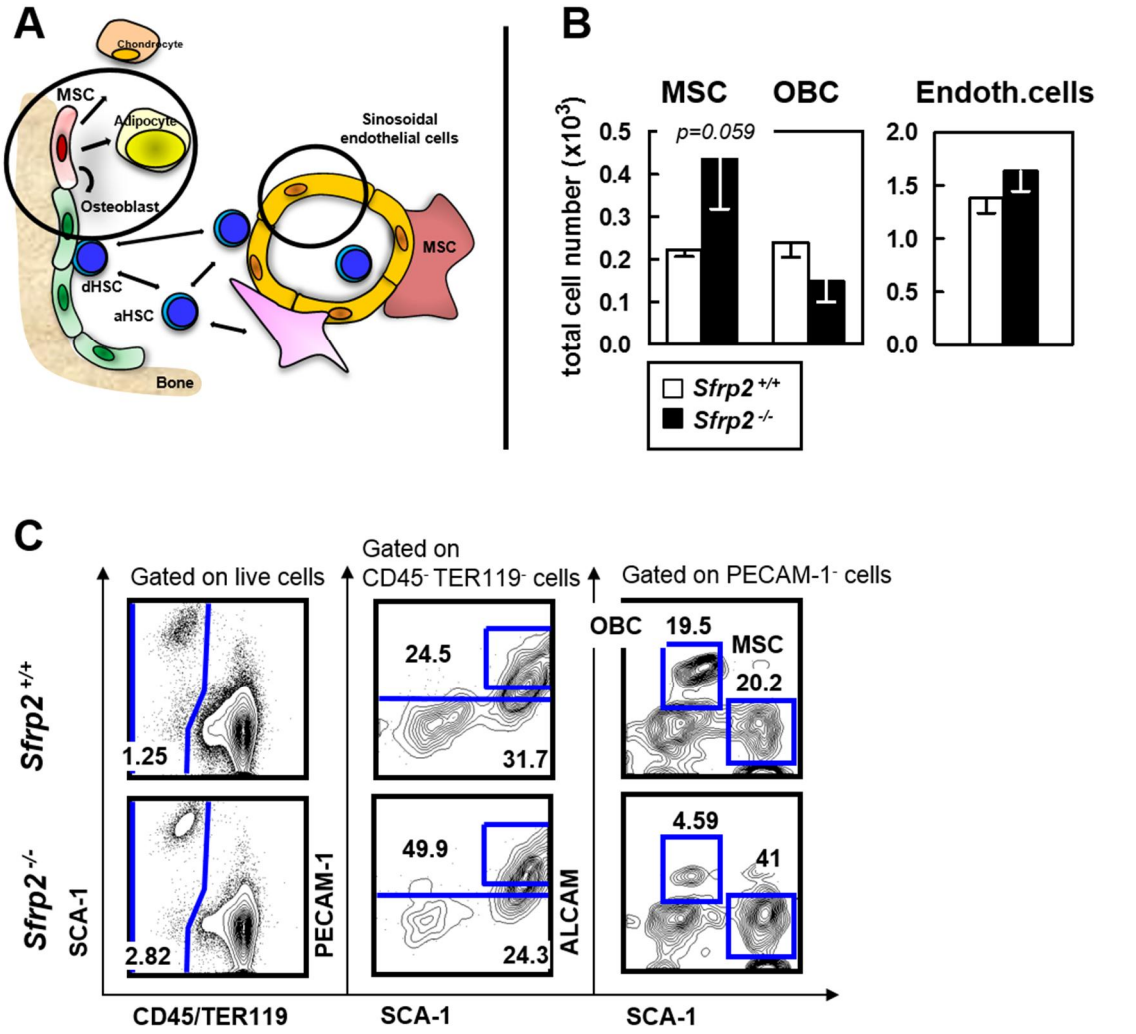

Figure 20. Niche cell types in Sfrp2 KO and WT mice. *(A) Composition of bone marrow niche. (B) Total cell number of mesenchymal stromal/stem cells (MSCs) osteoblasts (OCBs) and sinusoidal endothelial cells. (C) Representative FACS plots and gating strategy of niche cells. White bars: Sfrp2*$^{+/+}$ *littermates (n=9), black bars: Sfrp2*$^{-/-}$ *mice (n=8), Mean ± SEM, *p<0.05.*

MSCs have the potential to differentiate into osteoblasts, adipocytes or chondrocytes (Figure 20 A). To analyse the effect of *Sfrp2* deficiency on the differentiation capability of MSCs, osteogenic and adipogenic differentiation was induced (Chapter 3.9.). Interestingly, data showed a decreased number of Oil Red O-positive cells (indicative of cells with lipid vesicles) after adipogenic induction. The Von Kossa stain (indicative of cells with mineralizing calcium) was unchanged, indicating an unchanged differentiation potential into osteoblasts compared to wild type controls (Figure 21 C). Thus, the data

shows that *Sfrp2* may be required for adipogenic differentiation of MSCs, but does not influence the generation of osteoblasts.

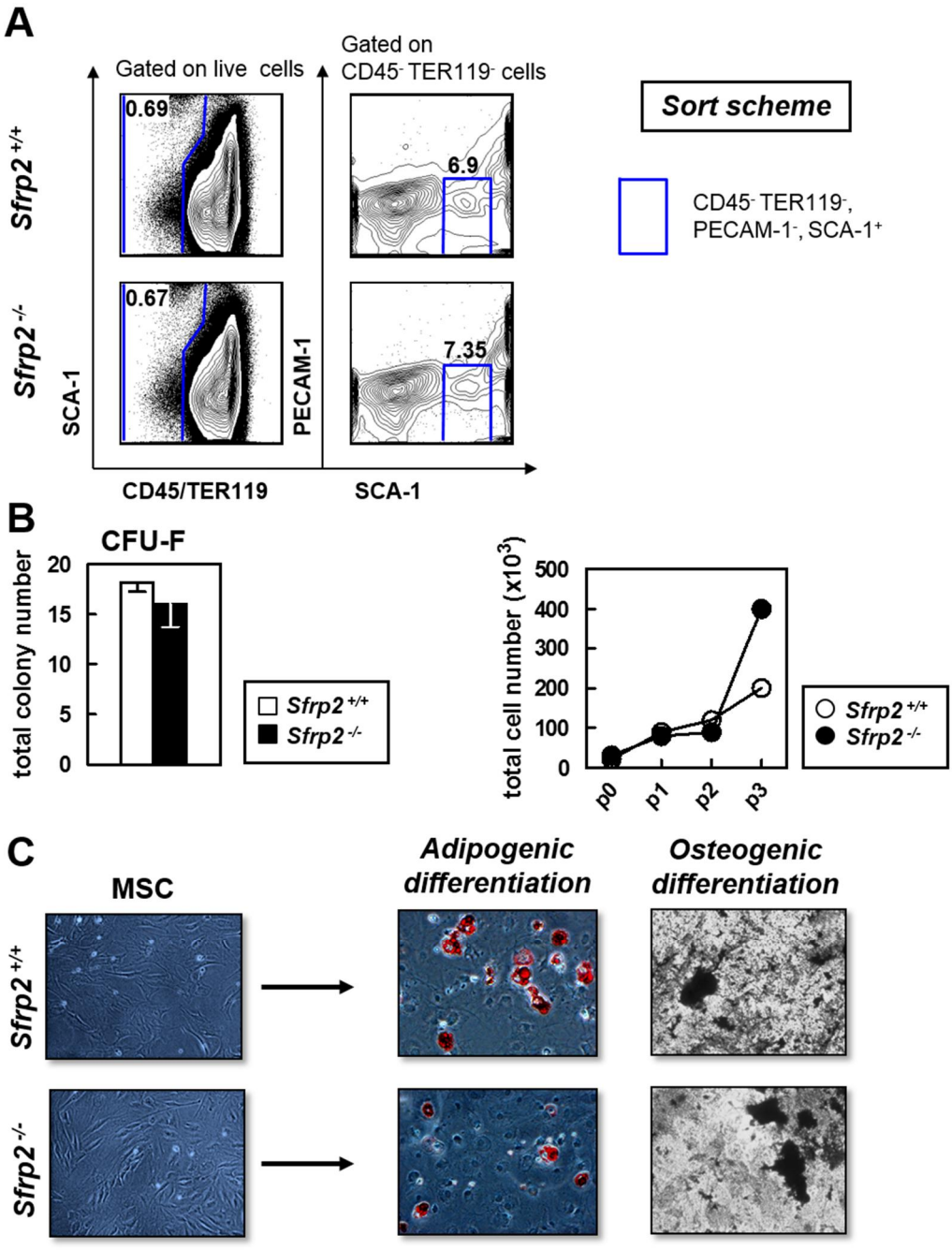

Figure 21. CFU-F and differentiation potential of MSCs. *(A) Sort scheme of MSCs (CD45- TER119- PECAM-1- SCA-1+) of WT and Sfrp2 KO mice. (B) Left panel: Total number of colonies formed by MSCs after ten days (CFU-F). Right panel: Growth curve of MSCs passage 0 (p0) to p3. (C) Adipogenic and osteogenic differentiation of MSCs, magnification x10. White bars and white circles: Sfrp2+/+ littermates (n=6), black bars and circles: Sfrp2-/- mice (n=6), Mean ± SEM.*

4.3. Decreased Wnt signalling activity in HSCs in the absence of sFRP-2

Wnt signalling was reported to be essential for blood cell production (Austin *et al.* 1997, Van Den Berg *et al.* 1998). Signalling through the catenin-dependent canonical Wnt pathway has been shown to be important for the regulation of HSC proliferation and cell-fate decisions (Kirstetter *et al.* 2006, Scheller *et al.* 2006, Nemeth *et al.* 2007). Non-canonical signalling cross-talks to the canonical pathway, and it was shown that Wnt-5a may inhibit catenin-dependent signalling, resulting in enhanced repopulating ability (Nemeth *et al.* 2007). Recently, Sugimura and colleagues showed that non-canonical Wnt signalling plays an essential role maintaining HSCs within their niche through stimulation of the Flamingo receptor (Sugimura *et al.* 2012). Further, Florian and group described a switch from canonical to non-canonical signalling in aged mice (Florian *et al.* 2013).

Secreted frizzled-related proteins play a role as regulators of Wnt signalling pathway (Kawano and Kypta 2003). SFRP-2 can directly bind to Wnt molecules and thus regulate the interaction of Wnts with canonical and non-canonical Frizzled (Fz) receptors (Suzuki *et al.* 2004).

The aim of the following experiments was to investigate the effect of *Sfrp2* deficiency on canonical and non-canonical Wnt signalling in LSK and progenitor cell populations isolated from *Sfrp2*$^{-/-}$ mice. For this purpose, I sorted LSKs, myeloid and lymphoid progenitor cells (MPs, CLPs) of eight to ten weeks old (young) mice. Since only small cell numbers can be isolated, I did not perform Western blot, but fixed 500 to 1000 cells on slides and stained candidates of Wnt signalling using immunofluorescence. The nuclei were counterstained with DAPI and protein expression was analysed by fluorescent microscope as described in detail in Chapter 3.4.

Canonical Wnt signalling

Firstly, members of Wnt/Beta-catenin signalling were investigated. In this pathway, Wnt ligand binds to Fz receptor, Dishevelled (DVL) then recruits GSK-3 beta to the cell

membrane. That results in the dissolution of a GSK-3 beta, Axin, APC complex, which, under non-stimulated conditions facilitates the phosphorylation and degradation of Beta-catenin. In the stimulated active state, Beta-catenin is stabilized, because its phosphorylation does not occur, and it can translocate to the nucleus, where it displaces the repressor Grouch from the transcription factor TCF allowing the recruitment of co-activators. The resulting activated transcription complex then initiates the expression of target genes such as Cyclin-D1 and c-Myc (Clevers and Nusse 2012) (Figure 2).

Compared to the wild type controls, the protein level of DVL-2, GSK-3 beta and Beta-catenin was significantly decreased in LSKs of *Sfrp2* KO mice. A decreased level of Beta-catenin suggests a decreased expression of target genes, which was confirmed examining Cyclin-D1 and c-Myc which both exhibited a decreased protein level (Figure 22 A, B and 23). In line with the results of a decreased Beta-catenin an increased level of phosphorylated Beta-catenin was found, indicating enhanced activity of the catenin destruction complex (Figure 22 A, B).

In myeloid and lymphoid progenitors the protein level of catenin-dependent Wnt signalling members was also decreased: The MPs exhibited a significantly lower level of DVL-2, GSK-3 beta, Beta-catenin and, surprisingly, also its phosphorylated state (Phospho-Beta-catenin) (Figure 22 C), suggesting catenin stability is regulated through other pathway members in MPs. Interestingly Cyclin-D1 (Figure 22 C) and c-Myc (Figure 23) expression level was significantly higher in MPs of *Sfrp2* KO mice compared to wild type control myeloid progenitors, suggesting that transcription of these targets may not depend solely on catenin, as we also found previously in $Ptn^{-/-}$ mice (Istvanffy *et al.* 2011). This may point to a cross-reaction with non-canonical Wnt signalling or other pathways or possible regulations on transcriptional level. In CLPs, results showed a significantly decreased level of DVL-2, Beta-catenin, Phospho-Beta-catenin and a highly decreased expression of c-Myc protein (Figure 22 C and 23). In addition, since the proliferation regulator c-Myc is increased in MPs and decreased in CLPs, the loss of *Sfrp2* may regulate myeloid-lymphoid cell fate decisions.

The observation that Beta-catenin-dependent Wnt signalling in stem and progenitor cells is reduced in *Sfrp2* knockout mice suggests a role of sFRP-2 as an activator for canonical Wnt signalling, perhaps in a similar manner as we observed for sFRP-1 (Renstrom *et al.* 2009).

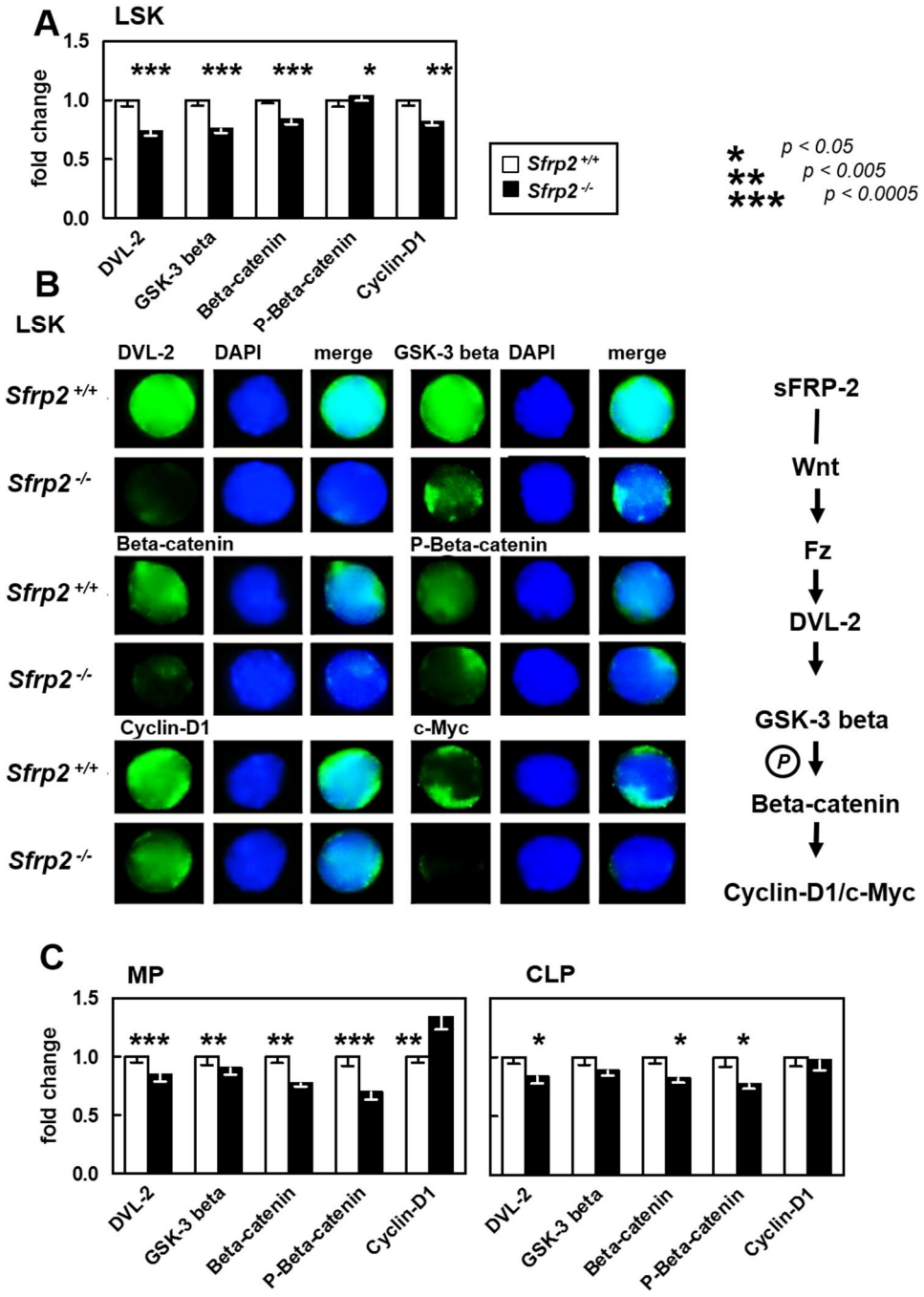

Figure 22. Protein level of candidates of Beta-catenin-dependent Wnt signalling in stem and progenitor cells of Sfrp2 KO and WT mice. *(A) Fold change of quantification of protein level of DVL-2, GSK-3 beta, Beta-catenin, Phospho-Beta-catenin and Cyclin-D1 of pooled and sorted LSKs of Sfrp2 KO and WT mice. (B) Representative pictures of single cell staining (LSKs) of DVL-2, GSK-3 beta, Beta-catenin, Phospho-Beta-catenin and c-Myc with primary rabbit anti-mouse antibodies and secondary FITC-labelled antibodies (left side), the nuclear counterstaining with DAPI (middle) and merge of both (right). For Cyclin-D1 staining a fourfold chain was used with primary anti-Cyclin-D1 rabbit anti-mouse antibody, second: Alexa Fluor488 goat anti rabbit, third: anti-Alexa Fluor rabbit, fourth: anti-rabbit FITC-labelled antibody. (C) Fold change of protein level of Beta-catenin-dependent Wnt signalling candidates in sorted MP and CLP populations. White bars: Sfrp2$^{+/+}$ littermates, black bars: Sfrp2$^{-/-}$ mice. Data were generated of two independent experiments with n=4 each. For quantification 20 cells were snapped on Leica fluorescent microscope, magnification x100. Total pixel were quantified by ImageJ software. Mean ± SEM, *p<0.05, **p<0.005, ***p<0.0005.*

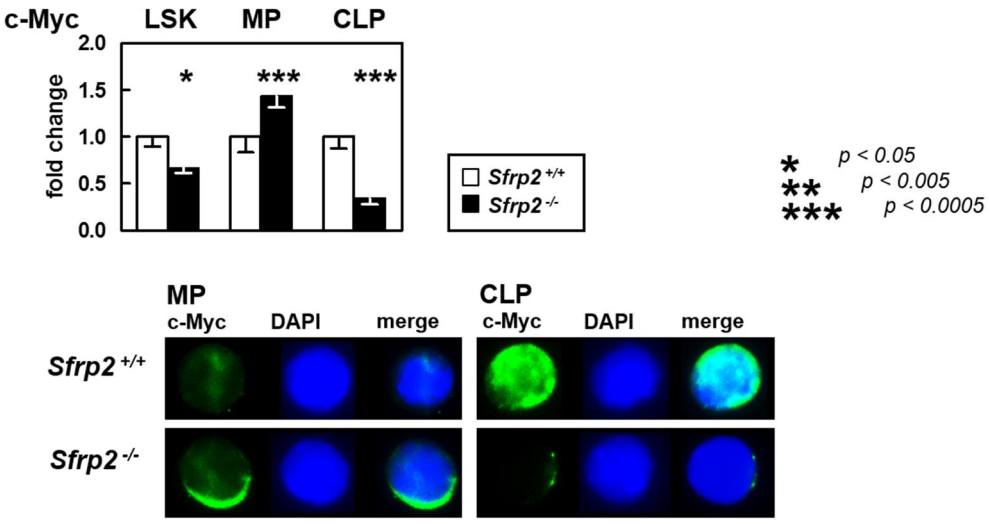

Figure 23. Protein level of canonical Wnt signalling pathway target c-Myc in sorted LSK and progenitor cells of Sfrp2 KO and WT mice. *Fold change of quantification of protein level of c-Myc in LSKs MPs and CLPs with representative pictures of single cell staining (MPs and CLPs) of c-Myc with primary rabbit anti-mouse antibodies and secondary FITC-labelled antibodie (left side), the nuclear counterstaining with DAPI (middle) and merge of both (right side). White bars: Sfrp2$^{+/+}$ littermates, black bars: Sfrp2$^{-/-}$ mice. Data were generated of two independent experiments with n=4 each. For quantification 20 cells were snapped on Leica fluorescent microscope, magnification x100. Total pixel were quantified by ImageJ software. Mean ± SEM, *p<0.05, **p<0.005, ***p<0.0005.*

Non-canonical Wnt signalling

In a second series of immunofluorescence experiments, signalling intermediates associated with the Ca^{2+}-dependent Wnt signalling pathway were analysed, which regulates C/EBP-alpha and PPAR-gamma through NF-ATc. In brief, Wnt binding to non-canonical Fz receptors leads to a release of Ca^{2+} (Florian *et al.* 2013), which triggers the activation of Ca^{2+} sensitive proteins: PKC, calcineurin, and the Ca^{2+}-calmodulin-dependent Kinase (CaMK-II). Calcineurin dephosphorylates NF-ATc which then translocates to the nucleus, where it regulates gene expression. The Ca^{2+}-dependent pathway also cross-talks with canonical Wnt signalling by inhibiting the Beta-catenin-TCF/LEF transcription complex through the CaMK-II TGF-beta activated Kinase1 (TAK1), Nemo like Kinase (NLK) signalling cascade (Yamada *et al.* 2006, Lv *et al.* 2014) (Figure 2). In *Sfrp2*$^{-/-}$ LSK cells, both CaMK-II and its activated form Phospho-CaMK-II (Thr286) protein levels were increased while the level of NLK was unchanged.

Interestingly the protein expression level of NF-ATc was highly decreased, which correlated with the results of decreased PPAR-gamma protein level (Figure 24 A, B).

Further, data indicate a decreased expression level of NF-ATc and C/EBP-alpha in myeloid progenitors. The additional decreased level of NLK might be linked to the enhanced protein level of canonical target genes c-Myc and Cyclin-D1 in MPs, as NLK inhibits Beta-catenin-dependent Wnt signalling. In contrast to LSK cells, the protein level of PPAR-gamma was highly increased in MPs (Figure 24 C). In lymphoid progenitors, an enhanced level of CaMK-II was found, but at the same time, the level of NLK was strongly decreased (Figure 24 C).

Figure 25 summarizes the results of protein level alterations of LSKs in canonical and non-canonical Wnt signalling and taken together, in LSK cells of adult mice the absence of sFRP-2 seems to result in a decrease of both canonical and non-canonical Wnt signalling activity.

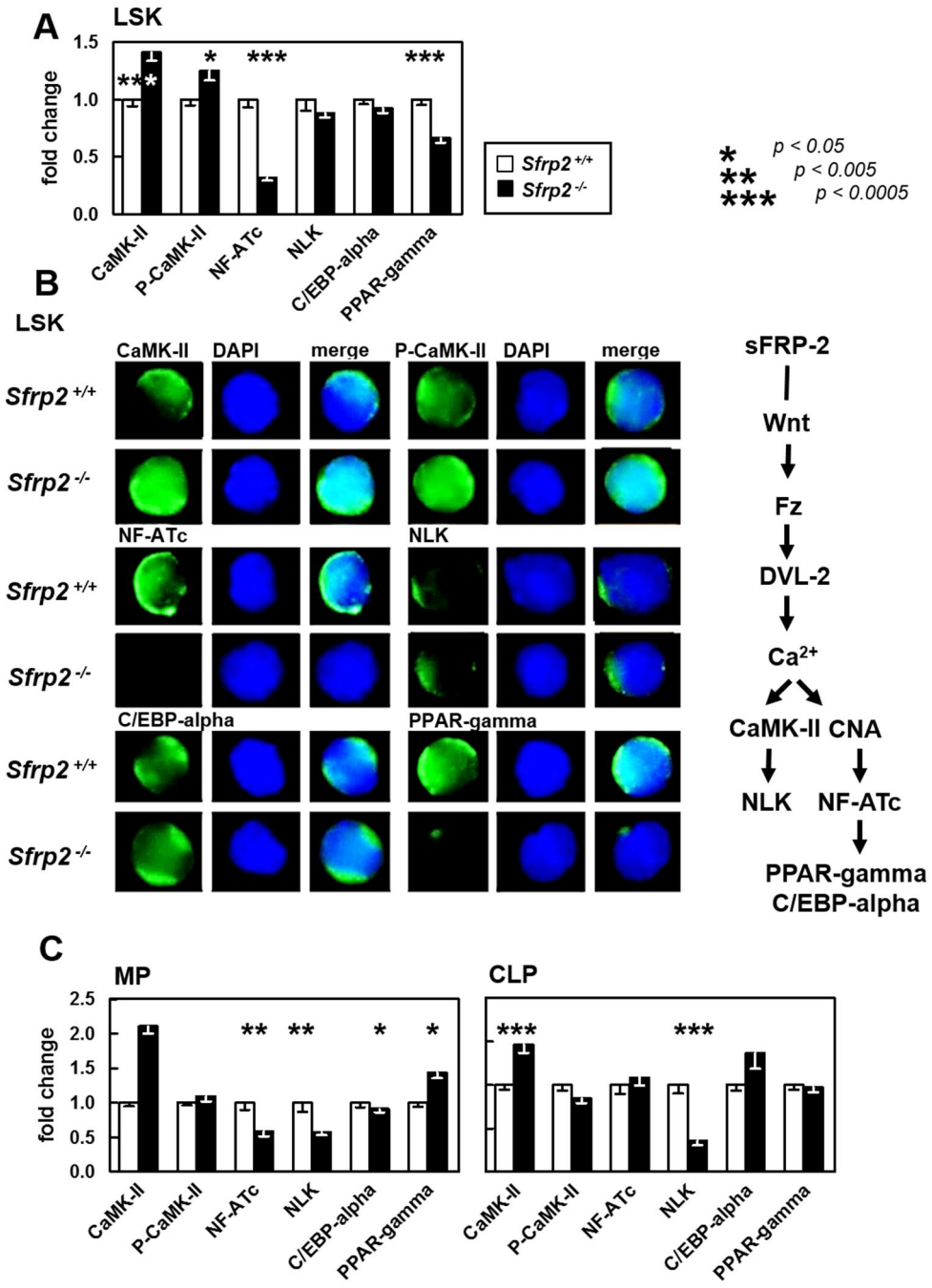

Figure 24. Protein level of candidates of Ca2+-dependent Wnt signalling in stem and progenitor cells of Sfrp2 KO and WT mice. *(A) Fold change of quantification of protein level of CaMK-II, P-CaMK-II, NLK, NF-ATc, PPAR-gamma and C/EPB-alpha in sorted LSKs of Sfrp2 KO and WT mice. (B) Representative pictures of single cell staining (LSKs) of CaMK-II, P-CaMK-II, NLK, PPAR-gamma and C/EPB-alpha with primary rabbit anti-mouse antibodies and secondary anti-rabbit FITC-labelled antibodies (left side), the nuclear counterstaining with DAPI (middle) and merge of both (right). NF-ATc primary antibody: mouse polyclonal antibody, second: Alexa Fluor488 goat anti-mouse, third: anti-Alexa Fluor rabbit, fourth: anti-rabbit FITC-labelled antibody. (C) Fold change of protein level of Ca^{2+}-dependent Wnt signalling candidates in sorted MP and CLP populations. White bars: $Sfrp2^{+/+}$ littermates, black bars: $Sfrp2^{-/-}$ mice. Data were generated of two independent experiments with n=4 each. For quantification 20 cells were snapped on Leica fluorescent microscope, magnification x100. Total pixel were quantified by ImageJ software. Mean ± SEM, *p<0.05, **p<0.005, ***p<0.0005.*

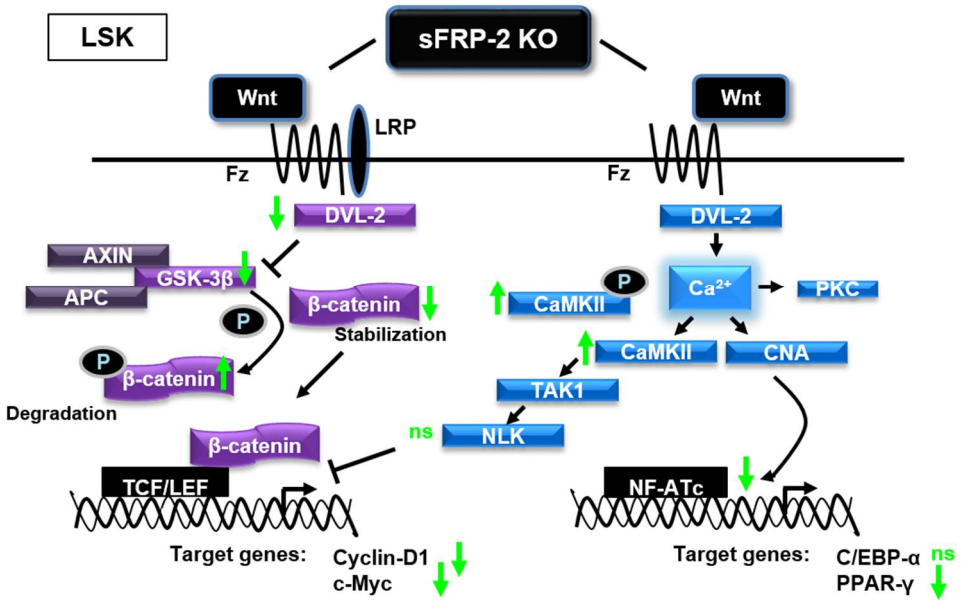

Figure 25. Alteration of protein level of Wnt signalling pathway in LSKs of Sfrp2 KO mice. *Candidate proteins of catenin-dependent Wnt signalling are shown in violet, proteins of Ca^{2+}-dependent Wnt signalling in blue. Green arrows represent the protein level in Sfrp2 KO in comparison to WT.*

4.4. Proliferation and stress-induced activation of HSC

The decreased number of long-term HSC-like $CD34^-$ $CD150^+$ LSKs in adult *Sfrp2* deficient mice and the decreased protein level of the critical cell cycle regulator Cyclin-D1, which is a target of canonical Wnt signalling, suggest a role for *Sfrp2* in cell cycle regulation of LSK and progenitor cells.

Haematopoietic stem cells are mostly present in a quiescent state in the niche (G0 phase) and divide only about five times per life. In events of haematopoietic stress, like infection, wounding, irradiation or chemical reagents, dormant HSCs are activated (G1 phase) to self-renew or differentiate to provide an appropriate amount of mature blood cells required for the challenge posed to the blood cell system (Wilson *et al.* 2008, Trumpp *et al.* 2010). The entry of HSCs into cell cycle is regulated by intrinsic factors and the microenvironment, respectively.

4.4.1. Decreased cell cycling activity of LSKs due to *Sfrp2* deficiency

To get insights into whether alterations in cell cycling behaviour of haematopoietic cell populations of *Sfrp2* KO mice are the reason for steady state changes in LSKs, two different approaches were started. First, the proliferative activity of cells of haematopoietic hierarchy was analysed by the expression of cell cycle marker Ki-67. Cells express the marker during activated G1 phase, synthesis phase (S-phase) and mitosis (G2/M) phase, but not when they are quiescent, in G0 phase of the cell cycle (Scholzen and Gerdes 2000). In further studies analysing cell cycle behaviour Bromodeoxyuridine (BrdU) was used. BrdU is incorporated into the newly synthesized DNA of replicating cells (S-phase) (Eidinoff *et al.* 1959, Gonchoroff *et al.* 1985). BrdU was injected in wild type and *Sfrp2*$^{-/-}$ mice and BM was analysed after 16 h. The staining of total DNA level with 7-AAD allows to detect the distribution of cells in G0/G1, S and G2/M phase of cell cycle.

In the first approach ten weeks old mice were sacrificed and haematopoietic cells were stained corresponding to their surface markers. After additional fixation and permeabilization, the bone marrow cells were stained over night with anti-Ki-67 antibody (Chapter 3.11.).

Analysis of Ki-67 showed significantly less bone marrow cells expressing Ki-67 (Figure 26 A). Closer examination of mature lymphoid and myeloid subpopulations demonstrated diminished Ki-67 expression in B220^{+} cells. Ki-67 expression in CD4^{+} CD8a^{+} T-cells as well as myeloid populations was unchanged with regard to the same populations in *Sfrp2*$^{+/+}$ controls (Figure 26 B). Analysis of stem and progenitor cell populations (LSKs, MPs and CLPs) indicated decreased percentages of LSK cells expressing Ki-67. This effect of *Sfrp2* deficiency was unique to these earliest haematopoietic cells, as it was found that the fraction of Ki-67-expressing myeloid and lymphoid progenitors was unchanged compared to WT controls (Figure 26 C). Thus, the results suggest a decreased proliferative activity of LSKs in *Sfrp2*$^{-/-}$ mice.

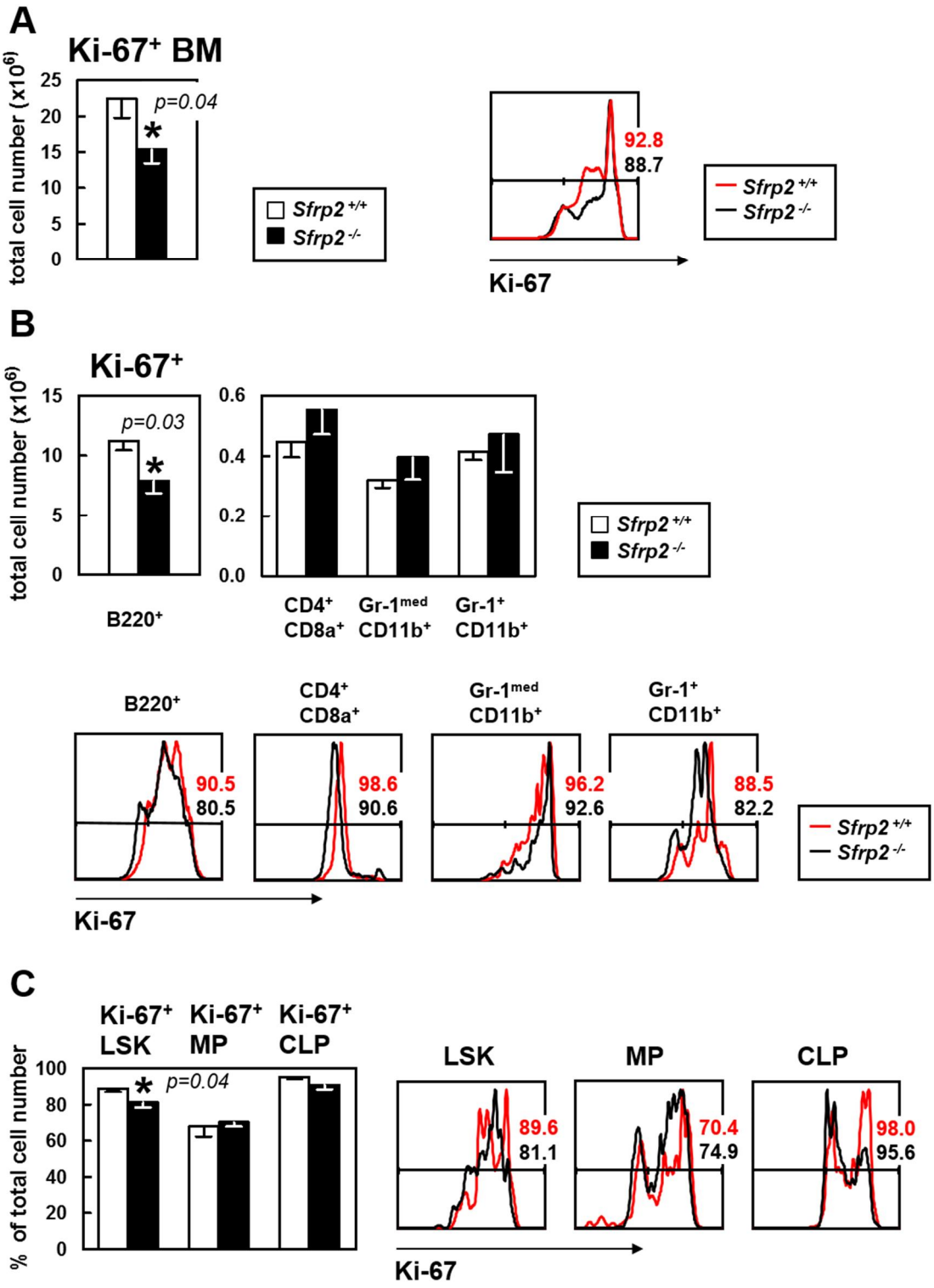

Figure 26. Proliferative activity of haematopoietic cells in bone marrow of Sfrp2 KO and WT mice measured by Ki-67 expression. *(A) Total cell number of Ki-67$^+$ whole BM analysed by flow cytometry (left side), with representative histogram on the right side. (B) Upper panel: Total cell number of Ki-67$^+$ mature haematopoietic populations (B220$^+$, CD4$^+$ CD8a$^+$, Gr-1^{med} CD11b$^+$ and Gr-1$^+$ CD11b$^+$). Lower panel: Representative histograms. Sfrp2 WT littermates (n=6), Sfrp2 KO mice (n=6). (C) Percentage of total cell number of Ki-67$^+$ LSKs, MPs and CLPs analysed by flow cytometry (left side) with representative histograms (right side). White bars and red lines: Sfrp2$^{+/+}$ 129xBL/6 (n=8), black bars and black lines: Sfrp2$^{-/-}$ mice (n=10), Mean ± SEM, *p<0.05.*

In the second approach to investigate the proliferative activity of haematopoietic cells in the absence of sFRP-2, BrdU incorporation into haematopoietic cells was analysed. For this experiment, as it is also described in Chapter 3.12., BrdU was injected intraperitoneal once and the incorporation into DNA was measured after 16 hours by FACS after fixation, permeabilization, BrdU and 7-AAD staining (Figure 27 A). Results exhibited an increased percentage of total bone marrow cells which incorporated BrdU (S phase, Figure 27 B) which was quite unexpected considering the decreased number of Ki-67$^+$ bone marrow cells. The mature myeloid (Gr-1^{med} CD11b$^+$, Gr-1$^+$ CD11b$^+$) and lymphoid (B220$^+$, CD4$^+$ CD8a$^+$) subpopulations exhibited an unchanged proliferative activity in all populations of *Sfrp2*$^{-/-}$ mice compared to wild type controls (Figure 27 C).

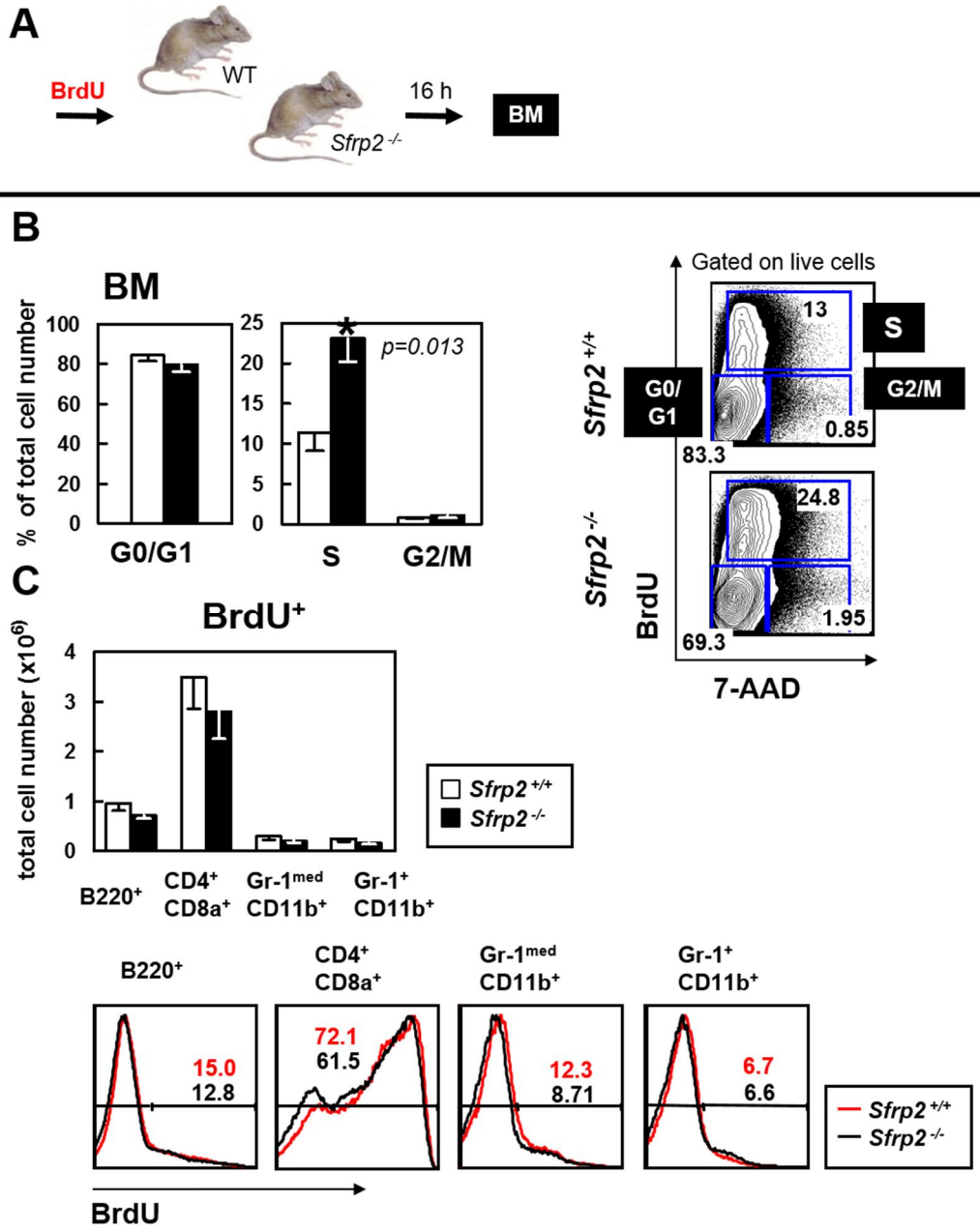

Figure 27. Proliferative activity of mature haematopoietic cells in bone marrow of Sfrp2 KO and WT mice measured by BrdU incorporation. *(A) Experimental design. (B) Percentage of BrdU and 7-AAD labelled whole bone marrow in G0/G1, S and G2/M phases of cell cycle analysed by flow cytometry (left side), with representative FACS plots on the right side. (C) Upper panel: Total cell number of BrdU$^+$ mature haematopoietic populations (B220$^+$, CD4$^+$ CD8a$^+$, Gr-1^{med} CD11b$^+$ and Gr-1$^+$ CD11b$^+$). Lower panel: Representative histograms. White bars and red lines: Sfrp2$^{+/+}$ littermates (n=6), black bars and black lines: Sfrp2$^{-/-}$ mice (n=4), Mean ± SEM, *p<0.05.*

Like the mature cell populations, LSK, MP and CLP cells had incorporated BrdU to similar levels in WT and *Sfrp2*$^{-/-}$ mice (Figure 28 A). However, regarding the cell cycle phases by analysing 7-AAD level, which stains DNA versus BrdU incorporation, the percentage of LSKs in S phase was detected to be significantly increased (Figure 28 B),

indicating an enhanced proliferative activity, which was unexpected regarding Ki-67 data and the decreased level of Cyclin-D1 in LSKs. One possible explanation could be, that BrdU is acting as a stress inductor for the mice, by incorporating into DNA. The absence of sFRP-2 might cause an altered stress response in the mice influencing the activation of HSCs.

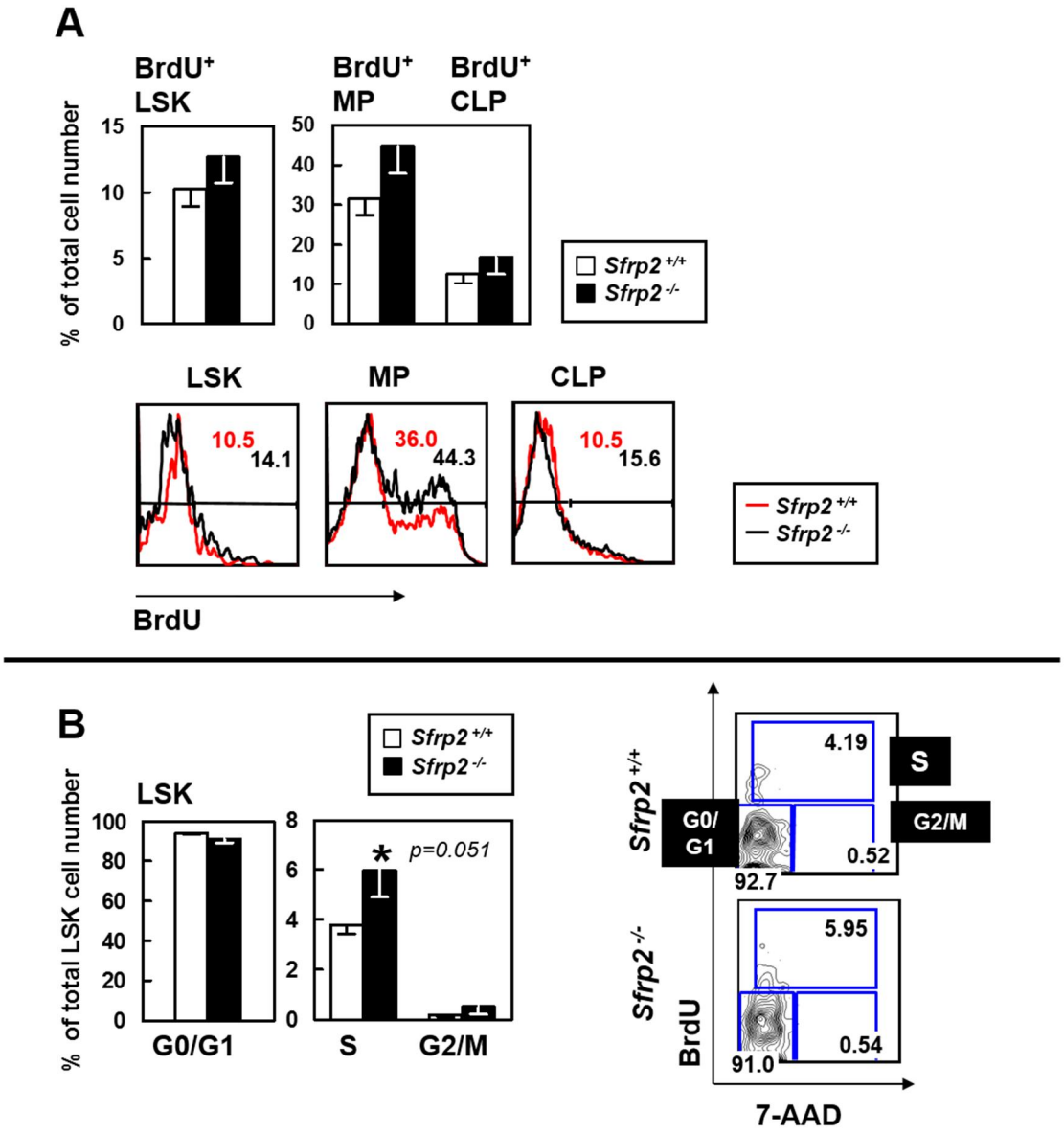

Figure 28. Proliferative activity of steady state LSKs and progenitor cells in bone marrow of Sfrp2 KO and WT mice. *(A) Percentage of total cell number of BrdU$^+$ LSKs, MPs and CLPs analysed by flow cytometry with representative histograms. (B) Percentage of BrdU and 7-AAD-labelled total LSK number in G0/G1, S and G2/M phases of cell cycle with representative FACS plots. White bars and red lines: Sfrp2$^{+/+}$ littermates (n=6); black bars and black lines: Sfrp2$^{-/-}$ mice (n=4), Mean ± SEM, *p<0.05.*

So far, short term BrdU incorporation was investigated. A third approach which would "awake" the dormant HSCs in the niche (Essers *et al.* 2009, Trumpp *et al.* 2010) was studied by long-term BrdU incorporation. To activate the quiescent long-term HSCs, BrdU was injected once followed by ten days of oral gavage (Chapter 3.12. and Figure 29). Seventy days later, the remaining incorporated BrdU was determined in subpopulations of cells. The more BrdU detected, the more quiescent that population would be. After 70 days a decreased number of CD34$^-$ LSK in most *Sfrp2* deficient mice was detected, but due to the inter-animal variation no significant alterations occurred (Figure 29). To further follow the hypothesis of an altered activation of HSCs in *Sfrp2* KO mice, further investigations dealt with stress-induced haematopoiesis and cell cycle behaviour (Chapter 4.4.2.).

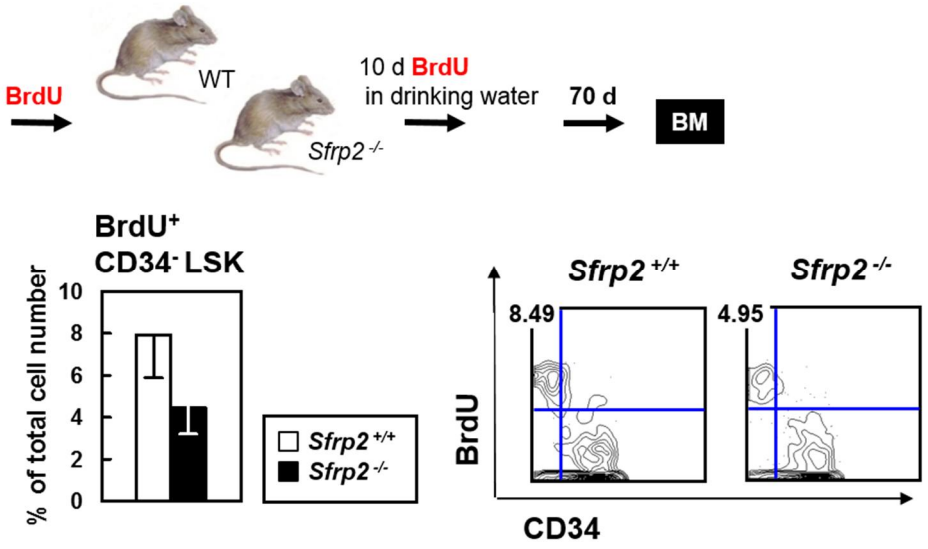

Figure 29. Long-term BrdU incorporation of CD34$^-$ LSKs. *Upper panel: Experimental design. Lower panel: Percentage of total cell number of BrdU$^+$ CD34$^-$ LSKs analysed by flow cytometry with representative FACS plots. Sfrp2 WT littermates (n=10), Sfrp2 KO mice (n=8). White bars: Sfrp2$^{+/+}$ littermates, black bars: Sfrp2$^{-/-}$ mice, Mean ± SEM, *p<0.05.*

4.4.2. Lack of *Sfrp2* leads to increased stress-induced activation of HSCs

Since there is no major involvement of *Sfrp2* in steady state haematopoiesis, and the last experiment suggested that *Sfrp2* might limit cell cycle induction after stress, I decided to study haematopoietic stress more closely.

The chemo-reagent 5-Fluorouracil (5-FU) is metabolized into several active metabolites, which disrupt RNA synthesis as well as interferes with DNA synthesis during phase (S-phase), by exchanging Thymidine with 5-FU (Longley *et al.* 2003). A detailed description of the mechanism of action of 5-FU is shown in Figure 30. The exchange results in p53-dependent cell death of actively dividing haematopoietic cells like mature and progenitor cells. As a result of this haematopoietic challenge, quiescent HSCs are activated to come out of the niche to proliferate and differentiate and regenerate the blood cell system.

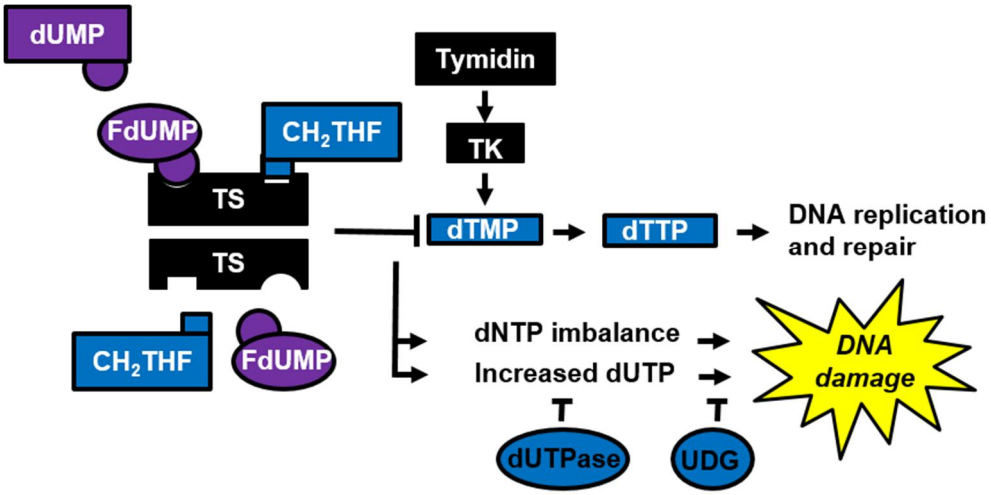

Figure 30. Mechanism of action of 5-FU. *Thymidylate synthase (TS) catalyses the conversion of deoxyuridine monophosphate (dUMP) to deoxythymidine monophosphate (dTMP) with 5,10-methylene tetrahydrofolate (CH2THF) as the methyl donor. The 5-fluorouracil (5-FU) active metabolite fluorodeoxyuridine monophosphate (FdUMP) binds to the nucleotide-binding site of TS and forms a stable ternary complex with TS and CH2THF, blocking access of dUMP to the nucleotide-binding site and inhibiting dTMP synthesis. This results in deoxynucleotide (dNTP) pool imbalances and increased levels of deoxyuridine triphosphate (dUTP), both of which cause DNA damage. The extent of DNA damage caused by dUTP is dependent on the levels of the pyrophosphatase dUTPase and uracil-DNA glycosylase (UDG). The dTMP can be salvaged from thymidine through the action of thymidine kinase (adapted from Longley et al., Nat Rev Cancer. 2003).*

For the experiments described here, 5-FU was injected intraperitoneally in *Sfrp2*$^{-/-}$ and WT control mice (Chapter 3.13., Figure 31 A). After four days, the initial regeneration of mature cells in peripheral blood was investigated. After six days, mice were sacrificed and blood and bone marrow was analysed. The results show that after four days, the percentage of B220^{+} B-cells was decreased, while the percentage of Gr-1^{med} CD11b^{+}

monocytes was increased in peripheral blood. Percentage of $CD4^+$ $CD8a^+$ T-cells as well as of Gr-1^+ $Cd11b^+$ granulocytes was unchanged. Six days after 5-FU injection, PB analysis exhibited an increased percentage of T-cells and a decreased number of monocytes, percentage of B-cells and granulocytes were unchanged (Figure 31 B). When the BM was investigated six days after injection of 5-FU, the number of total cells in the mature haematopoietic cell fractions was similar in WT and *Sfrp2*$^{-/-}$ mice (Figure 31 C).

To figure out whether the hypothesised phenotype of an altered HSC activation can be confirmed, stem and progenitor cells were analysed. Although there were neither changes in myeloid progenitors (MPs) nor in lymphoid progenitor cells (CLPs), interestingly, the total cell number of LSKs as well as of more primitive, and supposedly quiescent $CD34^-$ $CD150^+$ LSKs was significantly increased in *Sfrp2*$^{-/-}$ mice (Figure 31 D).

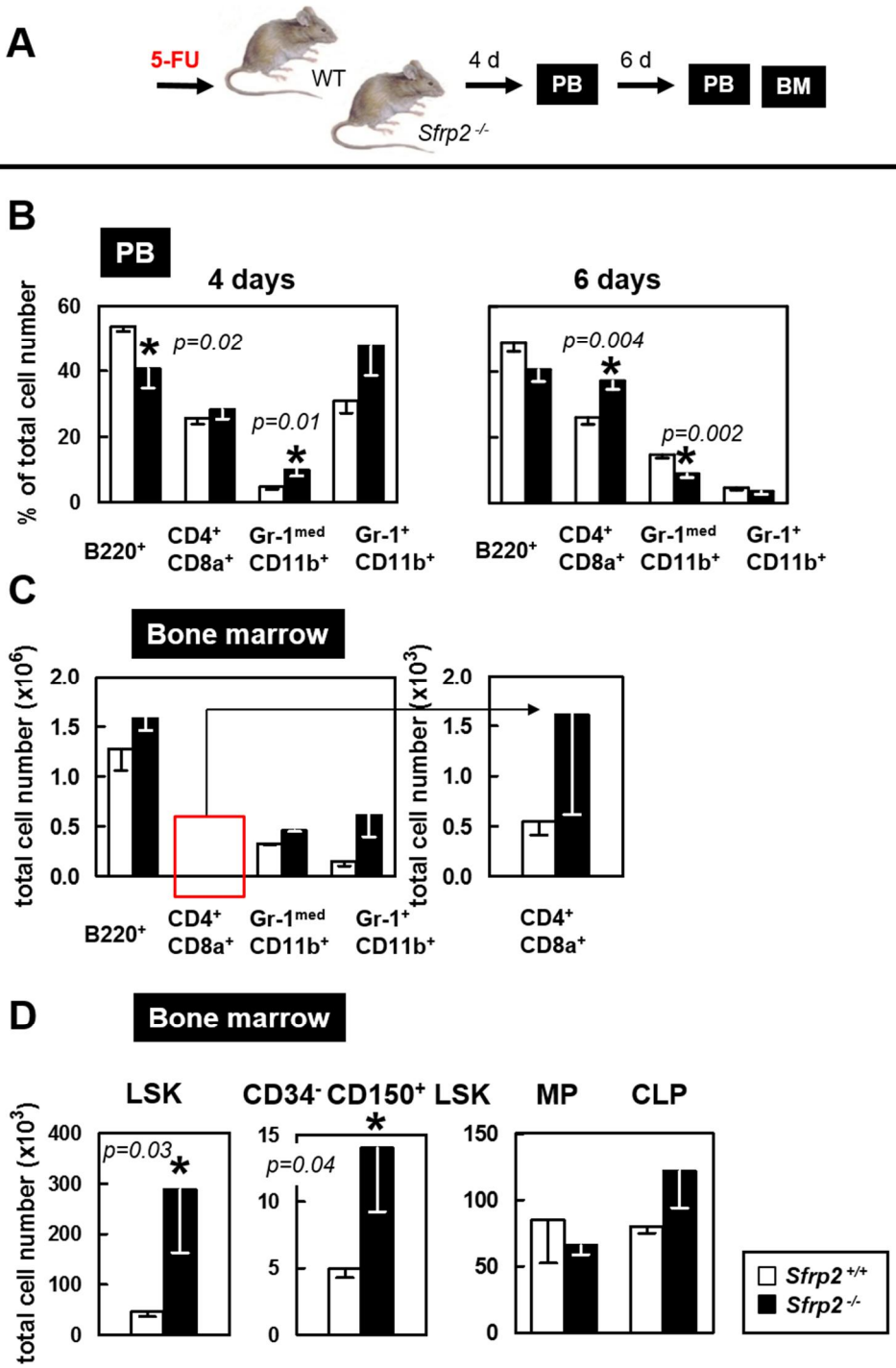

Figure 31. Stress- (5-FU) induced alterations of peripheral blood and bone marrow of haematopoietic cells in Sfrp2 KO and WT mice. *(A) Experimental design. (B) Percentage of mature lymphoid and myeloid cell populations (B220$^+$, CD4$^+$ CD8a$^+$, Gr-1^{med} CD11b$^+$ and Gr-1$^+$ CD11b$^+$) in peripheral blood (PB) four and six days post 5-FU injection and (C) total cell number of bone marrow mature cells six days post 5-FU injection. (D) Total cell number of LSKs and long-term HSC-like CD34$^-$ CD150$^+$ LSKs as well as MPs and CLPs. White bars: Sfrp2$^{+/+}$ littermates (n=10), black bars: Sfrp2$^{-/-}$ mice (n=7), Mean ± SEM, *p<0.05.*

The increased number of LSK cell populations might be due to either more cells remaining (less differentiation, or cell death) or more cells regenerated (more cell cycle activity or earlier return to quiescence). To study the latter possibility, increased cell cycling activity, BrdU was injected five days after 5-FU treatment to analyse its incorporation into DNA of S-phase cells in LSK and progenitor cells after stress induction (Figure 32 A). While the percentage of incorporated BrdU remained unchanged in myeloid and lymphoid progenitors (MPs, CLPs), interestingly, an increased BrdU incorporation in LSK cells and an increased number of $CD34^-$ LSK which had incorporated BrdU were found (Figure 32 B). Further, a highly increased percentage of LSKs in S-phase was detected, while G0/G1 cell fraction was significantly decreased in cells from *Sfrp2*$^{-/-}$ mice (Figure 32 C). This finding shows that early LSK phenotypes are less quiescent and more in S-phase, suggesting that mice deficient in *Sfrp2* show an enhanced activation of LSKs from G0/G1 to proliferative state (S-phase) of cell cycle after haematopoietic challenge. Since increased HSC activation may result in HSC exhaustion, this detection supports the finding of a decreased maintenance of HSC in *Sfrp2*$^{-/-}$ mice after stress.

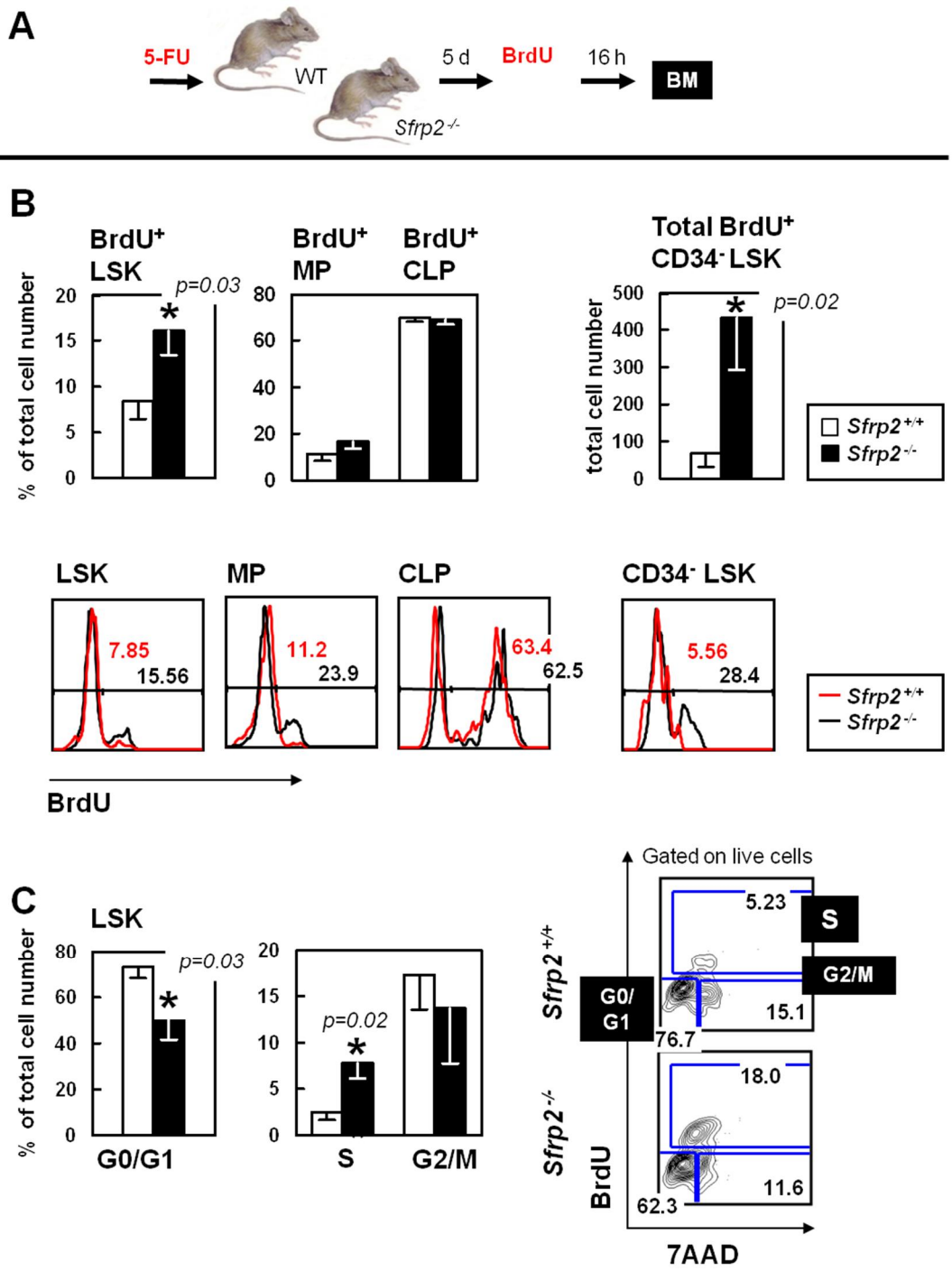

Figure 32. Proliferative activity of LSK and progenitor cells in bone marrow of Sfrp2 KO and WT mice after stress induction. *(A) Experimental design. (B) Percentage of total cell number of BrdU$^+$ LSKs and CD34$^-$ LSKs, as well as MPs and CLPs analysed by flow cytometry (upper panel) with representative histograms (lower panel). (C) Percentage of BrdU$^+$ and 7-AAD-labelled total LSK number in G0/G1, S and G2/M phases of cell cycle (left side), with representative FACS plots (right side). White bars and red lines: Sfrp2 WT littermates (n=11), black bars and black lines: Sfrp2 KO mice (n=10), Mean ± SEM, *p<0.05.*

4.5. No alterations of apoptotic behaviour of *Sfrp2*$^{-/-}$ haematopoietic cells

The changes in proliferation and activation of HSCs could also be caused by different sensitivity to cell death. Thus, possible alterations in apoptosis were studied, as cells might be sensitive for apoptotic signals after induction of proliferation by stress. Wnt signalling pathway was found not only to drive proliferation, but also to be associated with apoptosis by the regulation of BCL-2 (Ming *et al.* 2012). Considering the decreased number of LSKs in mice lacking *Sfrp2* and the decreased activity of Wnt signalling, apoptosis might be another mechanism the alterations could be caused by.

To examine apoptotic behaviour, bone marrow of ten weeks old *Sfrp2* knock out and control mice was cultured over night with growth factors (IL3, IL6, SCF). As also described in Chapter 3.14., apoptosis was then induced by cycloheximide, which blocks the protein biosynthesis (Figure 33 A). Bone marrow was analysed by flow cytometry showing an unchanged distribution of live (PI^- $AnnexinV^-$), apoptotic (PI^- $AnnexinV^+$) and necrotic (PI^+ $AnnexinV^-$) cells (Figure 33 B). Studying LSK and progenitor cells, the number of apoptotic cells was also unchanged in *Sfrp2* knockout bone marrow compared to wild type controls (Figure 33 C). Taken together the loss of *Sfrp2* does not influence the apoptotic behaviour of LSK and progenitor cells.

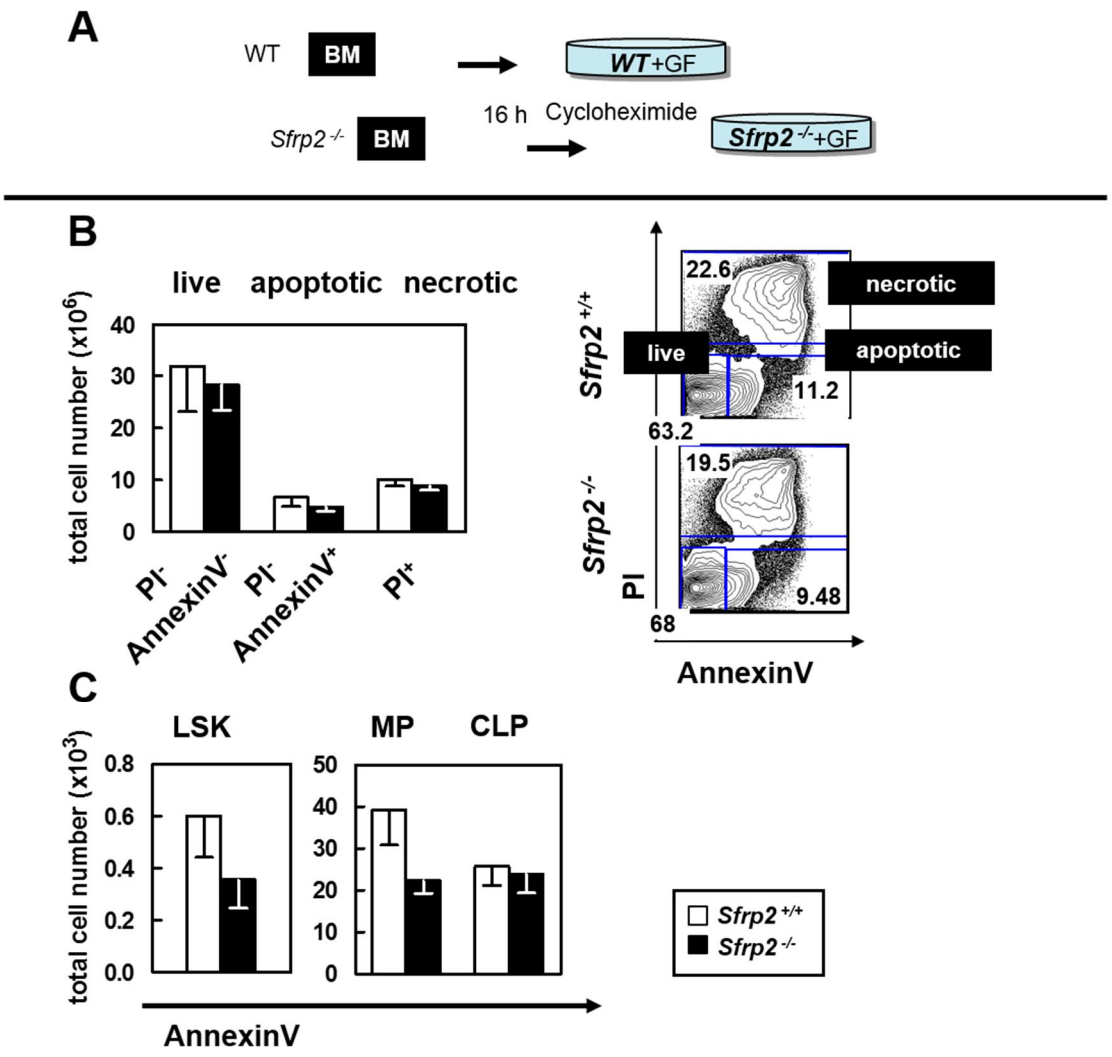

Figure 33. Apoptotic behaviour in steady state haematopoiesis of Sfrp2 KO and WT mice. *(A) Experimental design. (B) Total cell number of PI- and AnnexinV-labelled live, apoptotic and necrotic populations in bone marrow analysed by flow cytometry (left side) with representative FACS plots (right side). (C) Total cell number of AnnexinV$^+$ apoptotic LSKs, MPs and CLPs. White bars: Sfrp2$^{+/+}$ littermates (n=5), black bars: Sfrp2$^{-/-}$ mice (n=7), Mean ± SEM.*

4.6. SFRP-2 extrinsically alters HSCs

These studies show that in haematopoietic stress, cell cycle activity increases in early haematopoietic cells due to *Sfrp2* deficiency. Thus, *Sfrp2* may enhance activation under stress. As the effect might be intrinsic, dependent on *Sfrp2* deficiency in HSCs or extrinsic, based on the absence of sFRP-2 in the niche, transplantation models were used.

4.6.1. Intrinsic and extrinsic transplantation

Sfrp2 is highly secreted by mineralized osteoblasts in endosteal niche (Roux 2010) and is suggested to inhibit differentiation of HSCs by enhancing self-renewal. Stimulation of LT-HSCs with *Sfrp2 in vitro* results in an increased HSC engraftment in serial transplantation experiments (Nakajima *et al.* 2009). The family member sFRP-1 was previously shown to regulate the maintenance of HSCs through regulation of the cell cycle in an extrinsic manner (Renstrom *et al.* 2009).

SFPR-2 as well as sFRP-1 is overrepresented in HSC-supporting stromal cells UG26-1B6 (Oostendorp *et al.* 2005). While sFRP-1 was shown to be not expressed in haematopoietic stem and progenitor cells (Nakajima *et al.* 2009, Renstrom *et al.* 2009) the expression level of *Sfrp2* in haematopoietic cells themselves has not been published so far. Real time PCR analyses exhibited a very low expression of *Sfrp2* in LSK and myeloid progenitor cells as well as in mature $B220^+$ B-cells, $CD4^+$ $CD8a^+$ T-cells and $Gr\text{-}1^{med}$ $CD11b^+$ monocytes relative to the expression of *Rpl39* housekeeping gene. A higher expression was observed in lymphoid progenitors and $Gr\text{-}1^+$ $CD11b^+$ granulocytes (Figure 34) relative to *Rpl39* and also compared to the expression level of *Sfrp2* in UG26-1B6 stromal cells.

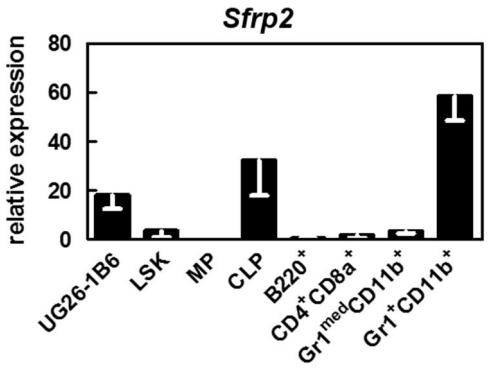

Figure 34. Relative expression of Sfrp2 in haematopoietic cell populations and stromal cell line. *Expression of Sfrp2 in UG26-1B6 stromal cell line, LSKs, MPs, CLPs, $B220^+$ B-cells, $CD4^+$ $CD8a^+$ T-cells, $Gr\text{-}1^{med}$ $CD11b^+$ monocytes and $Gr\text{-}1^+$ $CD11b^+$ granulocytes calculated on 2^delta CT x100 % values relative to Rpl39 housekeeping gene.*

After 5-FU treatment, cell cycle entry in $Sfrp2^{-/-}$ LSK cells is increased (Figure 32 C). Another model of haematopoietic stress is the repopulation assay (Chapter 3.10.). This assay has the additional advantage of dissecting whether possible differences in behaviour are displayed by the haematopoietic cells themselves (intrinsic effects) or are

caused by the microenvironment (extrinsic effects). In order to assess whether loss of *Sfrp2* in stem and progenitor cells themselves result in the altered engraftment of HSCs, I transplanted *Sfrp2*$^{-/-}$ and WT bone marrow cells (CD45.2, Ly5.2) in lethally irradiated (8.5 Gy) 129xLy5.1 mice (CD45.2 (Ly5.2) x CD45.1 (Ly5.1)) and followed engraftment for 16 weeks (Figure 35 A-C). The congenic system (CD45.1, CD45.2 surface marker expression) allows to distinguish donor and recipient cells by flow cytometry. As shown in Figure 35 the data demonstrated an unchanged engraftment of myeloid and lymphoid cells analysing peripheral blood five, ten and 16 weeks after transplantation (Figure 35 B) as well as bone marrow and spleen after 16 weeks (Figure 35 C and D). Additionally an unchanged number of functional *Sfrp2* deficient HSCs in BM 16 weeks after injection was examined (Figure 35 E), indicating that loss of *Sfrp2* in HSCs themselves does not influence their ability to engraft in primary recipients.

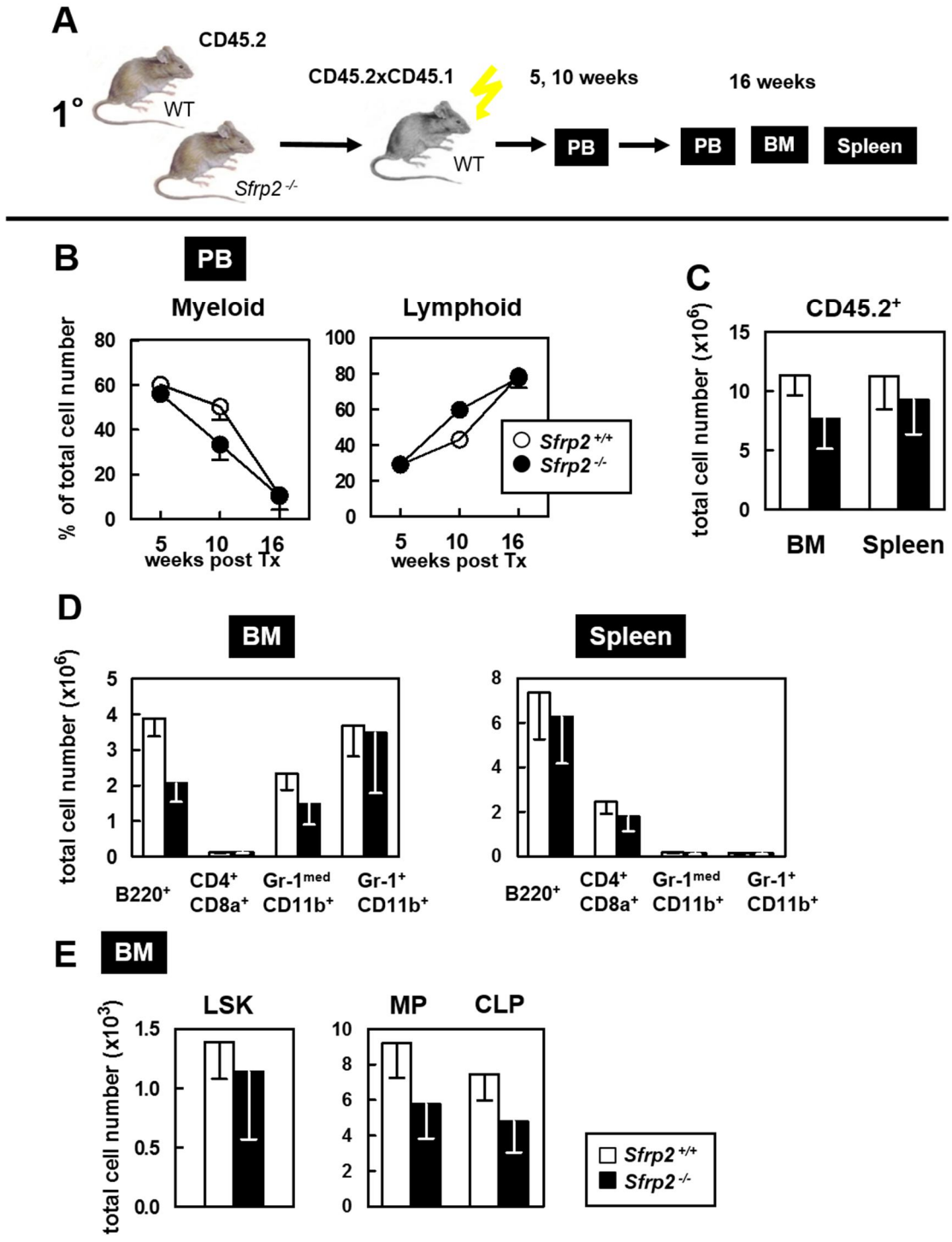

Figure 35. Intrinsic effect of Sfrp2 knockout. *(A) Experimental design. (B) Percentage of myeloid and lymphoid engraftment of WT and Sfrp2 KO bone marrow (in WT niche) five, ten and 16 weeks after transplantation in peripheral blood (PB). (C) Total cell number of engrafted (CD45.2$^+$) bone marrow (BM) and spleen cells. (D) Total cell number of donor B220$^+$, CD4$^+$ CD8a$^+$, Gr-1^{med} CD11b$^+$ and Gr-1$^+$ CD11b$^+$ in bone marrow and spleen. (E) Donor LSK, MP and CLP number in BM. White bars and white circles: Sfrp2$^{+/+}$ littermates (n=9), black bars and circles: Sfrp2$^{-/-}$ mice (n=10), Mean ± SEM.*

Conversely, the microenvironment might influence engraftment in an extrinsic manner. To study this, wild type donor bone marrow cells (Ly5.1, CD45.1) were injected into lethally irradiated *Sfrp2*$^{-/-}$ or WT control mice (CD45.2) and were analysed following the same procedure as in the previous paragraph (Figure 36 A). Five weeks after transplantation, an increased myeloid engraftment of WT donors in *Sfrp2* knockout mice was observed (Figure 36 B). This interesting finding could correspond with previously shown results of increased progenitor activity in steady state characterization of adult *Sfrp2* KO mice (Figure 17 B).

After 16 weeks, recipient mice were sacrificed, and the mice were analysed for donor cell engraftment in detail. The total engraftment of CD45.1 donor cells (Figure 36 C) as well as reconstitution of mature lineages (B220^{+}, CD4^{+} CD8a^{+}, Gr-1^{med} CD11b^{+}, Gr-1^{+} CD11b^{+}) in BM and spleen (Figure 36 D) was unchanged in *Sfrp2* knockout mice compared to their controls. Further, investigations of myeloid and lymphoid progenitors and LSKs which reside in the *Sfrp2* deficient environment for 16 weeks exhibited an unchanged number of MPs and CLPs. However, the number of LSKs was highly increased (Figure 36 E) in the bone marrow. This finding is in line with the increase in LSK cells after 5-FU treatment and suggests that the LSK cells have a higher cell cycle activity in *Sfrp2*$^{-/-}$ recipient mice.

Since this could be associated with loss of HSCs upon further transplantation, LSK cells from primary recipients were isolated and further transplanted into secondary recipients which is described below and is also seen in Figure 39.

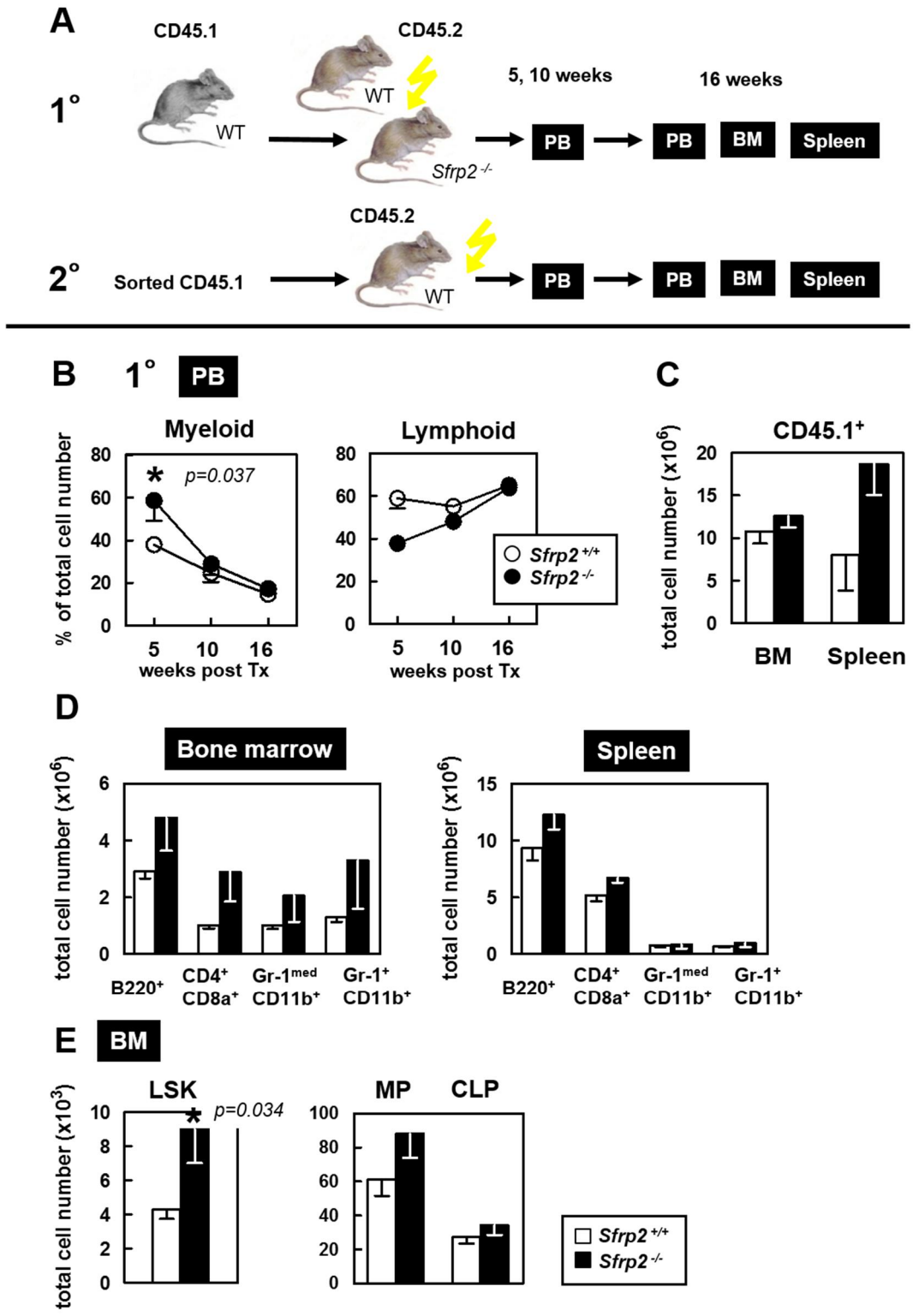

Figure 36. Extrinsic effect of Sfrp2 knockout. *(A) Experimental design. (B) Percentage of myeloid and lymphoid engraftment of WT bone marrow (in Sfrp2$^{-/-}$ or WT niche) five, ten and 16 weeks after transplantation in peripheral blood (PB). (C) Total cell number of engrafted (CD45.1^{+}) bone marrow (BM) and spleen cells. (D) Total cell number of donor B220^{+}, CD4^{+} CD8a^{+}, Gr-1^{med} CD11b^{+} and Gr-1^{+} CD11b^{+} in bone marrow and spleen. (E) Donor LSK, MP and CLP number in BM. White bars and white circles: Sfrp2$^{+/+}$ littermates (n=12), black bars and circles: Sfrp2$^{-/-}$ mice (n=17), Mean ± SEM, *p<0.05.*

4.6.2. Increased Wnt signalling activity of extrinsically altered HSCs

The experiments show that sFRP-2 limits the activation of HSCs after 5-FU- or repopulation-associated haematopoietic stress. To get a better idea of the changes in Wnt signalling in the stressed cells, the protein level of Wnt signalling candidates was analysed in WT donor LSK cells sorted from primary (1°) WT and *Sfrp2*$^{-/-}$ recipients.

For these experiments, 1° CD45.1^{+} LSK cells were spotted on slides and were stained with specific fluorescence-labelled antibodies for Wnt signalling proteins and with DAPI for nuclear counterstaining. Analysis was performed in the same manner as it was done for the investigations of Wnt signalling in untreated (steady state) adult mice described above (Chapter 4.3.).

Canonical Wnt signalling

While in steady-state haematopoiesis, the catenin-dependent Wnt pathway was detected to be inhibited, surprisingly, 16 weeks after injection, this Wnt pathway was more active in regenerated donor LSK cells. This was clear from significantly higher levels of DVL-2, catenin and the catenin target gene Cyclin-D1 (Figure 37 A, B)

Non-canonical Wnt signalling

Similarly, for Ca^{2+}-dependent Wnt signalling, staining of engrafted donor LSK cells suggest quite contrary results compared to steady state analysis: In LSKs of untreated (steady state) *Sfrp2* knockout mice the protein level of the transcription factor NF-ATc was highly decreased (Figure 24 A, B). Interestingly however, 16 weeks after transplantation, the protein level of NF-ATc was almost fourfold increased in donor LSK cells isolated from a *Sfrp2* deficient microenvironment compared to controls. Further, the protein level of Wnt signalling regulated C/EBP-alpha was significantly increased. Interestingly, protein level of CaMK-II was also increased which exclusively equals the steady state alteration in *Sfrp2*$^{-/-}$ mice compared to wild types (Figure 24 A, B and 38 A, B). Figure 38 C summarizes the results of protein level alterations of LSKs after

transplantation in canonical and non-canonical Wnt signalling, suggesting an activation of the pathway in HSCs residing in *Sfrp2* deficient niche for 16 weeks.

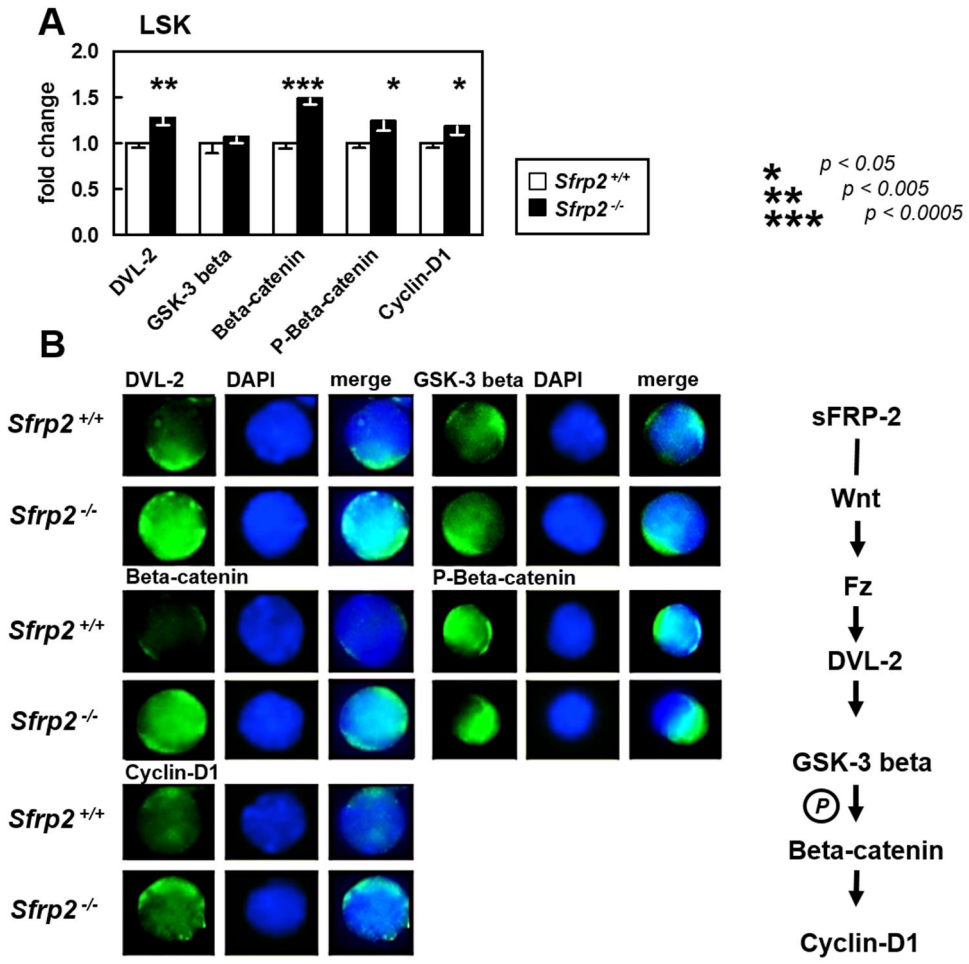

Figure 37. Protein level of candidates of Beta-catenin-dependent Wnt signalling of WT LSKs residing in Sfrp2 KO or WT environment for 16 weeks. *(A) Fold change of quantification of protein level of DVL-2, GSK-3 beta, Beta-catenin, P-Beta-catenin and Cyclin-D1 of pooled and sorted LSKs. (B) Representative pictures of single cell staining. White bars: Sfrp2$^{+/+}$ littermates (n=8), black bars: Sfrp2$^{-/-}$ mice (n=9). For quantification 20 cells were snapped on Leica fluorescent microscope, magnification x100. Total pixel were quantified by ImageJ. Mean ± SEM, *p<0.05, **p<0.005, ***p<0.0005.*

Figure 38. (Below); Protein level of candidates of Ca^{2+}-dependent Wnt signalling of WT LSKs, residing in Sfrp2 KO or WT environment for 16 weeks. *(A) Fold change of quantification of protein level of CaMK-II, P-CaMK-II, NLK, NF-ATc and C/EPB-alpha in sorted LSKs. (B) Representative pictures of single cell staining. White bars: Sfrp2$^{+/+}$ littermates (n=8), black bars: Sfrp2$^{-/-}$ mice (n=9). For quantification 20 cells were snapped on Leica fluorescent microscope, magnification x100. Total pixel were quantified by ImageJ. Mean ± SEM, *p<0.05, **p<0.005, ***p<0.0005. (C) Alteration of protein level of Wnt signalling pathway in donor LSKs: Candidate proteins of Beta-catenin-dependent Wnt signalling are shown in violet, proteins of Ca^{2+}-dependent Wnt signalling in blue. Green arrows represent the protein level in Sfrp2 KO in comparison to WT.*

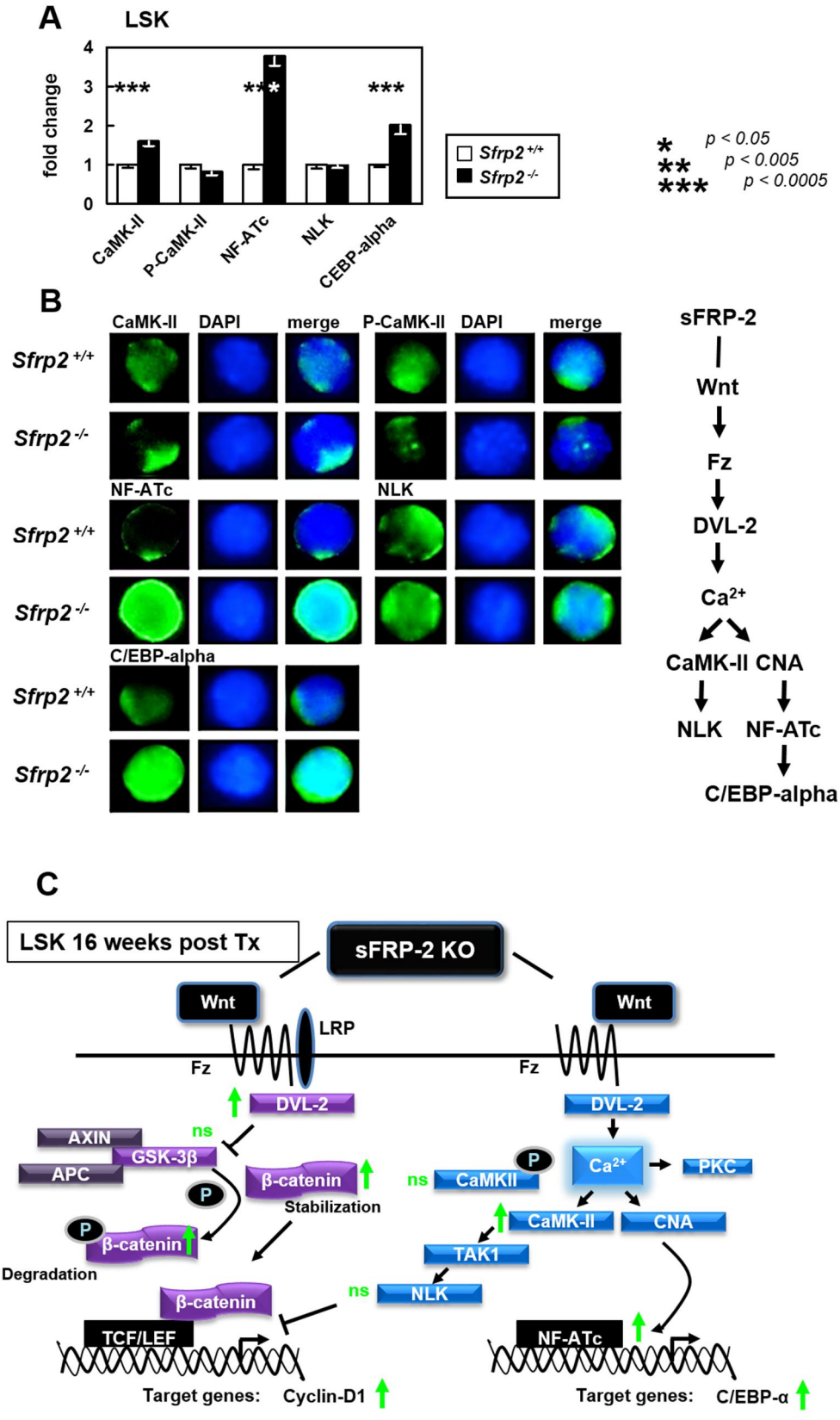
A
LSK
fold change
4
3
2
1
0
***
***
***
CaMK-II
P-CaMK-II
NF-ATc
NLK
CEBP-alpha
Sfrp2 +/+
Sfrp2 -/-
* p < 0.05
** p < 0.005
*** p < 0.0005
B
CaMK-II
DAPI
merge
P-CaMK-II
DAPI
merge
Sfrp2 +/+
Sfrp2 -/-
NF-ATc
NLK
Sfrp2 +/+
Sfrp2 -/-
C/EBP-alpha
Sfrp2 +/+
Sfrp2 -/-
sFRP-2
Wnt
Fz
DVL-2
Ca2+
CaMK-II CNA
NLK NF-ATc
C/EBP-alpha
C
LSK 16 weeks post Tx
sFRP-2 KO
Wnt
LRP
Fz
DVL-2
AXIN
GSK-3β
APC
ns
β-catenin
Stabilization
P
β-catenin
Degradation
β-catenin
TCF/LEF
Target genes: Cyclin-D1
Wnt
Fz
DVL-2
P
CaMKII
ns
Ca2+
PKC
CaMK-II
CNA
TAK1
NLK
ns
NF-ATc
Target genes: C/EBP-α

4.6.3. Reduction of extrinsically altered HSCs after secondary transplantation

Since the results could be associated with loss of HSCs upon further transplantation, LSK cells from primary recipients were isolated and transplanted into secondary recipients (Figure 36 A). As the previously published *Sfrp1* data showed a significant decrease of donor LSKs in secondary recipients after 16 weeks (Renstrom *et al.* 2009), an effect in *Sfrp2* knockout mice was hypothesised. Donor cells were sorted out according to their expression of surface markers CD45.1, Lin, KIT and SCA-1, also attending the number of LSK cells (Figure 39 A). Afterwards, 2000 donor LSK equivalents of KIT^+ cells were re-transplanted into lethally irradiated wild type recipients (BL/6, CD45.2). Secondary transplantation analyses were performed as described above in primary transplantation studies.

Five and ten weeks after transplantation the initial engraftment of donor cells was analysed in peripheral blood. The myeloid engraftment was slightly decreased five weeks after injection. The lymphoid engraftment was unchanged (Figure 39 B).

Sixteen weeks after transplantation, mice were sacrificed and peripheral blood, bone marrow and spleen were analysed. In peripheral blood, the myeloid and lymphoid engraftment of Ly5.1 cells out of *Sfrp2* deficient microenvironment was unchanged compared to the controls (Figure 39 B). Also total engraftment in bone marrow and spleen was not significantly altered (Figure 39 C). Analysing lineage reconstitution in bone marrow and spleen, a significantly increased number of $Gr\text{-}1^{med}$ $CD11b^+$ monocytes was detected in the spleen (Figure 39 D).

Primary in *Sfrp2* deficient microenvironment injected WT cells exhibited a highly increased number of LSK cells 16 weeks after transplantation (Figure 36 E). More interestingly, 16 weeks after re-transplanting an equal number of LSKs into secondary WT recipients, data exhibited a significantly decreased number of LSKs, which resided within the *Sfrp2* KO niche during the first 16 weeks (Figure 39 E). The results suggest that sFRP-2 itself might be an important factor maintaining the stem cell quality of LSK

cells in adult mice, as the loss of sFRP-2 seems to induce a reduction of HSC repopulation potential.

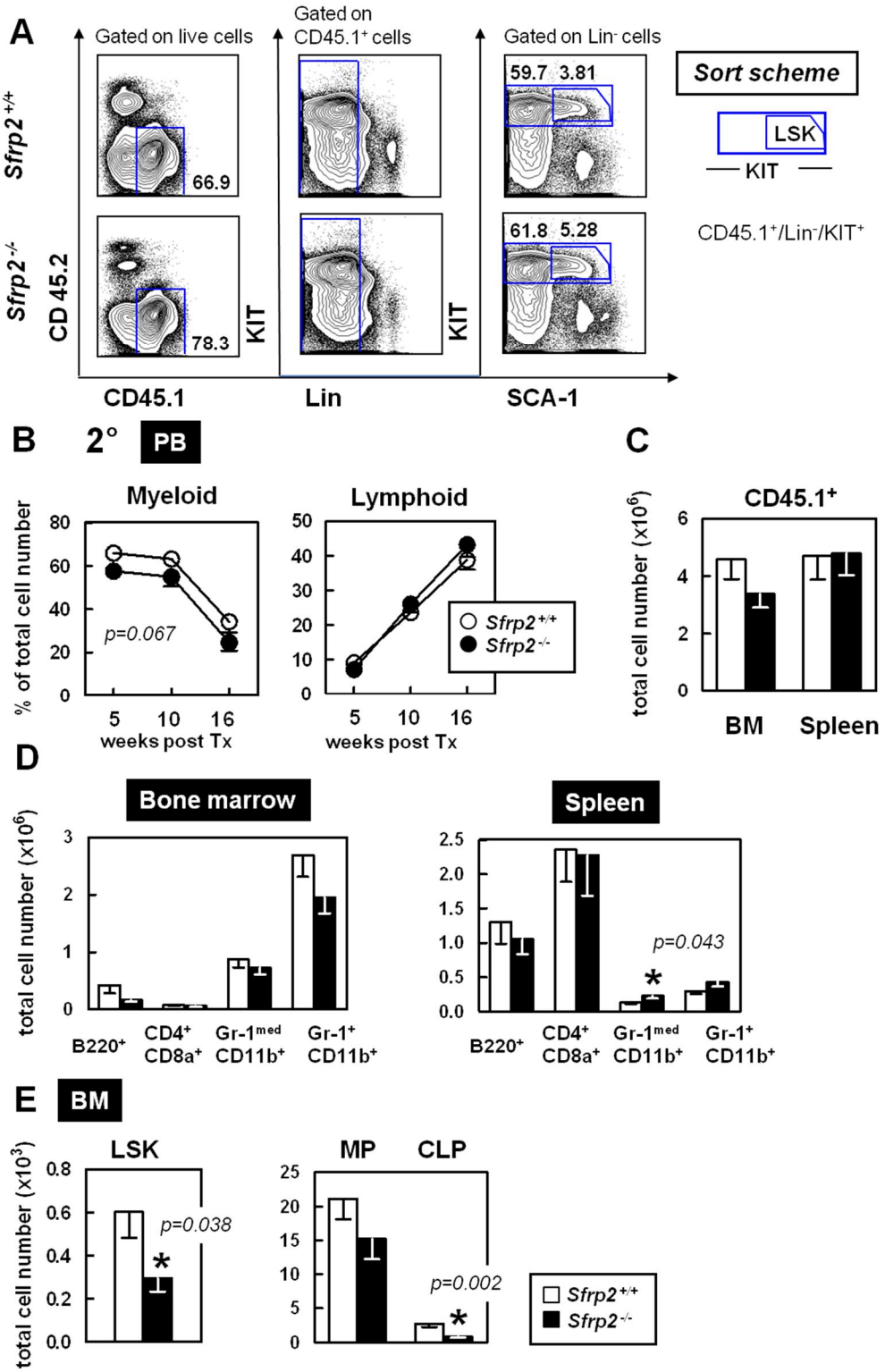

Figure 39. Secondary transplantation of extrinsically altered cells. *(A) Sort scheme of 1° CD45.1$^+$ Lin$^-$ KIT$^+$ cells for secondary injection in WT mice. (B) Percentage of myeloid and lymphoid engraftment of CD45.1$^+$ cells five, ten and 16 weeks after re-transplantation in peripheral blood (PB). (C) Total cell number of engrafted (CD45.1$^+$) bone marrow (BM) and spleen cells. (D) Total cell number of B220$^+$, CD4$^+$ CD8a$^+$, Gr-1^{med} CD11b$^+$ and Gr-1$^+$ CD11b$^+$ in bone marrow and spleen. (E) Donor LSK, MP and CLP number in BM. White bars and white cycles: Sfrp2$^{+/+}$ littermates (n=12), black bars and cycles: Sfrp2$^{-/-}$ mice ((A-D): n=9, (E): n=8), Mean ± SEM, *p<0.05.*

4.7. SFRP-2 in leukaemia

Various publications indicate that aberrant Wnt signalling mediates tumor progression. For instance in CML patients it was shown, that Beta-catenin is required for the progression from the chronic phase into blast crisis (Zhao *et al.* 2007). As described in the introduction (Chapter 1.3.3.) the epigenetic regulation of Wnt modulator is involved in the development of solid tumours as well as in leukaemia. The *Sfrp2* gene is silenced in AML (Jost *et al.* 2008), ALL (Roman-Gomez *et al.* 2006) and CLL (Rahmatpanah *et al.* 2009) (Chapter 1.3.3.) leading to constitutive activation of Wnt signalling. Although in multiple myeloma cells an up-regulation of *Sfrp2* is associated with malformations (Oshima *et al.* 2005). Thus, the role of *Sfrp2* in leukaemogenesis is quite controversial. In 2009, the family member *Sfrp1* was shown to be silenced in a rare population of CML patients. The silencing was associated with a resistance to Imatinib and may provide a key biological difference in therapy resistant patients (Pehlivan *et al.* 2009).

To maintain leukaemic stem cells (LSCs) they are-as well as normal HSCs-dependent on their microenvironment. However, as described in detail in Chapter 1.2.2., evidence is accumulating that the cellular composition and the signals from the niche are altered in the presence of leukaemic cells. For instance, CLL cells were observed to hijack the niche (Lutzny *et al.* 2013), or the other way round transformed niche cells caused HSC mutations (Rupec *et al.* 2005). In myeloproliferative neoplasia the niche was shown to be remodelled to an LSC-supporting niche (Schepers *et al.* 2013).

So far, there is only rare knowledge about Wnt signalling in niche cells in the presence of malignantly transformed HSCs. Here, I studied the effect of *Sfrp2* KO in the niche during leukaemogenesis. As it is described above in the thesis, *Sfrp2* extrinsically regulates haematopoietic stem cells (Chapter 4.6.). In the following studies the extent of *Sfrp2* KO on leukaemogenesis is further elucidated. Therefore p185 BCR-ABL^{+} HSCs (described below) were injected in *Sfrp2*$^{-/-}$ mice and haematopoietic cells as well as their niche were analysed after the outbreak of the disease. In the following chapter different

BCR-ABL fusion proteins and their association to various types of leukaemia are described.

4.7.1. The Philadelphia chromosome: a fusion of BCR and ABL genes

The Philadelphia (Ph) chromosome was discovered in chronic myeloid leukaemia (CML) by Peter Nowell and David Hungerford in 1960 in Philadelphia, giving the chromosomes name (Nowell and Hungerford 1960). The fusion of *Abl* tyrosine kinase (*or Abl1: Abelson Musine Leukaemia Viral Oncogene Homolog 1)* on chromosome 9 and *Bcr* (*breakpoint cluster region*) on chromosome 22 leads to a constitutively active ABL tyrosine kinase, a proto-oncogene (Abelson and Rabstein 1970, Laneuville 1995, Li *et al.* 1999). The Ph chromosome is detected in 95 % of CML patients (Ph^+) and in 20-30 % of patients suffering from acute lymphoid leukaemia (ALL) (Faderl *et al.* 1999, Ottmann and Wassmann 2005, Melo and Barnes 2007).

Different breakpoints located on *Bcr* gene can give raise to various BCR-ABL fusion proteins, also reviewed by Deininger and colleagues (Deininger *et al.* 2000). As it is seen in Figure 40, the breakpoint within the *Abl* gene occurs upstream of exon Ib, downstream of exon Ia or between the two exons, which is the most frequent event (Melo 1996). The break in *Bcr* gene is located in one of three breakpoint cluster regions (*bcr*). As a hallmark of CML and in about 33 % of ALL the break in *Bcr* gene occurs within the major *bcr* (M-*bcr*) and forms together with ABL a 210 kD fusion protein. Alternative splicing leads to different fusion transcripts with b2a2 or b3a2 junctions. Another breakpoint is located in the so called minor *bcr* (m-*bcr*) mapping to the first intron of *Bcr* gene. The e1a2 junction gives rise to a 185 kD fusion protein, associated with only few CML patients and about 2/3 of ALL (Melo *et al.* 1994, Ravandi *et al.* 1999). A 230 kD fusion protein with breakpoint in µ-*bcr* region and junction of e19a2 was observed in a rare population of chronic neutrophilic leukaemia (Pane *et al.* 1996) (Figure 40).

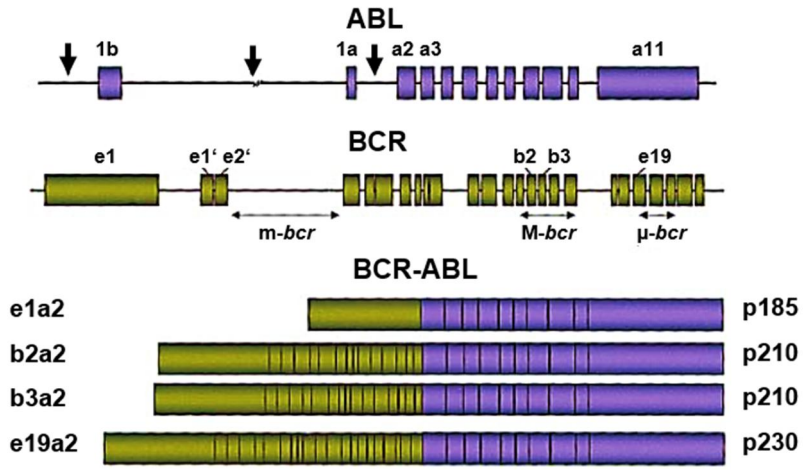

Figure 40. Location of breakpoints in ABL and BCR genes. *Adapted from the review of Deininger et al., Blood, 2000.*

4.7.2. Unchanged leukaemogenesis in *Sfrp2* deficient microenvironment

There was a significant increase of LSK number after 16 weeks in *Sfrp2* deficient microenvironment (Figure 36 E) and a decreased number in secondary transplantations (Figure 39 E). This suggests an increased HSC cycling activity in the *Sfrp2*$^{-/-}$ environment and it was considered, whether the absence of sFPR-2 in the mice might also influence cycling of LSCs and alter the course of myeloproliferative diseases by alterations of stem cell function and quality.

For that, WT donor mice were treated with 5-FU to augment the population of haematopoietic stem and progenitor cells and BM was isolated four days after injection. The BM was infected with p185 e1a2 BCR-ABL and GFP containing retrovirus, which was produced in Phoenix E cells (Chapter 3.15. and 3.16.). As a control MIG empty vector was used. Lethally irradiated *Sfrp2*$^{-/-}$ and WT littermate control mice were transplanted with 1x10^5 GFP$^+$ BCR-ABL or MIG infected bone marrow cells (Figure 41 A). Health state of mice was checked daily. In an average time span of three to four weeks BCR-ABL transplanted mice began to disease. Mice were sacrificed, when general state of health was strongly reduced, following the criteria described below. The analysis of healthy mice was performed after 120 days.

The criteria are based on our standards for determination of burdens on the animal (stress) in animal experiment.

I General state of health:

Reduced: arched back, ruffled fur, slow moving, enforced breathing, sunken flanks

Strongly reduced: dehydrated, apathetic, cold body surface, agonal respiration, swelling, anaemia

II Dietary intake:

Reduced dietary intake > 24 h, reduced body weight

Reduced dietary intake < 24 h, reduced body weight

III Movement activity

Reclusively (sitting in edge of cage), sleepy

Lying without movement

IV Behaviour

Disinterest on environment

Automutilation, apathetic, isolated

V Defecation

Rectal bleeding or diarrhoea >24 h; no defecation

To determine lympho-myeloproliferative disease (LMPD) in the mice after they were sacrificed, I additionally oriented on the physiological criteria of Bethesda proposals for classification of nonlymphoid haematopoietic neoplasms in mice (Kogan *et al.* 2002):

Physiological disease criteria:

Anaemia (RBC $<10^7$/µl)

Leucocytosis (WBC >15,000/µl)

Splenomegaly

Increasing BCR-ABL$^+$ (GFP$^+$) population in PB

The median survival of WT BCR-ABL treated mice was 28 days and 25 days for BCR-ABL treated *Sfrp2* knockout mice which is shown in Kaplan Meier survival curve in

Figure 41 B. Interestingly, all BCR-ABL treated WT mice succumbed to LMPD, while two out of 14 BCR-ABL treated *Sfrp2*$^{-/-}$ mice (14 %) did not develop disease (Figure 41 B).

Peripheral blood, bone marrow and spleen were analysed from moribund recipients. Healthy mice were analysed after a 120 days observation period (17 weeks). After sacrificing mice, the spleen weights of the healthy MIG control mice after a time period of 120 days was 80 mg (±7 mg, n=10). The spleen weight of the two healthy *Sfrp2*$^{-/-}$ mice which received BCR-ABL^{+} cells was found at the higher end of the values of the MIG spleens (100 mg). As expected, BCR-ABL diseased mice developed splenomegaly and the spleen size and weight was strongly increased compared to MIG animal's spleens (Figure 41 C).

The GFP^{+} bone marrow cells were highly increased in mice which developed leukaemia compared to MIG controls and the two not diseased (ND) *Sfrp2*$^{-/-}$ recipients of BCR-ABL^{+} GFP^{+} cells (Figure 41 D left side). Comparing WT and *Sfrp2*$^{-/-}$ recipients of BCR-ABL GFP expressing bone marrow cells, similar total numbers of GFP^{+} cells were found in WT recipients (about 200,000 GFP^{+} cells), while the distribution of total bone marrow cell numbers of *Sfrp2*$^{-/-}$ recipients varied from 60,000 to $1x10^{6}$ (Figure 41 D).

The total white blood cell number (WBC), as analysed by animal blood counter, is in a range from $3x10^{3}$ to $15x10^{3}$ in healthy and MIG control mice. WBC number of BCR-ABL^{+} WT and *Sfrp2*$^{-/-}$ recipient mice was significantly increased compared to MIG control mice, but there was no significant difference between WT and *Sfrp2*$^{-/-}$ recipients. The two *Sfrp2*$^{-/-}$ recipients which did not develop lympho-myeloproliferation exhibited a lower WBC number than the average number in healthy mice ($<1x10^{3}$) (Figure 42).

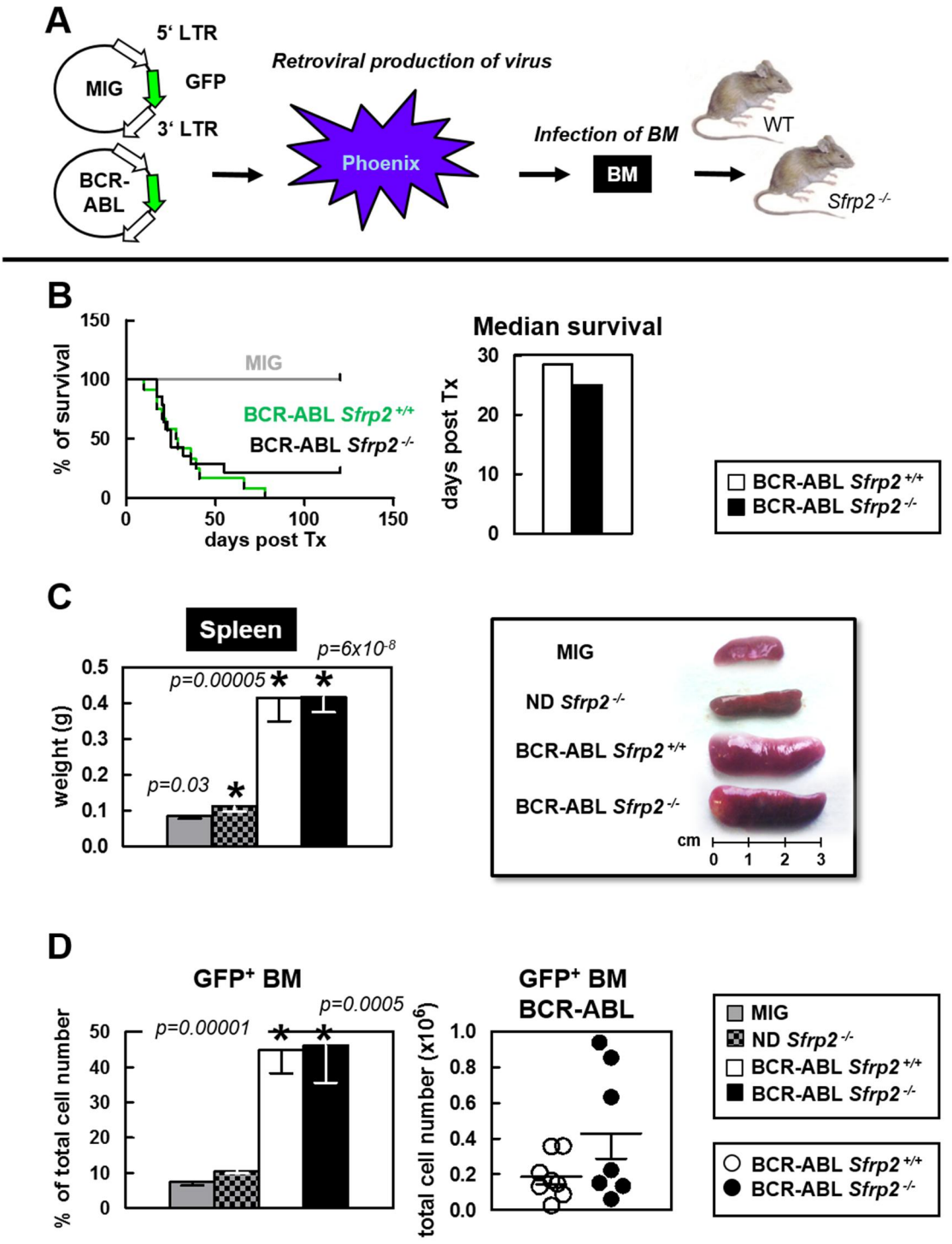

Figure 41. BCR-ABL-induced alterations in Sfrp2 KO and WT mice. *(A) Experimental design. (B) Kaplan-Meier Survival curve MIG (n=15), BCR-ABL Sfrp2 WT littermates (n=12), BCR-ABL Sfrp2 KO (n=14) and median survival in bar plots. (C) Spleen weight (g) and representative pictures of spleens. (D) GFP⁺ bone marrow. Grey line and grey bars: MIG (n=10), checked bars: Sfrp2 not diseased (ND, n=2), Green line, white bars and white circles: Sfrp2$^{+/-}$ littermates and 129xBL/6 (n=8), black line, black bars and circles: BCR-ABL Sfrp2$^{-/-}$ mice (n=7), Mean ± SEM, *p<0.05.*

P185 BCR-ABL mainly induces CML (95 %) and 20-30 % ALL (reviewed by (Deininger *et al.* 2000)). Although, diseased mice exhibited three different types of proliferative disease. The myeloid type (MPD) describes mice with more than 30 % of myeloid cells and less than 10 % of lymphoid cells. The lymphoid type (LPD) is represented by animals expressing more than 30 % lymphoid cells and less than 10 % of myeloid cells. The third type, the mixed form (LMPD), is defined with more than 30 % of both myeloid and lymphoid cells, respectively. Interestingly, *Sfrp2* deficient mice revealed all three types, whereas WT recipient mice showed LPD and LMPD but none of the eight WT mice showed evidence of MPD (Figure 42, 43 and Table 16).

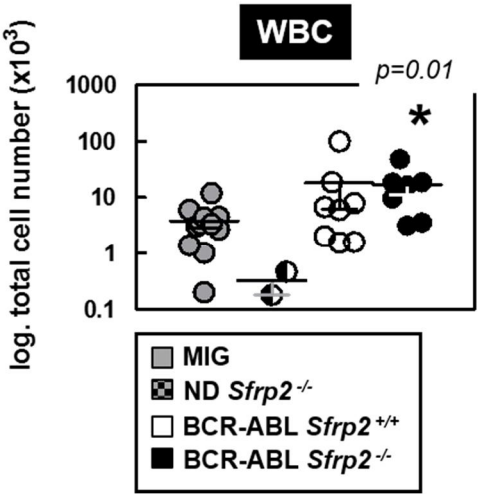

Table 16: Types of leukaemia

Type of leukaemia	*Sfrp2*$^{+/+}$ (n=8)	*Sfrp2*$^{-/-}$ (n=8)
myeloid	-	1
lymphoid	3	1
mixed	5	6

Figure 42. White blood cell number (WBC) and types of leukaemic disease in PB of BCR-ABL treated and control mice. *Left: WBC number. Grey circles: MIG (n=10), checked circles: Sfrp2 KO ND (n=2), white circles: BCR-ABL Sfrp2*$^{+/+}$ *littermates and 129xBL/6 (n=8), black circles: BCR-ABL Sfrp2*$^{-/-}$ *mice (n=8), Mean ± SEM, *p<0.05.*

Table 16: Types of leukaemia. Distribution of types of leukaemia in BCR-ABL *Sfrp2*$^{+/+}$ littermates and 129xBL/6 and BCR-ABL *Sfrp2*$^{-/-}$ mice.

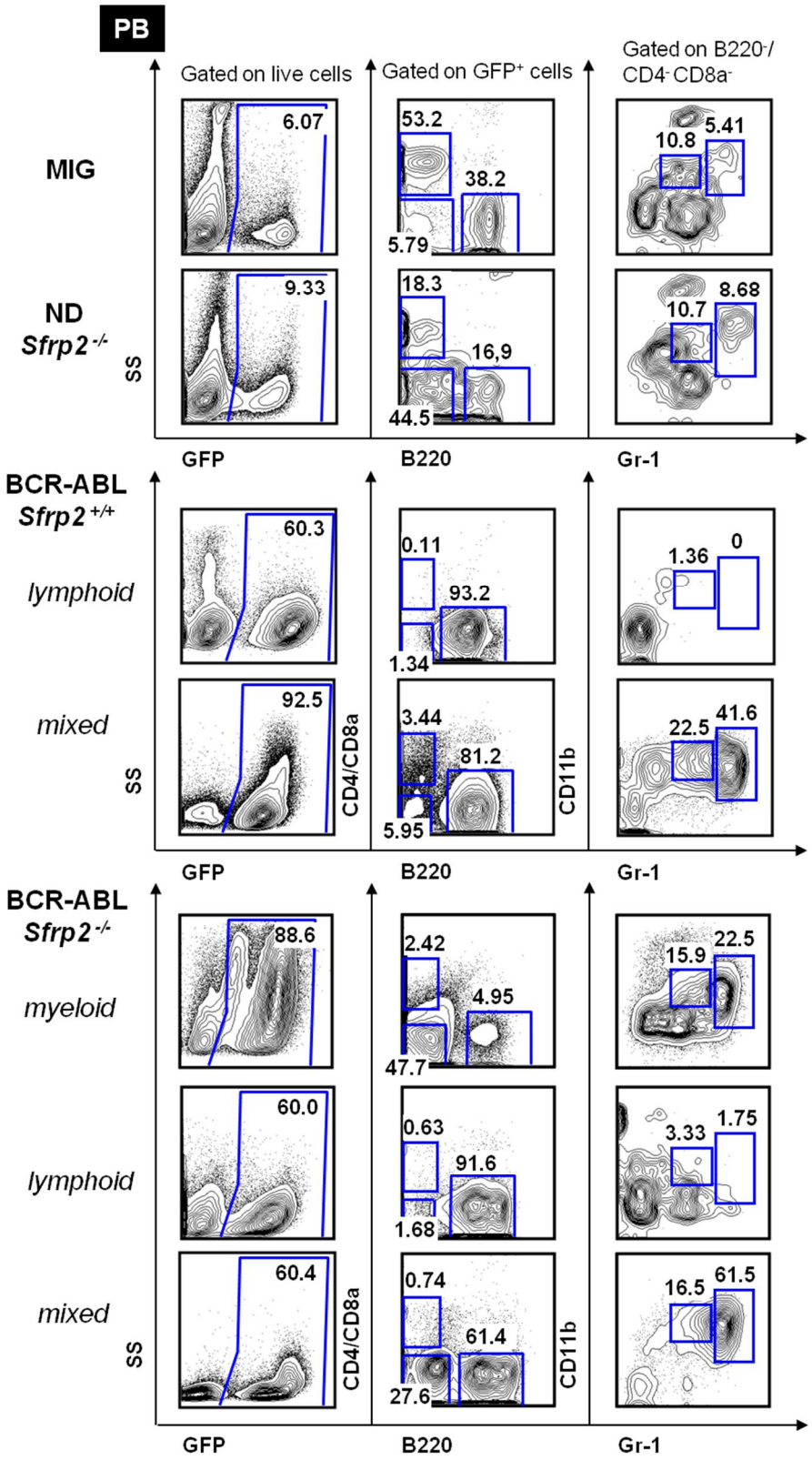

Figure 43. Types of leukaemic disease in PB of BCR-ABL treated and control mice. *Representative FACS plots of lymphoid and myeloid populations in MIG and Sfrp2 KO ND mice (upper panel), BCR-ABL WT littermates with lymphoid and mixed type (middle panel) and BCR-ABL Sfrp2$^{-/-}$ mice, myeloid, lymphoid and mixed type (lower panel).*

However, no major differences were found in BCR-ABL$^+$ LMPD in WT and *Sfrp2*$^{-/-}$ recipient mice (Figure 44 A). To find out whether the earliest GFP$^+$ stem and progenitor cells showed changes, LSKs as well as myeloid and lymphoid progenitors were analysed. Comparing BCR-ABL diseased animals to MIG controls, the WT recipients exhibited a significant increased number of LSKs in the bone marrow. Interestingly, total LSK number of BCR-ABL *Sfrp2*$^{-/-}$ recipient mice was unchanged in comparison to MIG LSKs (Figure 44 B left side). However, statistical analysis comparing BCR-ABL WT and BCR-ABL *Sfrp2*$^{-/-}$ recipients, the total LSK number was unchanged due to the high variation in the number of GFP$^+$ LSKs in WT recipients (Figure 44 B right side). Total number of myeloid and lymphoid progenitor cells was unchanged in BCR-ABL *Sfrp2*$^{-/-}$ mice compared to wild type mice (Figure 44 B right side).

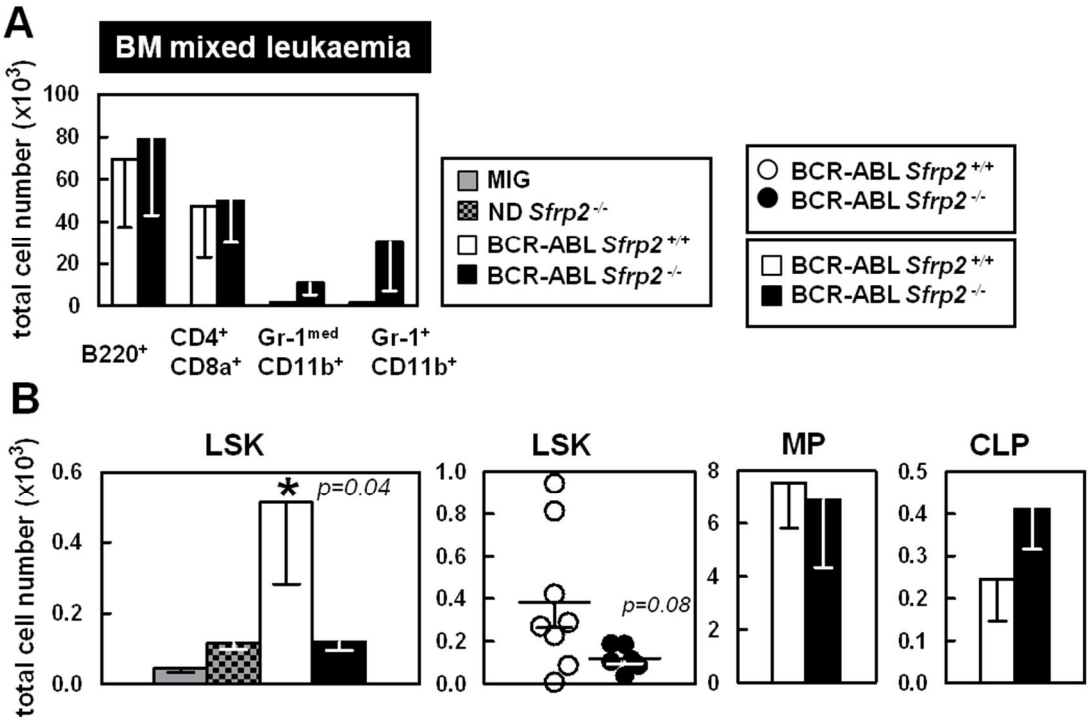

Figure 44. BCR-ABL-induced alterations of haematopoietic mature, progenitor and stem cells in bone marrow of Sfrp2 KOs and WTs. *(A) Total cell number of B220$^+$, CD4$^+$ CD8a$^+$, Gr-1^{med} CD11b$^+$ and Gr-1$^+$ CD11b$^+$ mature haematopoietic cells. (B) Total cell number of LSKs, MPs and CLPs. Grey bars: MIG (n=10), checked bars: ND Sfrp2$^{-/-}$ (n=2), white bars and white circles: BCR-ABL Sfrp2$^{+/+}$ littermates and 129xBL/6 (n=8), black bars and circles: BCR-ABL Sfrp2$^{-/-}$ mice (n=8), Mean ± SEM, *p<0.05.*

To confirm that the BCR-ABL$^+$ disease can be categorized as leukaemia, (LSC) should be able to re-induce the disease in secondary recipients. To find out whether LSCs were

formed in WT and *Sfrp2*$^{-/-}$ recipients, spleen cells of diseased mice were re-transplanted into WT recipients. BCR-ABL WT as well as BCR-ABL *Sfrp2*$^{-/-}$ spleen cells exhibited the capability to re-induce the disease within the same time frame (28-35 days). In peripheral blood about 75 % of GFP^{+} cells were detected. The cells reconstituted all mature lineages (Figure 45).

In summary, the absence of sFRP-2 does not play a major role in haematopoietic cell proliferation and differentiation in a model of BCR-ABL-induced LMPD.

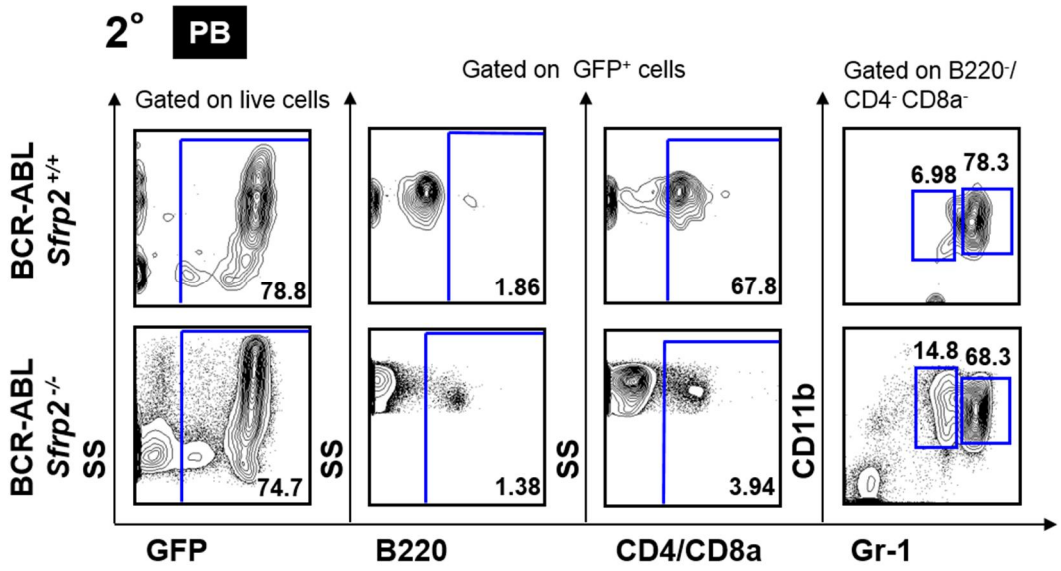

Figure 45. Secondary engraftment and lineage reconstitution of spleen cells of BCR-ABL diseased mice in peripheral blood of WT recipients. *Representative FACS plots; BCR-ABL Sfrp2*$^{+/+}$ *(upper row) and BCR-ABL Sfrp2*$^{-/-}$ *(lower row).*

LSCs from different malignant diseases have been shown to alter the balance and function of niche cells, so called niche hijacking (Lutzny *et al.* 2013). Interestingly, a reduced function of OBCs and strongly reduced bone mineralization was observed in AML mouse model (Frisch *et al.* 2012). Additionally the niche can be remodelled, as myeloid leukaemic cells stimulate MSCs to produce a high number of transformed OBCs in a transgenic model of BCR-ABL^{+} LMPD (Schepers *et al.* 2013). Thus, the question arose, whether leukaemia-induced alterations of the microenvironment may be different in *Sfrp2*$^{-/-}$ mice compared to the WT recipients.

In order to analyse this aspect of leukaemia, the number of mesenchymal stromal/stem cells (MSCs), osteoblastic cells (OBCs), and endothelial cells was determined in WT and *Sfrp2*$^{-/-}$ mice transplanted with MIG or BCR-ABL^{+} cells. The definition of niche cell populations followed the same scheme as in steady state analysis of the niche cell phenotypes (Nakamura *et al.* 2010) (Chapter 4.2.4).

Comparing niche cells of WT and *Sfrp2*$^{-/-}$ mice with BCR-ABL^{+} LMPD demonstrated no significant alterations in the number of MSCs, OBCs or endothelial cell populations (Figure 46 left side).

Nevertheless, some interesting differences were detected, comparing niche cells from control (MIG) WT and *Sfrp2*$^{-/-}$ recipients with mice receiving BCR-ABL-expressing cells (BCR-ABL WT, BCR-ABL *Sfrp2*$^{-/-}$ and BCR-ABL ND). The total cell number of MSCs was significantly increased in the two healthy *Sfrp2*$^{-/-}$ recipients receiving BCR-ABL cells. In addition, OBCs also exhibited an increase in these ND mice compared to MIG controls, suggesting that in these recipients, the niche might actively suppress the formation of LSCs. In endothelial cell fractions, the cell number was strongly decreased in all BCR-ABL treated mice in general (Figure 46 right side).

These results show the important role of the niche which changes after transplantation. Also, the results show that the niche in WT and *Sfrp2*$^{-/-}$ is remodelled in a similar manner. In summary, the data indicate that the niche is altered by leukaemia. However, the niche remodelling is mainly driven by BCR-ABL^{+} cells and does not seem to be dependent on *Sfrp2* deficiency in niche cells.

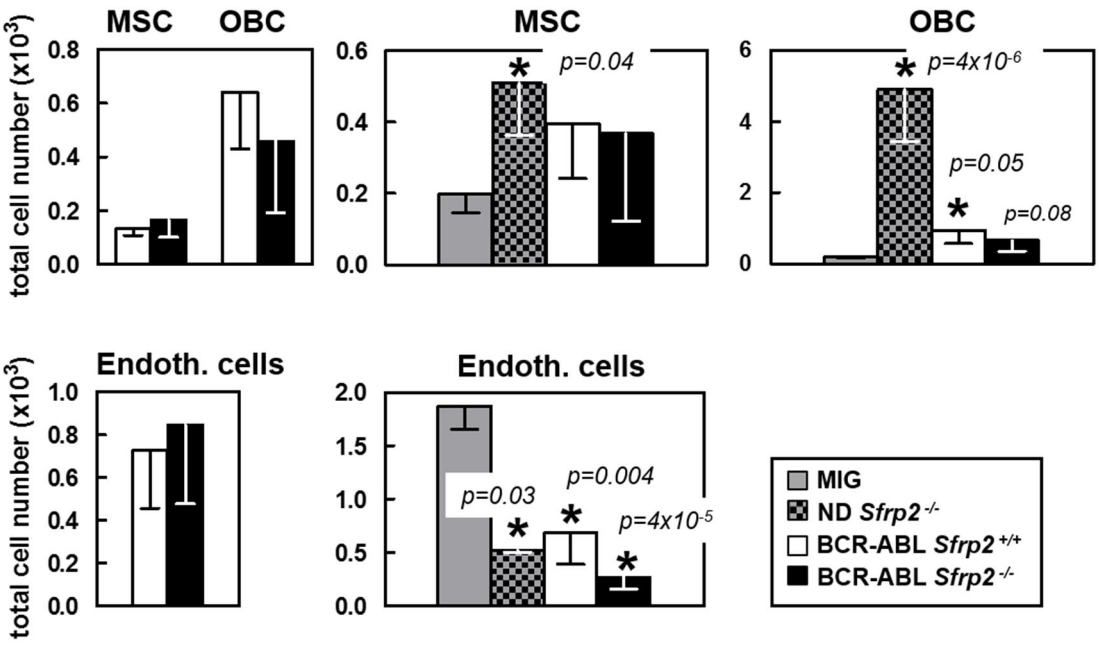

Figure 46. BCR-ABL-induced alterations of bone marrow niche in Sfrp2 KO and WT mice. *Total cell number of MSCs, OBCs (upper panel) and endothelial cells (lower panel). Grey bars: MIG (n=10), checked bars: Sfrp2 KO ND (n=2), white bars: Sfrp2$^{+/+}$ littermates and 129xBL/6 (n=8), black bars: BCR-ABL Sfrp2$^{-/-}$ mice (n=8), Mean ± SEM, *p<0.05.*

5. Discussion

Haematopoietic stem cells are a rare population of cells, residing within the bone marrow niche in a quiescent state throughout lifetime in adult mammals. The crucial role of the microenvironment in the regulation of HSC self-renewal, activation and differentiation processes is slowly elucidated. The maintenance of HSCs in G0/G1 phase of cell cycle and HSC activation to reconstitute the blood system in particular, are sensitive to the interaction of HSCs and the niche. The regulation of HSCs by the niche is governed by adhesion molecules, extracellular matrix and soluble factors. A central class of soluble niche factors shown by several investigators to modulate HSC number and quality, are members of the Wnt signalling pathway. Wnt-3a (Luis *et al.* 2009) is mainly secreted by haematopoietic cells themselves and activates the canonical Beta-catenin-dependent pathway (Cobas *et al.* 2004, Kirstetter *et al.* 2006, Jeannet *et al.* 2008, Koch *et al.* 2008, Luis *et al.* 2011). Although the focus in the study of Wnt signalling has been on canonical signalling for a long time, non-canonical signals, for instance through Wnt-5a (Liang *et al.* 2003, Murdoch *et al.* 2003, Nemeth *et al.* 2007) or Frizzled 8 (Fz-8) and Flamingo (Fmi) (Sugimura *et al.* 2012) are now known to be also crucial in HSC-niche interactions.

In HSC-supportive embryo derived stromal cell lines, the soluble Wnt regulators sFRP-1 and sFRP-2 were highly overexpressed compared to their expression level in non-supportive cell lines (Oostendorp *et al.* 2005) and sFRP-1 and sFRP-2 are expressed in important niche cells, the osteoblasts (Nakajima *et al.* 2009). Our previously published data showed that sFRP-1 extrinsically regulates HSC maintenance through the cell cycle (Renstrom *et al.* 2009). In this thesis, I studied the effect of *Sfrp2* deficiency on HSCs and their interaction with bone marrow microenvironment in steady state and after stress induction. I did not only study haematopoietic cells, but since recent data suggests that sFRP-2 might influence the niche cells themselves (Alfaro *et al.* 2008), I also studied the number of niche cells and the differentiation potential of mesenchymal stromal/stem cells.

My studies show that sFRP-2 affects the activation and repopulation behaviour of LSKs after transplantation and after genotoxic or natural stress induction.

5.1. *Sfrp2* KO in steady state haematopoiesis and in BM niche

5.1.1. Alterations in adult steady state haematopoiesis and Wnt signalling

When the adult mouse haematopoietic hierarchy was analysed, I found unchanged number of mature lymphoid and myeloid haematopoietic cells, regardless of the haematopoietic tissue studied (BM, spleen and peripheral blood (Figure 13, 14)). Further, an unchanged number of myeloid and lymphoid progenitors (MPs, CLPs) and LSK cells was detected in adult mice (Figure 15, 16). These results show that haematopoiesis in *Sfrp2*$^{-/-}$ mice is similar as in WT mice. Interestingly, however, data indicate a significantly decreased number of the earliest HSC-like CD34^{-} CD150^{+} LSK cell population (Figure 17 A). Additionally, a decreased proliferative activity was shown in staining for Ki-67 (Figure 26) and Cyclin-D1 in LSK cells (Figure 22 A, B). Cyclin-D1 is a known target of Wnt signalling (Figure 2). Indeed, canonical Wnt signalling appeared to be diminished (Figure 22, 23, 25), suggesting a Wnt signalling stimulating role of sFRP-2, which was contrary to the expectations, since sFRP-2 has been reported to inhibit canonical Wnt signalling (Kim *et al.* 2001, Suzuki *et al.* 2004, Shaham *et al.* 2009). But it was also reported that sFRP-2 augments Wnt-3a-dependent Wnt signalling (von Marschall and Fisher 2010). The background of these seemingly contrary data could be that sFRP-2 elicits different responses, depending on the constellation of Fz receptors expressed. Thus, sFRP-2 was recently shown to inhibit Wnt-3a signalling in the context of the expression of Fz-2, but augment Wnt-3a signalling in the context of Fz-5 receptors (Xavier *et al.* 2014). This context-dependent outcome of Fz signalling has not systematically been studied on different haematopoietic populations. Although LSK cells express Fz-4 (Buckley *et al.* 2011) and other reports show expression of Fz-3, -4, -6 and -9 in fetal liver-derived LSK (Heinonen *et al.* 2011), future studies should resolve which contexts promote, and which contexts inhibit Wnt signalling in HSCs.

The non-canonical Wnt signalling pathway has been studied only sparsely in haematopoiesis, but recently, it has become more weight through studies about Wnt-4 (Heinonen *et al.* 2011) Wnt-5a (Nemeth *et al.* 2007) and Flamingo (Sugimura *et al.* 2012). The effect of *Sfrp2* in non-canonical signalling was not studied so far, and the thesis' results show that activity of this pathway is decreased, as protein levels of NF-ATc and PPAR-gamma were significantly reduced in LSKs (Figure 24 A, B and Figure 25). Conform to this hypothesis, it has been shown that stimulation of endothelial cells with sFRP-2 activates Ca^{2+}-dependent Wnt signalling via calcineurin/NF-AT (Courtwright *et al.* 2009). My results thus strongly suggest that sFRP-2 is an activator of both canonical and non-canonical Wnt signalling in haematopoiesis in LSK cells.

As it is presented in Figures 22 C, 23 and 24 C, canonical and non-canonical Wnt signalling is also reduced in the absence of sFRP-2 in myeloid and lymphoid progenitors (MPs and CLPs), but surprisingly, canonical target Cyclin-D1 and c-Myc level was enhanced in MPs, showing differential Wnt signalling in different progenitor populations. Non-canonical signalling member NLK negatively regulates Beta-catenin-dependent Wnt signalling over phosphorylation of TCF/LEF, inhibiting the binding of Beta-catenin/TCF/LEF complex to DNA for transcriptional activation of its target genes (Yamada *et al.* 2006, Lv *et al.* 2014) and the overexpression of NLK suppressed the Beta-catenin/LEF binding (Xu *et al.* 2014). Thus, a reduced NLK level in *Sfrp2* knockout cells might indirectly increase canonical target protein level compared to the WT.

Taken together, the absence of sFRP-2 reduces both canonical and Ca^{2+}-dependent non-canonical Wnt signalling in primitive haematopoietic cells. As the effect of sFRP-2 is also Fz-dependent (Xavier *et al.* 2014), it will be interesting to further study the expression profile of Fz proteins in early haematopoietic cell populations in *Sfrp2*$^{-/-}$ and WT mice. This analysis could further clarify the context of the expression of different Fzs on different populations in the presence or absence of Wnt modulator sFRP-2.

5.1.2. Decreased adipogenic differentiation of MSCs

The investigations of niche cell components indicated a slightly enhanced number of MSCs but no changes in osteoblastic cell number of *Sfrp2* knockout mice compared to WT controls (Figure 20 B). Interestingly, MSCs deficient in *Sfrp2* showed a strongly reduced potential to differentiate into adipocytes, while the osteogenic differentiation does not seem to be affected (Figure 21 C).

SFRP-2 has been proposed to be a key mediator of MSC regulation. However the literature's results are quite contrary to the thesis' data showing a reduced number of MSCs. It has been published that recombinant sFRP-2 enhances MSC self-renewal (Alfaro *et al.* 2008). These authors defined MSCs are untreated granulo-monocytic-depleted murine bone marrow cells, which were cultured on fibronectin-coated dishes with supplements. In this thesis, I used a different definition of MSCs. Here, MSCs are defined as a population of cells, isolated from collagenase-treated flushed bones and further defined through described surface marker (Nakamura *et al.* 2010) (Figure 6). More importantly, the cells I isolated as MSCs were not cultured. Thus, the results are hardly comparable.

The absence of sFRP-2 was shown to restrict differentiation of cultured MSC into adipogenic lineage, but does not influence osteogenic differentiation potential (Figure 21 C). Although it was out of the thesis' scope, it would be interesting to further study molecular regulators of adipo- and osteogenesis, such as PPAR-gamma, Runx2 and C/EBP-alpha in WT and *Sfrp2*$^{-/-}$ MSCs. Peroxisome proliferator-activated receptor-gamma (PPAR-gamma) and Runt-related transcription factor 2 (Runx-2) are key regulators of the balance between osteogenic and adipogenic differentiation (reviewed by (James 2013)) as well as C/EPB-alpha (Fan *et al.* 2009).

The complete knockout of *Sfrp2* does not influence the differentiation of MSC into osteogenic lineage cells (Figure 21 C). Thus, sFRP-2 does not seem to affect the number of cells capable of osteogenesis. Further downstream events of osteogenesis, such as

bone formation itself, were not studied in the thesis. Published reports suggest that efficient bone formation depends on sFRP-2 (Roux 2010), particularly in mineralization of mature osteoblasts. It may also be of interest that sFRP-2 is highly secreted by mineralized osteoblasts in the endosteal niche (Roux 2010), suggesting that sFRP-2 constitutes an autocrine mechanism in the promotion of bone. Interestingly, there are also contrary studies, which describe sFRP-2 as a suppressor of bone formation in malformations like multiple myeloma (Oshima *et al.* 2005) and ameloblastoma (Sathi *et al.* 2009). The studies referred to, are not directly comparable and raise new questions. Such as that sFRP-2 may have different functions under steady state conditions and conditions of cancer cell modified niche function.

The data presented in my thesis show for the first time that *in vivo*, the MSCs are increased in number, dependent on *Sfrp2* deficiency. My data also suggest that the balance between adipo- and osteogenesis is disturbed in *Sfrp2* deficient mice. Whether these *in vitro* findings mean that bone structure of *Sfrp2* deficient mice *in vivo* is also changed should be part of future studies.

5.2. *Sfrp2* KO vs. *Sfrp1* KO in adult steady state haematopoiesis

The haematopoietic niche is essential for the developing haematopoiesis and the regulation of HSCs in the adult system. Recently, several genes were found to be overrepresented in HSC-supporting stromal cells including *Sfrp2* and its family member *Sfrp1* (Oostendorp *et al.* 2005, Ledran *et al.* 2008). SFRP-1 was recently described to extrinsically regulate haematopoietic stem cells (Renstrom *et al.* 2009).

The fetal liver (FL) is one of the first haematopoietic tissues in the developing embryo. HSCs are in a highly proliferative state during embryogenesis and the fetal program is driven until three to four weeks after birth (Bowie *et al.* 2007, Kim *et al.* 2007). I found a reduced total cell number of fetal liver cells in *Sfrp2*$^{-/-}$ mice (Figure 11), as well as an enhanced fraction of LSKs and also long-term repopulating CD34^{+} LSKs in fetal livers of

Sfrp2$^{-/-}$ mice (Figure 12 B). So far, the effect of either *Sfrp2*$^{-/-}$ or *Sfrp1*$^{-/-}$ in fetal haematopoiesis has not been reported.

In former studies, our group published the sFRP-1-dependent extrinsic regulation of HSCs (Renstrom *et al.* 2009). Considering the reported redundancy of sFRP-1 and sFRP-2 (also described in Chapter 1.4.1. and 1.4.2.), we expected a similar phenotype of *Sfrp1*$^{-/-}$ and *Sfrp2*$^{-/-}$ mice. Surprisingly, in adult *Sfrp2* KO mice the HSC-like CD34^{-} CD150^{+} LSKs were significantly reduced (Figure 17 A), while in contrast, this population is increased in *Sfrp1*$^{-/-}$ mice. Further, Figure 17 B presents an enhanced clonogenic potential of myeloid progenitors in *Sfrp2*$^{-/-}$ mice, but we previously showed a decreased number of CFU-GM in the absence of sFRP-1. Thus, LSK cells from *Sfrp1*$^{-/-}$ and *Sfrp2*$^{-/-}$ do not behave similar. However, in line with the results of a reduced proliferative activity of *Sfrp2* deficient HSCs (Figure 22 (Cyclin-D1) and Figure 26 (Ki-67)), *Sfrp1*$^{-/-}$ mice showed a decreased cell cycling activity as less BrdU incorporation was detected accompanied with a decreased expression of the Wnt signalling target *Cyclin-D1* on transcriptional level (Renstrom *et al.* 2009). Additionally, Beta-catenin protein was reduced in both *Sfrp1*$^{-/-}$ and *Sfrp2*$^{-/-}$ LSK cells (Figure 22). One possible explanation for these disparities and similarities observed, is exemplified by *in vitro* data of Xavier and colleagues, who found that different levels of sFRP-1 determines its role as inhibitor or activator of Wnt signalling. Interestingly, sFRP-2 was also shown to dose-independently activated canonical Wnt signalling (Xavier *et al.* 2014).

In summary, sFRP-2 is integrated in a sensitive network of regulatory mechanisms of various pathways interacting with the other niche factors, like for instance sFRP-1. My results strongly suggest that sFRP-2 and sFRP-1 are not interchangeable redundant factors in the regulation of maintenance and self-renewal of HSCs. However, I did not find such differences in the activation of canonical Wnt signalling in LSK cells from these mice. The possible role of non-canonical Wnt signalling was not explored in detail, since this pathway consists of several parallel and interacting pathways, which include Ca^{2+}-dependent and small GTPase-dependent planar cell polarity signalling.

Perhaps sFRP-1 and sFRP-2 are neither strictly redundant nor non-redundant. Considering publications of Esteve and group (Esteve *et al.* 2011) or Xavier and colleagues (Xavier *et al.* 2014), it is well possible that depending on tissue, dose, or Fz expression pattern, sFRP-1 and sFRP-2 may be redundant, or not. However, the dose of the two sFRPs, or the Fz patterns of different haematopoietic stem and progenitor cells have, so far, not been investigated.

5.3. *Sfrp2* KO alters the activation of HSCs

5.3.1. SFRP-2-dependent extrinsic activation of HSC

In mice the detailed expression pattern of sFRP-2 was only studied during embryogenesis (Leimeister *et al.* 1998), so far. SFRP-2 was mainly found in mesenchymal compartments, particularly in craniofacial mesenchyme and smooth muscle cells.

I have also found expression of *Sfrp2* transcript in haematopoietic cells (Figure 34), suggesting that loss of *Sfrp2* in HSCs might have intrinsic consequences for their regulation. However, in line with our previous experiments with *Sfrp1*$^{-/-}$ mice (Renstrom *et al.* 2009), intrinsic transplantation studies, did not show any significant alterations in the long-term repopulation ability of *Sfrp2*$^{-/-}$ HSCs (Figure 35). This indicates that intrinsic loss of *Sfrp2* in HSCs does not affect stem cell self-renewal, maintenance or differentiation.

In experiments designed to determine extrinsic effects of *Sfrp2* loss, *in vitro* co-cultures exhibited an increased number of LSKs co-cultured on *Sfrp2* KD stroma, and their clonogenic activity was also increased (Figure 10). This finding is in line with our previous findings showing an increased clonogenic activity of myeloid progenitors in co-cultures on *Sfrp1* KD stroma (Renstrom *et al.* 2009). This *in vitro* system provides evidence that sFRP-2 is involved in extrinsic regulation of HSC activation.

In the thesis, I further studied extrinsic effects of *Sfrp2* deficiency in the niche through injection of WT cells into *Sfrp2* KO mice. My findings show that in this model of

regenerative stress, LSKs are over-activated, as exemplified by Wnt signalling-dependent increased cell cycle activity (Figure 37) and an increase in cell number (Figure 36 E).

Very interestingly, after secondary transplantation, the HSCs were reduced (Figure 39 E and cartoon Figure 47 1° and 2°). Since over-activation of HSCs may indicate reduced ability to return to a quiescent state, this finding could be attributed to stem cell exhaustion.

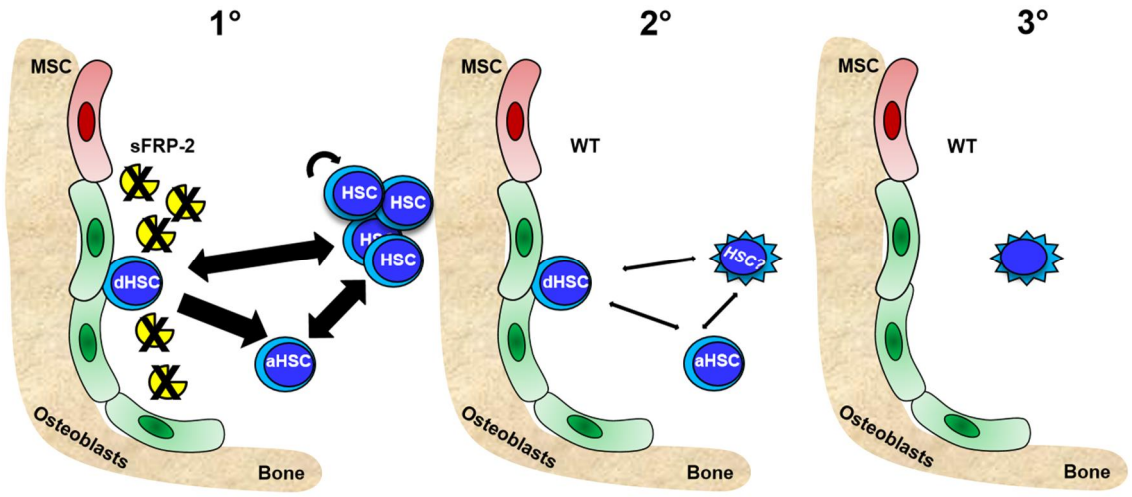

Figure 47. Extrinsic effect of Sfrp2 KO in serial transplantations of WT LSKs. *In endosteal niche OBs and MSCs regulate HSC homeostasis. (1°) HSC over-activation after primary transplantation in Sfrp2$^{-/-}$ recipients. (2°) Reduction of HSCs in secondary recipients. 1° and 2° summarize the thesis' data described in Chapter 4.6. (3°) Hypothesised HSC exhaustion after tertiary transplantation.*

Indeed, when I calculate the percentage of engrafted LSKs after first and secondary transplantation (Figure 48), 80 % of WT LSKs were able to engraft into a *Sfrp2* deficient niche, but seem to lose their quality as engraftment level decreases to 15 % in secondary recipients. If this trend is extrapolated into 3° recipients, one could envision very low engraftment level or even graft failure. This experiment has, in fact been performed. As it is a long-term transplantation assay, the results are not finalized at the time of submission of this thesis (Figure 47 3°).

Thus, my results suggest that sFRP-2 is required for the long-term maintenance of the self-renewing pool of HSCs. This hypothesis is supported by data showing that

CD34$^-$ LSK cells cultured with SCF, TPO and sFRP-2 exhibit a highly increased long-term repopulating potential compared to CD34$^-$ LSK cells cultured with only SCF and TPO (Nakajima *et al.* 2009).

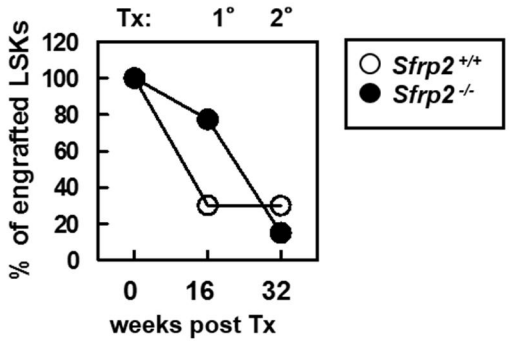

Figure 48. Percentage of engrafted LSKs after 1° and 2° transplantation. *White circles: Sfrp2$^{+/+}$ littermates, black circles: Sfrp2$^{-/-}$ mice.*

5.3.2. Over-activation of HSCs due to genotoxic and natural stress, but not after inflammatory stress induction

In vivo extrinsic transplantation studies revealed that HSCs are over-activated and their quality is diminished after regenerative activation in the absence of sFRP-2. These results suggest that sFRP-2 is required for proper regeneration, when the haematopoietic system is challenged. In my thesis, I have set up several experimental approaches to investigate activation of HSCs of *Sfrp2* KO mice, using models of genotoxic (5-FU), natural (aging), or inflammatory stress (leukaemia).

Genotoxic stress induced by 5-FU

Genotoxicity describes events inducing DNA damage, which leads to mutations and may induce cancer. Cells prevent genotoxic stress by DNA repair or apoptosis. Shim and colleagues previously analysed the response of Drosophila blood cells to events of stress conditions like oxidative stress, hypoxia and infection. They showed that systemic and nutritional signals maintained haematopoietic progenitors in a Wingless signalling-dependent way (Wnt in mammals) (Shim *et al.* 2012). So far, *Sfrp2* has not directly been linked to a response to genotoxic stress. It is, however, entirely possible that stress regulates the level of sFRP-2, since sFRP-2 is targeted for suppression by a transforming

mutant of the stress sensor p53 (p53 (val135) (Yam *et al.* 1999). This mutant promotes cellular proliferation, a feature which would be consistent with decreased sFRP-2 levels.

The chemotoxic reagent 5-FU induced genotoxic stress by causing an imbalance of the dNTP pool, which leads to DNA damage (Figure 30). After treatment of *Sfrp2* KO mice with 5-FU, LSKs and $CD34^-$ $CD150^+$ LSKs were strongly increased (Figure 31 D) due to a larger proportion of cells in S-phase (Figure 32 C). This finding indicates increased proliferative activity in *Sfrp2*$^{-/-}$ mice compared to WT mice. This could mean that the regenerating activated LSK cells actually have a decreased long-term-repopulating ability. This could be studied in transplantation experiments using LSK cells from 5-FU-treated donors.

Natural stress: Aging

In the thesis, aging is defined as “natural stress”. Under pathogen-free conditions, aging HSCs undergo various qualitative and quantitative changes (Waterstrat and Van Zant 2009). The pool size of $CD150^+$ $CD48^-$ LSKs increases, lymphoid-biased HSCs get lost and more myeloid-biased HSCs occur, while they have a reduced potential to reconstitute mature blood cells (Dykstra *et al.* 2011), and they also exhibited reduced long-term repopulating activity.

In this thesis, in “middle aged” (twelve to 16 months old) *Sfrp2*$^{-/-}$ mice, the number of LSKs and $CD34^-$ $CD150^+$ LSKs was highly increased compared to WT mice (Figure 19 A, B). This is consistent with the already discussed results of increased number of LSKs after genotoxic stress induction via 5-FU and the regenerative stress HSC phenotype after 1° transplantation. An enhanced relative number of LSKs in aged mice compared to young mice has been found by several investigators (Morrison *et al.* 1996, Sudo *et al.* 2000, Rossi *et al.* 2007, Dykstra and de Haan 2008, Dykstra *et al.* 2011). Surprisingly, the thesis’ data showed, that the absolute LSK number is reduced in aged WT compared to young WT mice, while LSK number of *Sfrp2*$^{-/-}$ mice remains consistent during aging (Figure 19 C). Compared to recently published data of Dykstra and colleagues, a possible explanation for the controversy results might be, that in the thesis twelve to 16

months old “middle aged mice” were used, while old mice are described at the age of 24 to 26 months (Dykstra *et al.* 2011). Indeed, a kinetic analysis from young to old, combined with analysis at several time points leading up to 24 months and more has not been reported, so far. A second possible reason might be that there are differences between strains of mice (129xBL/6 in our study, compared to BL/6 in other studies, Dykstra *et al.*, 2011). Consistent with other data, however, a highly increased $CD34^-$ $CD150^+$ LSK pool was found compared to young animals (14-fold in WT and even over 50-fold in *Sfrp2*$^{-/-}$ (Figure 17 and 19)). Thus, the increase of primitive $CD34^-$ $CD150^+$ LSKs is already detectable in middle aged mice. Furthermore, the deficiency of *Sfrp2* enhances the increase even further, probably due to a more pronounced stress response.

Taken together, my data indicate that sFRP-2 is crucial in the events of stress and activation. Primary transplantations as well as genotoxic (5-FU) or natural (aging) stress showed similar strong increases in LSKs, particularly the most primitive $CD34^-$ $CD150^+$ LSK cell populations. In a forced over-activated regenerative response, a strongly decreased LSK number is shown in secondary recipients at a total of 32 weeks after initial transplantation, due to *Sfrp2* deficiency. This suggests a beginning (accelerated?) HSC exhaustion, dependent on the absence of sFRP-2. Thus, my data support the view that sFRP-2 is required to maintain the most primitive $CD34^-$ $CD150^+$ LSK population containing the long-term repopulating cells.

Inflammatory stress induced by oncogene BCR-ABL

During aging, lymphoid-biased HSCs get lost. Consequently, there is a reduced number of lymphocytes, which results in an impaired immune-response in disease and cancer in age (Cho *et al.* 2008). Concomitantly, an increased myelopoiesis is observed, increasing the chance of myeloid malignancies. Thus, considering my findings of a strongly increased population of $CD34^-$ $CD150^+$ LSK cells in middle-aged mice, I studied the question, whether *Sfrp2* might also influence HSCs during leukaemogenesis. Recent evidence has shown that the niche changes in the presence of malignant haematopoietic cells and undergoes inflammatory conversion changes (Lutzny *et al.* 2013, Schepers *et*

al. 2013, Kode *et al.* 2014, Medyouf *et al.* 2014). Thus, increased DNA damage, and thus genotoxic stress may occur during leukaemogenesis.

Considering the over-activation and possible exhaustion in extrinsic transplantations and the increased number of LSKs after natural or genotoxic stress, alterations in lag-time and severity of leukaemogenesis in *Sfrp2*$^{-/-}$ mice were anticipated. However, no alteration in latency time was detected in the development of BCR-ABL^{+} LMPD in *Sfrp2* KO recipient mice compared to WT recipients (Figure 41 B).

Very little is known about the state of Wnt signalling and its modulators in non-haematopoietic niche cells in the presence of leukaemic cells. Whether the expression of Wnt inhibitors and activators is affected, or if signal transduction through this pathway is altered in cells of the leukaemic niche, still needs to be elucidated. Therefore, it would be interesting to perform qPCR analysis of niche cells of WT BCR-ABL diseased mice, to investigate the expression level of *Sfrp2* on RNA level. Also the sFRP-2 protein expression level should be analysed in MSCs OBCs and endothelial cells by immunofluorescence single cell staining.

Although no significant changes were detected in cells of haematopoietic hierarchy in the BM, interestingly, the LSK number was even fourfold decreased in diseased *Sfrp2*$^{-/-}$ BCR-ABL treated mice (Mean= 100) compared to controls (Mean= 400). As the data did not show significant alterations in myeloid and lymphoid progenitor or mature cells, differentiation seems not to be affected. Although the changes in primitive BCR-ABL^{+} cells in *Sfrp2*$^{-/-}$ recipients leave room for speculation, all mice transplanted with GFP^{+} cells from either WT or *Sfrp2*$^{-/-}$ recipients developed secondary LMPD, indicating that leukaemic stem cells developed regardless of the niche genotype. Thus, contrary to other forms of stress (5-FU, regeneration, aging), loss of *Sfrp2* does not affect BCR-ABL^{+} leukaemogenesis.

5.4. Conclusion

In my PhD thesis' project, the role of Wnt signalling modulator Secreted frizzled-related protein 2, *Sfrp2*, in steady state haematopoiesis and haematopoietic stress conditions was investigated.

My results indicate that sFRP-2 is important in steady state haematopoiesis, as *Sfrp2* deficiency reduces the number of HSC-like $CD34^-$ $CD150^+$ LSKs (Figure 49). However, *Sfrp2*$^{-/-}$ HSCs repopulate WT recipients similarly as WT donor HSCs, showing that despite that sFRP-2 expression is detectable in CLPs and $Gr\text{-}1^+$ $CD11b^+$ haematopoietic cells, there are no intrinsic functional differences in *Sfrp2*$^{-/-}$ HSCs compared to WT HSCs.

Under stress conditions the role of sFRP-2 has never been investigated before. The thesis' results demonstrate for the first time a clear increase of HSCs in *Sfrp2* deficient mice under challenging conditions. Figure 49 presents the imbalance of HSC homeostasis under challenging conditions (Figure 49 right), manifesting itself in an over-activation of HSCs. The increase in donor LSKs after *in vivo* transplantation of WT HSC into *Sfrp2*$^{-/-}$ recipients indicate a niche-dependant, extrinsic effect of *Sfrp2* deficiency. In the latter experiments of regenerative stress, further transplantations of regenerated HSCs from *Sfrp2*$^{-/-}$ recipients showed a decrease of LSKs in secondary recipients, suggesting a slow exhaustion of repopulating HSCs after serial transplantation. Since serial transplantation is a functional assay of self-renewal, these results indicate that HSC maintenance and self-renewal is reduced in *Sfrp2*$^{-/-}$ recipients. In Figure 47 a model of exhaustion of the LT-HSC pool is proposed.

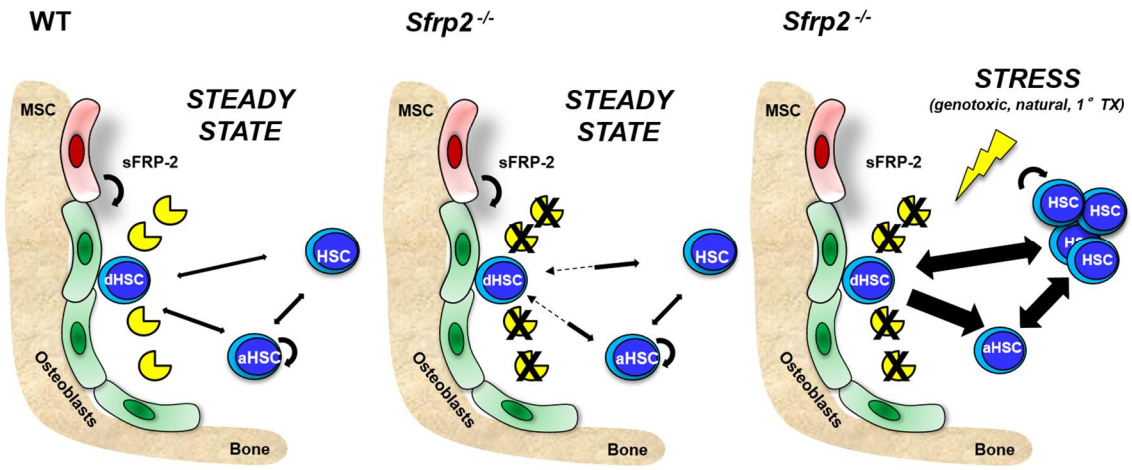

Figure 49. HSC behaviour in endosteal bone marrow niche. *Steady state haematopoiesis WT (left) and Sfrp2$^{-/-}$ mice (middle); HSC behaviour under genotoxic and natural stress conditions and after 1° extrinsic transplantation in Sfrp2$^{-/-}$ mice (right).*

Thus my results demonstrate for the first time that sFRP-2 is required for long-term maintenance of the self-renewing pool of long-term repopulating HSCs. Together with recently published data for sFRP-1 and PTN (Renstrom *et al.* 2009, Istvanffy *et al.* 2011), sFRP-2 is another candidate of niche secretome which is crucial for cell-cell interaction of HSCs and the niche. Beyond, sFRP-2 was demonstrated to be an important regulator of dHSC activation under stress conditions. After serial transplantations *Sfrp2* deficiency impairs HSC phenotype and function.

6. Appendices

6.1. List of Figures

6.2. List of Tables

6.3. List of Abbreviations

5-FU	5-Fluorouracile
7-AAD	7-amino-actinomycin D
ABL	Abelson Musine Leukaemia Viral Oncogene Homolog 1
ALCAM	Activated leukocyte cell adhesion molecule
ALL	Acute lymphoid leukaemia
AML	Acute myeloid leukaemia
APC	Allophycocyanin
BCR	Breakpoint cluster region
BM	Bone marrow
BrdU	5-bromo-2'-deoxyuridine
BSA	Bovine serum albumine
Ca^{2+}	$Calcium^{2+}$
CLL	Chronic lymphoid leukaemia
CML	Chronic myeloid leukaemia
CNA	Calcineurin A
CaMK-II	Calcium/calmodulin-dependent protein kinase type II
CD	Cluster of differentiation
C/EBP alpha	CCAAT/enhancer-binding protein alpha
CFU	Colony forming unity
CLP	Common lymphoid progenitor
CMP	Common myeloid progenitors
c-Myc	Proto-oncogene c-Myc
Cy	Cyanine
Cyclin-D1	G1/S-specific cyclin-D1
CXCR4	C-X-C chemokine receptor type 4
CXCL12	C-X-C motif chemokine 12 (Stromal cell-derived factor 1/SDF-1)
DAPI	4,6-diamino-2-phenylindole dihydrochloride
DMEM	Dulbecco´s modified Eagle´s medium
DMSO	Dimetylsulfoxide
DNA	Desoxyribonucleic acid
DVL-2	Segment polarity protein dishevelled homolog DVL-2
Eos	Eosinophiles
FACS	Fluorescence activated cell sorting
FCS	Fetal Calf Serum
FITC	Fluoresceinisothiocyanat
Fz	Frizzled
GF	Growth factors
GFP	Green fluorescent protein

GMP	Granulocyte-monocyte-progenitor
Gran	Granulocytes
GSK-3 beta	Glycogen synthase kinase-3 beta
HCT	Haematocrit
HBSS	Hank´s buffered salt solution
HEPES	2-(4-(2-Hydroxyethyl)- 1-piperazinyl)-ethansulfonsäure
HSC	Haematopoietic stem cells
Ig	Immunoglobulin
IL	Interleukin
JNK1	Stress-activated protein kinase JNK1
KD	Knockdown
KO	Knockout
LMPD	Lympho-Myeloproliferative disease
LPD	Lymphoproliferative disease
LSC	Leukaemic stem cells
LSK	$Lin^- SCA\text{-}1^+ KIT^+$
LT-HSC	Long-term repopulating haematopoietic stem cell
Lymph	Lymphoids
MEP	Megakaryocyte-erythrocyte progenitor
MIG	Murine stem cell virus (**M**SCV), internal ribosomal entry side (**I**RES), green fluorescent protein (**G**FP)
Mono	Monocytes
MPD	Myeloproliferative disease
mRNA	Messenger ribonucleic acid
MP	Multipotent progenitor
NF-ATc	Nuclear factor of activated T-cells, cytoplasmic
NLK	Serine/threonine-protein kinase NLK (Nemo-like kinase)
PB	Peripheral blood
PBS	phosphate buffered saline
PCR	Polymerase chain reaction
PE	R-Phycoerythrin
PI	Propidium iodide
PLC-beta-3	1-phosphatidylinositol 4,5-bisphosphate phosphodiesterase beta-3
pLKO.1	Plasmid, LKO.1 5': sequencing primer within human U6 promoter
PLT	Platelets
PPAR-gamma	Peroxisome proliferator-activated receptor gamma
PTN	Pleiotrophin
qRT-PCR	quantitative real time PCR
RBC	Red blood cells

RNA	Ribonucleic acid
ROR2	Tyrosine-protein kinase transmembrane receptor ROR2
Rpl	Ribosomal protein L
RYK	Tyrosine-protein kinase RYK
sFRP	Secreted frizzled-related protein
shRNA	Small hairpin ribonucleic acid
ST-HSC	Short-term repopulating haematopoietic stem cell
WBC	White blood cells
Wnt	Wingless-type MMTV integration site family member
WT	Wild type

7. Publication

- Istvanffy,R., Kröger M., Eckl C**.**, Gitzelmann S., Vilne B., **Bock F.,** Graf S., Schiemann M., Keller U.B., Peschel C. & Oostendorp R.A.J. *Stromal pleiotrophin regulates repopulation-behavior of hematopoetic stem cells*. Blood, 2011.

- Schreck, C.,* **Bock, F**.,* Grziwok, S., Oostendorp, R. A., Istvanffy, R. *Regulation of hematopoiesis by activators and inhibitors of Wnt signaling from the niche.* Ann N Y Acad Sci, 2014.

  * *These two authors contributed equally*

8. Acknowledgements

Ich möchte mich an dieser Stelle bei allen herzlich bedanken, die zum Gelingen meiner Arbeit beigetragen haben.

Mein besonderer Dank gilt Professor Christian Peschel, der mir die Möglichkeit gegeben hat an diesem interessanten und anspruchsvollen Projekt im wissenschaftlichen Umfeld der III. Medizinischen Klinik am Klinikum rechts der Isar zu arbeiten.

Ganz herzlich bedanke ich mich bei meinem Doktorvater Professor Robert Oostendorp, der mir stets mit fachlichem Rat zur Seite stand und mir darüber hinaus die Möglichkeit gab mein Promotionsprojekt und auch mich selbst weiterzuentwickeln.

Vielen Dank an meine lieben Kolleginnen der Ag. Oostendorp für die Einarbeitung, unsere Diskussionen und die schöne Zeit. Vielen lieben Dank vor allem an Dr. Rouzanna Istvanffy, Christina Schreck und Charlotta Pagel, die mich in allen Phasen der Promotion wunderbar unterstützt haben.

Danke auch an die Mikrobiologie für die langjährige Möglichkeit das FACS-Gerät mitzubenutzen, sowie an Matthias Schiemann und Lynette Henkel für die Sort-Termine.

Das Projekt wurde von der Deutschen Forschungsgemeinschaft (DFG) sowie der José Carreras Leukämie-Stiftung e.V. finanziert.

Vielen Dank an meine Familie und meine Freunde, die mir immer den nötigen Ausgleich gegeben haben. Von ganzem Herzen danke ich meinem Mann Philipp für seine liebe Unterstützung und Geduld. Du hast mir den Rückhalt und den Glauben an mich selbst gegeben, um dieses Projekt meistern zu können. Es wäre ohne dich nicht möglich gewesen.

9. References

Abelson, H. T. and L. S. Rabstein (1970). "Lymphosarcoma: virus-induced thymic-independent disease in mice." Cancer Res **30**(8): 2213-2222.

Adolfsson, J., R. Mansson, et al. (2005). "Identification of Flt3+ lympho-myeloid stem cells lacking erythro-megakaryocytic potential a revised road map for adult blood lineage commitment." Cell **121**(2): 295-306.

Akashi, K., M. Kondo, et al. (1998). "Role of interleukin-7 in T-cell development from hematopoietic stem cells." Immunol Rev **165**: 13-28.

Alfaro, M. P., M. Pagni, et al. (2008). "The Wnt modulator sFRP2 enhances mesenchymal stem cell engraftment, granulation tissue formation and myocardial repair." Proc Natl Acad Sci U S A **105**(47): 18366-18371.

Austin, T. W., G. P. Solar, et al. (1997). "A role for the Wnt gene family in hematopoiesis: expansion of multilineage progenitor cells." Blood **89**(10): 3624-3635.

Baksh, D., G. M. Boland, et al. (2007). "Cross-talk between Wnt signaling pathways in human mesenchymal stem cells leads to functional antagonism during osteogenic differentiation." J Cell Biochem **101**(5): 1109-1124.

Balazs, A. B., A. J. Fabian, et al. (2006). "Endothelial protein C receptor (CD201) explicitly identifies hematopoietic stem cells in murine bone marrow." Blood **107**(6): 2317-2321.

Beals, C. R., N. A. Clipstone, et al. (1997). "Nuclear localization of NF-ATc by a calcineurin-dependent, cyclosporin-sensitive intramolecular interaction." Genes Dev **11**(7): 824-834.

Beals, C. R., C. M. Sheridan, et al. (1997). "Nuclear export of NF-ATc enhanced by glycogen synthase kinase-3." Science **275**(5308): 1930-1934.

Beerman, I., D. Bhattacharya, et al. (2010). "Functionally distinct hematopoietic stem cells modulate hematopoietic lineage potential during aging by a mechanism of clonal expansion." Proc Natl Acad Sci U S A **107**(12): 5465-5470.

Beerman, I., W. J. Maloney, et al. (2010). "Stem cells and the aging hematopoietic system." Curr Opin Immunol **22**(4): 500-506.

Benz, C., M. R. Copley, et al. (2012). "Hematopoietic stem cell subtypes expand differentially during development and display distinct lymphopoietic programs." Cell Stem Cell **10**(3): 273-283.

Blackshaw, S., S. Harpavat, et al. (2004). "Genomic analysis of mouse retinal development." PLoS Biol **2**(9): E247.

Boudin, E., I. Fijalkowski, et al. (2013). "The role of extracellular modulators of canonical Wnt signaling in bone metabolism and diseases." Semin Arthritis Rheum.

Bowie, M. B., D. G. Kent, et al. (2007). "Steel factor responsiveness regulates the high self-renewal phenotype of fetal hematopoietic stem cells." Blood **109**(11): 5043-5048.

Buckley, S. M., F. Ulloa-Montoya, et al. (2011). "Maintenance of HSC by Wnt5a secreting AGM-derived stromal cell line." Exp Hematol **39**(1): 114-123 e111-115.

Burda, P., N. Curik, et al. (2009). "PU.1 activation relieves GATA-1-mediated repression of Cebpa and Cbfb during leukemia differentiation." Mol Cancer Res **7**(10): 1693-1703.

Calvi, L. M., G. B. Adams, et al. (2003). "Osteoblastic cells regulate the haematopoietic stem cell niche." Nature **425**(6960): 841-846.

Chan, C. K., P. Lindau, et al. (2013). "Clonal precursor of bone, cartilage, and hematopoietic niche stromal cells." Proc Natl Acad Sci U S A **110**(31): 12643-12648.

Cho, J. S., S. H. Kook, et al. (2013). "Cell autonomous and nonautonomous mechanisms drive hematopoietic stem/progenitor cell loss in the absence of DNA repair." Stem Cells **31**(3): 511-525.

Cho, R. H., H. B. Sieburg, et al. (2008). "A new mechanism for the aging of hematopoietic stem cells: aging changes the clonal composition of the stem cell compartment but not individual stem cells." Blood **111**(12): 5553-5561.

Christensen, J. L. and I. L. Weissman (2001). "Flk-2 is a marker in hematopoietic stem cell differentiation: a simple method to isolate long-term stem cells." Proc Natl Acad Sci U S A **98**(25): 14541-14546.

Clevers, H. and R. Nusse (2012). "Wnt/beta-catenin signaling and disease." Cell **149**(6): 1192-1205.

Cobas, M., A. Wilson, et al. (2004). "Beta-catenin is dispensable for hematopoiesis and lymphopoiesis." J Exp Med **199**(2): 221-229.

Courtwright, A., S. Siamakpour-Reihani, et al. (2009). "Secreted frizzle-related protein 2 stimulates angiogenesis via a calcineurin/NFAT signaling pathway." Cancer Res **69**(11): 4621-4628.

Curtis, K. M., L. A. Gomez, et al. (2010). "EF1alpha and RPL13a represent normalization genes suitable for RT-qPCR analysis of bone marrow derived mesenchymal stem cells." BMC Mol Biol **11**: 61.

de Bruijn, M. F., N. A. Speck, et al. (2000). "Definitive hematopoietic stem cells first develop within the major arterial regions of the mouse embryo." EMBO J **19**(11): 2465-2474.

Deininger, M. W., J. M. Goldman, et al. (2000). "The molecular biology of chronic myeloid leukemia." Blood **96**(10): 3343-3356.

Ding, L., T. L. Saunders, et al. (2012). "Endothelial and perivascular cells maintain haematopoietic stem cells." Nature **481**(7382): 457-462.

Dykstra, B. and G. de Haan (2008). "Hematopoietic stem cell aging and self-renewal." Cell Tissue Res **331**(1): 91-101.

Dykstra, B., D. Kent, et al. (2007). "Long-term propagation of distinct hematopoietic differentiation programs in vivo." Cell Stem Cell **1**(2): 218-229.

Dykstra, B., S. Olthof, et al. (2011). "Clonal analysis reveals multiple functional defects of aged murine hematopoietic stem cells." J Exp Med **208**(13): 2691-2703.

Dzierzak, E. and N. A. Speck (2008). "Of lineage and legacy: the development of mammalian hematopoietic stem cells." Nat Immunol **9**(2): 129-136.

Ehninger, A. and A. Trumpp (2011). "The bone marrow stem cell niche grows up: mesenchymal stem cells and macrophages move in." J Exp Med **208**(3): 421-428.

Eidinoff, M. L., L. Cheong, et al. (1959). "Incorporation of unnatural pyrimidine bases into deoxyribonucleic acid of mammalian cells." Science **129**(3362): 1550-1551.

Essers, M. A., S. Offner, et al. (2009). "IFNalpha activates dormant haematopoietic stem cells in vivo." Nature **458**(7240): 904-908.

Essers, M. A. and A. Trumpp (2010). "Targeting leukemic stem cells by breaking their dormancy." Mol Oncol **4**(5): 443-450.

Esteve, P., A. Sandonis, et al. (2011). "Secreted frizzled-related proteins are required for Wnt/beta-catenin signalling activation in the vertebrate optic cup." Development **138**(19): 4179-4184.

Faderl, S., M. Talpaz, et al. (1999). "The biology of chronic myeloid leukemia." N Engl J Med **341**(3): 164-172.

Fan, Q., T. Tang, et al. (2009). "The role of CCAAT/enhancer binding protein (C/EBP)-alpha in osteogenesis of C3H10T1/2 cells induced by BMP-2." J Cell Mol Med **13**(8B): 2489-2505.

Fleming, H. E., V. Janzen, et al. (2008). "Wnt signaling in the niche enforces hematopoietic stem cell quiescence and is necessary to preserve self-renewal in vivo." Cell Stem Cell **2**(3): 274-283.

Florian, M. C., K. J. Nattamai, et al. (2013). "A canonical to non-canonical Wnt signalling switch in haematopoietic stem-cell ageing." Nature **503**(7476): 392-396.

Frassoni, F., N. G. Testa, et al. (1982). "The relative spatial distribution of erythroid progenitor cells (BFUe and CFUe) in the normal mouse femur." Cell Tissue Kinet **15**(4): 447-455.

Frenette, P. S., S. Pinho, et al. (2013). "Mesenchymal stem cell: keystone of the hematopoietic stem cell niche and a stepping-stone for regenerative medicine." Annu Rev Immunol **31**: 285-316.

Friedenstein, A. J., R. K. Chailakhyan, et al. (1987). "Bone marrow osteogenic stem cells: in vitro cultivation and transplantation in diffusion chambers." Cell Tissue Kinet **20**(3): 263-272.

Friedenstein, A. J., U. F. Deriglasova, et al. (1974). "Precursors for fibroblasts in different populations of hematopoietic cells as detected by the in vitro colony assay method." Exp Hematol **2**(2): 83-92.

Frisch, B. J., J. M. Ashton, et al. (2012). "Functional inhibition of osteoblastic cells in an in vivo mouse model of myeloid leukemia." Blood **119**(2): 540-550.

Fuchs, E., T. Tumbar, et al. (2004). "Socializing with the neighbors: stem cells and their niche." Cell **116**(6): 769-778.

Garrett, R. W. and S. G. Emerson (2009). "Bone and blood vessels: the hard and the soft of hematopoietic stem cell niches." Cell Stem Cell **4**(6): 503-506.

Gekas, C., F. Dieterlen-Lievre, et al. (2005). "The placenta is a niche for hematopoietic stem cells." Dev Cell **8**(3): 365-375.

Geyh, S., S. Oz, et al. (2013). "Insufficient stromal support in MDS results from molecular and functional deficits of mesenchymal stromal cells." Leukemia **27**(9): 1841-1851.

Gonchoroff, N. J., P. R. Greipp, et al. (1985). "A monoclonal antibody reactive with 5-bromo-2-deoxyuridine that does not require DNA denaturation." Cytometry **6**(6): 506-512.

Goodell, M. A., M. Rosenzweig, et al. (1997). "Dye efflux studies suggest that hematopoietic stem cells expressing low or undetectable levels of CD34 antigen exist in multiple species." Nat Med **3**(12): 1337-1345.

Heinonen, K. M., J. R. Vanegas, et al. (2011). "Wnt4 enhances murine hematopoietic progenitor cell expansion through a planar cell polarity-like pathway." PLoS One **6**(4): e19279.

Ikegawa, M., H. Han, et al. (2008). "Syndactyly and preaxial synpolydactyly in the single Sfrp2 deleted mutant mice." Dev Dyn **237**(9): 2506-2517.

Ikuta, K. and I. L. Weissman (1992). "Evidence that hematopoietic stem cells express mouse c-kit but do not depend on steel factor for their generation." Proc Natl Acad Sci U S A **89**(4): 1502-1506.

Istvanffy, R., M. Kroger, et al. (2011). "Stromal pleiotrophin regulates repopulation behavior of hematopoietic stem cells." Blood **118**(10): 2712-2722.

Jaiswal, N., S. E. Haynesworth, et al. (1997). "Osteogenic differentiation of purified, culture-expanded human mesenchymal stem cells in vitro." J Cell Biochem **64**(2): 295-312.

James, A. W. (2013). "Review of Signaling Pathways Governing MSC Osteogenic and Adipogenic Differentiation." Scientifica (Cairo) **2013**: 684736.

Jeannet, G., M. Scheller, et al. (2008). "Long-term, multilineage hematopoiesis occurs in the combined absence of beta-catenin and gamma-catenin." Blood **111**(1): 142-149.

Jin, L., K. J. Hope, et al. (2006). "Targeting of CD44 eradicates human acute myeloid leukemic stem cells." Nat Med **12**(10): 1167-1174.

Jones, S. E. and C. Jomary (2002). "Secreted Frizzled-related proteins: searching for relationships and patterns." Bioessays **24**(9): 811-820.

Jost, E., J. Schmid, et al. (2008). "Epigenetic inactivation of secreted Frizzled-related proteins in acute myeloid leukaemia." Br J Haematol **142**(5): 745-753.

Kawano, Y. and R. Kypta (2003). "Secreted antagonists of the Wnt signalling pathway." J Cell Sci **116**(Pt 13): 2627-2634.

Kele, J., E. R. Andersson, et al. (2012). "SFRP1 and SFRP2 dose-dependently regulate midbrain dopamine neuron development in vivo and in embryonic stem cells." Stem Cells **30**(5): 865-875.

Kent, D. G., M. R. Copley, et al. (2009). "Prospective isolation and molecular characterization of hematopoietic stem cells with durable self-renewal potential." Blood **113**(25): 6342-6350.

Kiel, M. J., M. Acar, et al. (2009). "Hematopoietic stem cells do not depend on N-cadherin to regulate their maintenance." Cell Stem Cell **4**(2): 170-179.

Kiel, M. J. and S. J. Morrison (2008). "Uncertainty in the niches that maintain haematopoietic stem cells." Nat Rev Immunol **8**(4): 290-301.

Kiel, M. J., G. L. Radice, et al. (2007). "Lack of evidence that hematopoietic stem cells depend on N-cadherin-mediated adhesion to osteoblasts for their maintenance." Cell Stem Cell **1**(2): 204-217.

Kiel, M. J., O. H. Yilmaz, et al. (2005). "SLAM family receptors distinguish hematopoietic stem and progenitor cells and reveal endothelial niches for stem cells." Cell **121**(7): 1109-1121.

Kieslinger, M., S. Hiechinger, et al. (2010). "Early B cell factor 2 regulates hematopoietic stem cell homeostasis in a cell-nonautonomous manner." Cell Stem Cell **7**(4): 496-507.

Kim, A. S., S. A. Anderson, et al. (2001). "Pax-6 regulates expression of SFRP-2 and Wnt-7b in the developing CNS." J Neurosci **21**(5): RC132.

Kim, I., T. L. Saunders, et al. (2007). "Sox17 dependence distinguishes the transcriptional regulation of fetal from adult hematopoietic stem cells." Cell **130**(3): 470-483.

Kirstetter, P., K. Anderson, et al. (2006). "Activation of the canonical Wnt pathway leads to loss of hematopoietic stem cell repopulation and multilineage differentiation block." Nat Immunol **7**(10): 1048-1056.

Kobayashi, K., M. Luo, et al. (2009). "Secreted Frizzled-related protein 2 is a procollagen C proteinase enhancer with a role in fibrosis associated with myocardial infarction." Nat Cell Biol **11**(1): 46-55.

Koch, U., A. Wilson, et al. (2008). "Simultaneous loss of beta- and gamma-catenin does not perturb hematopoiesis or lymphopoiesis." Blood **111**(1): 160-164.

Kode, A., J. S. Manavalan, et al. (2014). "Leukaemogenesis induced by an activating beta-catenin mutation in osteoblasts." Nature **506**(7487): 240-244.

Kogan, S. C., J. M. Ward, et al. (2002). "Bethesda proposals for classification of nonlymphoid hematopoietic neoplasms in mice." Blood **100**(1): 238-245.

Kondo, M., I. L. Weissman, et al. (1997). "Identification of clonogenic common lymphoid progenitors in mouse bone marrow." Cell **91**(5): 661-672.

Krause, D. S., K. Fulzele, et al. (2013). "Differential regulation of myeloid leukemias by the bone marrow microenvironment." Nat Med **19**(11): 1513-1517.

Krause, D. S., K. Lazarides, et al. (2006). "Requirement for CD44 in homing and engraftment of BCR-ABL-expressing leukemic stem cells." Nat Med **12**(10): 1175-1180.

Laneuville, P. (1995). "Abl tyrosine protein kinase." Semin Immunol **7**(4): 255-266.

Ledran, M. H., A. Krassowska, et al. (2008). "Efficient hematopoietic differentiation of human embryonic stem cells on stromal cells derived from hematopoietic niches." Cell Stem Cell **3**(1): 85-98.

Lee, J. L., C. T. Lin, et al. (2004). "Autocrine/paracrine secreted Frizzled-related protein 2 induces cellular resistance to apoptosis: a possible mechanism of mammary tumorigenesis." J Biol Chem **279**(15): 14602-14609.

Leimeister, C., A. Bach, et al. (1998). "Developmental expression patterns of mouse sFRP genes encoding members of the secreted frizzled related protein family." Mech Dev **75**(1-2): 29-42.

Li, B., A. S. Bailey, et al. (2010). "Endothelial cells mediate the regeneration of hematopoietic stem cells." Stem Cell Res **4**(1): 17-24.

Li, S., R. L. Ilaria, Jr., et al. (1999). "The P190, P210, and P230 forms of the BCR/ABL oncogene induce a similar chronic myeloid leukemia-like syndrome in mice but have different lymphoid leukemogenic activity." J Exp Med **189**(9): 1399-1412.

Liang, H., Q. Chen, et al. (2003). "Wnt5a inhibits B cell proliferation and functions as a tumor suppressor in hematopoietic tissue." Cancer Cell **4**(5): 349-360.

Lo Celso, C., H. E. Fleming, et al. (2009). "Live-animal tracking of individual haematopoietic stem/progenitor cells in their niche." Nature **457**(7225): 92-96.

Lodygin, D., A. Epanchintsev, et al. (2005). "Functional epigenomics identifies genes frequently silenced in prostate cancer." Cancer Res **65**(10): 4218-4227.

Logan, C. Y. and R. Nusse (2004). "The Wnt signaling pathway in development and disease." Annu Rev Cell Dev Biol **20**: 781-810.

Longley, D. B., D. P. Harkin, et al. (2003). "5-fluorouracil: mechanisms of action and clinical strategies." Nat Rev Cancer **3**(5): 330-338.

Luis, T. C., B. A. Naber, et al. (2011). "Canonical wnt signaling regulates hematopoiesis in a dosage-dependent fashion." Cell Stem Cell **9**(4): 345-356.

Luis, T. C., F. Weerkamp, et al. (2009). "Wnt3a deficiency irreversibly impairs hematopoietic stem cell self-renewal and leads to defects in progenitor cell differentiation." Blood **113**(3): 546-554.

Lutzny, G., T. Kocher, et al. (2013). "Protein kinase c-beta-dependent activation of NF-kappaB in stromal cells is indispensable for the survival of chronic lymphocytic leukemia B cells in vivo." Cancer Cell **23**(1): 77-92.

Lv, L., C. Wan, et al. (2014). "Nemo-like kinase (NLK) inhibits the progression of NSCLC via negatively modulating WNT signaling pathway." J Cell Biochem **115**(1): 81-92.

Ma, Y. D., C. Park, et al. (2009). "Defects in osteoblast function but no changes in long-term repopulating potential of hematopoietic stem cells in a mouse chronic inflammatory arthritis model." Blood **114**(20): 4402-4410.

Mak, K. S., A. P. Funnell, et al. (2011). "PU.1 and Haematopoietic Cell Fate: Dosage Matters." Int J Cell Biol **2011**: 808524.

Maltseva, D. V., N. A. Khaustova, et al. (2013). "High-throughput identification of reference genes for research and clinical RT-qPCR analysis of breast cancer samples." J Clin Bioinforma **3**(1): 13.

Mao, B., W. Wu, et al. (2002). "Kremen proteins are Dickkopf receptors that regulate Wnt/beta-catenin signalling." Nature **417**(6889): 664-667.

Mao, J., J. Wang, et al. (2001). "Low-density lipoprotein receptor-related protein-5 binds to Axin and regulates the canonical Wnt signaling pathway." Mol Cell **7**(4): 801-809.

Martin, V., X. Agirre, et al. (2008). "Methylation status of Wnt signaling pathway genes affects the clinical outcome of Philadelphia-positive acute lymphoblastic leukemia." Cancer Sci **99**(9): 1865-1868.

Martin, V., A. Valencia, et al. (2010). "Epigenetic regulation of the non-canonical Wnt pathway in acute myeloid leukemia." Cancer Sci **101**(2): 425-432.

Matsuoka, S., Y. Ebihara, et al. (2001). "CD34 expression on long-term repopulating hematopoietic stem cells changes during developmental stages." Blood **97**(2): 419-425.

Medvinsky, A. and E. Dzierzak (1996). "Definitive hematopoiesis is autonomously initiated by the AGM region." Cell **86**(6): 897-906.

Medyouf, H., M. Mossner, et al. (2014). "Myelodysplastic cells in patients reprogram mesenchymal stromal cells to establish a transplantable stem cell niche disease unit." Cell Stem Cell **14**(6): 824-837.

Melo, J. V. (1996). "The diversity of BCR-ABL fusion proteins and their relationship to leukemia phenotype." Blood **88**(7): 2375-2384.

Melo, J. V. and D. J. Barnes (2007). "Chronic myeloid leukaemia as a model of disease evolution in human cancer." Nat Rev Cancer **7**(6): 441-453.

Melo, J. V., H. Myint, et al. (1994). "P190BCR-ABL chronic myeloid leukaemia: the missing link with chronic myelomonocytic leukaemia?" Leukemia **8**(1): 208-211.

Mendez-Ferrer, S., T. V. Michurina, et al. (2010). "Mesenchymal and haematopoietic stem cells form a unique bone marrow niche." Nature **466**(7308): 829-834.

Miething, C., C. Mugler, et al. (2003). "Phosphorylation of tyrosine 393 in the kinase domain of Bcr-Abl influences the sensitivity towards imatinib in vivo." Leukemia **17**(9): 1695-1699.

Mikkola, H. K. and S. H. Orkin (2006). "The journey of developing hematopoietic stem cells." Development **133**(19): 3733-3744.

Ming, M., S. Wang, et al. (2012). "Activation of Wnt/beta-catenin protein signaling induces mitochondria-mediated apoptosis in hematopoietic progenitor cells." J Biol Chem **287**(27): 22683-22690.

Mirotsou, M., Z. Zhang, et al. (2007). "Secreted frizzled related protein 2 (Sfrp2) is the key Akt-mesenchymal stem cell-released paracrine factor mediating myocardial survival and repair." Proc Natl Acad Sci U S A **104**(5): 1643-1648.

Mohrin, M., E. Bourke, et al. (2010). "Hematopoietic stem cell quiescence promotes error-prone DNA repair and mutagenesis." Cell Stem Cell **7**(2): 174-185.

Moore, M. A. and D. Metcalf (1970). "Ontogeny of the haemopoietic system: yolk sac origin of in vivo and in vitro colony forming cells in the developing mouse embryo." Br J Haematol **18**(3): 279-296.

Morello, R., T. K. Bertin, et al. (2008). "Brachy-syndactyly caused by loss of Sfrp2 function." J Cell Physiol **217**(1): 127-137.

Morikawa, S., Y. Mabuchi, et al. (2009). "Prospective identification, isolation, and systemic transplantation of multipotent mesenchymal stem cells in murine bone marrow." J Exp Med **206**(11): 2483-2496.

Morita, Y., H. Ema, et al. (2010). "Heterogeneity and hierarchy within the most primitive hematopoietic stem cell compartment." J Exp Med **207**(6): 1173-1182.

Morrison, S. J. and A. C. Spradling (2008). "Stem cells and niches: mechanisms that promote stem cell maintenance throughout life." Cell **132**(4): 598-611.

Morrison, S. J., A. M. Wandycz, et al. (1996). "The aging of hematopoietic stem cells." Nat Med **2**(9): 1011-1016.

Morrison, S. J. and I. L. Weissman (1994). "The long-term repopulating subset of hematopoietic stem cells is deterministic and isolatable by phenotype." Immunity **1**(8): 661-673.

Muller, A. M., A. Medvinsky, et al. (1994). "Development of hematopoietic stem cell activity in the mouse embryo." Immunity **1**(4): 291-301.

Murdoch, B., K. Chadwick, et al. (2003). "Wnt-5A augments repopulating capacity and primitive hematopoietic development of human blood stem cells in vivo." Proc Natl Acad Sci U S A **100**(6): 3422-3427.

Nagasawa, T., Y. Omatsu, et al. (2011). "Control of hematopoietic stem cells by the bone marrow stromal niche: the role of reticular cells." Trends Immunol **32**(7): 315-320.

Nakajima, H., M. Ito, et al. (2009). "Wnt modulators, SFRP-1, and SFRP-2 are expressed in osteoblasts and differentially regulate hematopoietic stem cells." Biochem Biophys Res Commun **390**(1): 65-70.

Nakamura, Y., F. Arai, et al. (2010). "Isolation and characterization of endosteal niche cell populations that regulate hematopoietic stem cells." Blood **116**(9): 1422-1432.

Neering, S. J., T. Bushnell, et al. (2007). "Leukemia stem cells in a genetically defined murine model of blast-crisis CML." Blood **110**(7): 2578-2585.

Nemeth, M. J., L. Topol, et al. (2007). "Wnt5a inhibits canonical Wnt signaling in hematopoietic stem cells and enhances repopulation." Proc Natl Acad Sci U S A **104**(39): 15436-15441.

Nojima, M., H. Suzuki, et al. (2007). "Frequent epigenetic inactivation of SFRP genes and constitutive activation of Wnt signaling in gastric cancer." Oncogene **26**(32): 4699-4713.

Nowell, P. C. and D. A. Hungerford (1960). "Chromosome studies on normal and leukemic human leukocytes." J Natl Cancer Inst **25**: 85-109.

Nygren, M. K., G. Dosen, et al. (2007). "Wnt3A activates canonical Wnt signalling in acute lymphoblastic leukaemia (ALL) cells and inhibits the proliferation of B-ALL cell lines." Br J Haematol **136**(3): 400-413.

Oostendorp, R. A., K. N. Harvey, et al. (2002). "Stromal cell lines from mouse aorta-gonads-mesonephros subregions are potent supporters of hematopoietic stem cell activity." Blood **99**(4): 1183-1189.

Oostendorp, R. A., A. J. Medvinsky, et al. (2002). "Embryonal subregion-derived stromal cell lines from novel temperature-sensitive SV40 T antigen transgenic mice support hematopoiesis." J Cell Sci **115**(Pt 10): 2099-2108.

Oostendorp, R. A., C. Robin, et al. (2005). "Long-term maintenance of hematopoietic stem cells does not require contact with embryo-derived stromal cells in cocultures." Stem Cells **23**(6): 842-851.

Orford, K. W. and D. T. Scadden (2008). "Deconstructing stem cell self-renewal: genetic insights into cell-cycle regulation." Nat Rev Genet **9**(2): 115-128.

Osawa, M., K. Hanada, et al. (1996). "Long-term lymphohematopoietic reconstitution by a single CD34-low/negative hematopoietic stem cell." Science **273**(5272): 242-245.

Oshima, T., M. Abe, et al. (2005). "Myeloma cells suppress bone formation by secreting a soluble Wnt inhibitor, sFRP-2." Blood **106**(9): 3160-3165.

Ottersbach, K. and E. Dzierzak (2005). "The murine placenta contains hematopoietic stem cells within the vascular labyrinth region." Dev Cell **8**(3): 377-387.

Ottmann, O. G. and B. Wassmann (2005). "Treatment of Philadelphia chromosome-positive acute lymphoblastic leukemia." Hematology Am Soc Hematol Educ Program: 118-122.

Palis, J. and M. C. Yoder (2001). "Yolk-sac hematopoiesis: the first blood cells of mouse and man." Exp Hematol **29**(8): 927-936.

Pane, F., F. Frigeri, et al. (1996). "Neutrophilic-chronic myeloid leukemia: a distinct disease with a specific molecular marker (BCR/ABL with C3/A2 junction)." Blood **88**(7): 2410-2414.

Passegue, E., A. J. Wagers, et al. (2005). "Global analysis of proliferation and cell cycle gene expression in the regulation of hematopoietic stem and progenitor cell fates." J Exp Med **202**(11): 1599-1611.

Pehlivan, M., Z. Sercan, et al. (2009). "sFRP1 promoter methylation is associated with persistent Philadelphia chromosome in chronic myeloid leukemia." Leuk Res **33**(8): 1062-1067.

Pinho, S., J. Lacombe, et al. (2013). "PDGFRalpha and CD51 mark human nestin+ sphere-forming mesenchymal stem cells capable of hematopoietic progenitor cell expansion." J Exp Med **210**(7): 1351-1367.

Pittenger, M. F., A. M. Mackay, et al. (1999). "Multilineage potential of adult human mesenchymal stem cells." Science **284**(5411): 143-147.

Raaijmakers, M. H., S. Mukherjee, et al. (2010). "Bone progenitor dysfunction induces myelodysplasia and secondary leukaemia." Nature **464**(7290): 852-857.

Rahmatpanah, F. B., S. Carstens, et al. (2009). "Large-scale analysis of DNA methylation in chronic lymphocytic leukemia." Epigenomics **1**(1): 39-61.

Ravandi, F., J. Cortes, et al. (1999). "Chronic myelogenous leukaemia with p185(BCR/ABL) expression: characteristics and clinical significance." Br J Haematol **107**(3): 581-586.

Rekhtman, N., F. Radparvar, et al. (1999). "Direct interaction of hematopoietic transcription factors PU.1 and GATA-1: functional antagonism in erythroid cells." Genes Dev **13**(11): 1398-1411.

Renstrom, J., R. Istvanffy, et al. (2009). "Secreted frizzled-related protein 1 extrinsically regulates cycling activity and maintenance of hematopoietic stem cells." Cell Stem Cell **5**(2): 157-167.

Renstrom, J., M. Kroger, et al. (2010). "How the niche regulates hematopoietic stem cells." Chem Biol Interact **184**(1-2): 7-15.

Reya, T., S. J. Morrison, et al. (2001). "Stem cells, cancer, and cancer stem cells." Nature **414**(6859): 105-111.

Risinger, J. I., G. L. Maxwell, et al. (2005). "Gene expression profiling of microsatellite unstable and microsatellite stable endometrial cancers indicates distinct pathways of aberrant signaling." Cancer Res **65**(12): 5031-5037.

Roman-Gomez, J., L. Cordeu, et al. (2007). "Epigenetic regulation of Wnt-signaling pathway in acute lymphoblastic leukemia." Blood **109**(8): 3462-3469.

Roman-Gomez, J., A. Jimenez-Velasco, et al. (2006). "CpG island methylator phenotype redefines the prognostic effect of t(12;21) in childhood acute lymphoblastic leukemia." Clin Cancer Res **12**(16): 4845-4850.

Rombouts, E. J., B. Pavic, et al. (2004). "Relation between CXCR-4 expression, Flt3 mutations, and unfavorable prognosis of adult acute myeloid leukemia." Blood **104**(2): 550-557.

Rossi, D. J., D. Bryder, et al. (2007). "Deficiencies in DNA damage repair limit the function of haematopoietic stem cells with age." Nature **447**(7145): 725-729.

Rossi, D. J., D. Bryder, et al. (2007). "Hematopoietic stem cell aging: mechanism and consequence." Exp Gerontol **42**(5): 385-390.

Roux, S. (2010). "New treatment targets in osteoporosis." Joint Bone Spine **77**(3): 222-228.

Rupec, R. A., F. Jundt, et al. (2005). "Stroma-mediated dysregulation of myelopoiesis in mice lacking I kappa B alpha." Immunity **22**(4): 479-491.

Salter, A. B., S. K. Meadows, et al. (2009). "Endothelial progenitor cell infusion induces hematopoietic stem cell reconstitution in vivo." Blood **113**(9): 2104-2107.

Sathi, G. A., M. Inoue, et al. (2009). "Secreted frizzled related protein (sFRP)-2 inhibits bone formation and promotes cell proliferation in ameloblastoma." Oral Oncol **45**(10): 856-860.

Satoh, W., T. Gotoh, et al. (2006). "Sfrp1 and Sfrp2 regulate anteroposterior axis elongation and somite segmentation during mouse embryogenesis." Development **133**(6): 989-999.

Satoh, W., M. Matsuyama, et al. (2008). "Sfrp1, Sfrp2, and Sfrp5 regulate the Wnt/beta-catenin and the planar cell polarity pathways during early trunk formation in mouse." Genesis **46**(2): 92-103.

Schaniel, C., D. Sirabella, et al. (2011). "Wnt-inhibitory factor 1 dysregulation of the bone marrow niche exhausts hematopoietic stem cells." Blood **118**(9): 2420-2429.

Scheller, M., J. Huelsken, et al. (2006). "Hematopoietic stem cell and multilineage defects generated by constitutive beta-catenin activation." Nat Immunol **7**(10): 1037-1047.

Schepers, K., E. M. Pietras, et al. (2013). "Myeloproliferative neoplasia remodels the endosteal bone marrow niche into a self-reinforcing leukemic niche." Cell Stem Cell **13**(3): 285-299.

Schofield, R. (1978). "The relationship between the spleen colony-forming cell and the haemopoietic stem cell." Blood Cells **4**(1-2): 7-25.

Scholzen, T. and J. Gerdes (2000). "The Ki-67 protein: from the known and the unknown." J Cell Physiol **182**(3): 311-322.

Schreck, C., F. Bock, et al. (2014). "Regulation of hematopoiesis by activators and inhibitors of Wnt signaling from the niche." Ann N Y Acad Sci **1310**: 32-43.

Seita, J. and I. L. Weissman (2010). "Hematopoietic stem cell: self-renewal versus differentiation." Wiley Interdiscip Rev Syst Biol Med **2**(6): 640-653.

Sesler, C. L. and M. Zayzafoon (2013). "NFAT signaling in osteoblasts regulates the hematopoietic niche in the bone microenvironment." Clin Dev Immunol **2013**: 107321.

Shaham, O., A. N. Smith, et al. (2009). "Pax6 is essential for lens fiber cell differentiation." Development **136**(15): 2567-2578.

Shim, J., T. Mukherjee, et al. (2012). "Direct sensing of systemic and nutritional signals by haematopoietic progenitors in Drosophila." Nat Cell Biol **14**(4): 394-400.

Shimono, A. and R. R. Behringer (2003). "Angiomotin regulates visceral endoderm movements during mouse embryogenesis." Curr Biol **13**(7): 613-617.

Shirozu, M., H. Tada, et al. (1996). "Characterization of novel secreted and membrane proteins isolated by the signal sequence trap method." Genomics **37**(3): 273-280.

Sipkins, D. A., X. Wei, et al. (2005). "In vivo imaging of specialized bone marrow endothelial microdomains for tumour engraftment." Nature **435**(7044): 969-973.

Stoehr, R., C. Wissmann, et al. (2004). "Deletions of chromosome 8p and loss of sFRP1 expression are progression markers of papillary bladder cancer." Lab Invest **84**(4): 465-478.

Sudo, K., H. Ema, et al. (2000). "Age-associated characteristics of murine hematopoietic stem cells." J Exp Med **192**(9): 1273-1280.

Sugimura, R., X. C. He, et al. (2012). "Noncanonical Wnt signaling maintains hematopoietic stem cells in the niche." Cell **150**(2): 351-365.

Sugiyama, T., H. Kohara, et al. (2006). "Maintenance of the hematopoietic stem cell pool by CXCL12-CXCR4 chemokine signaling in bone marrow stromal cell niches." Immunity **25**(6): 977-988.

Sugiyama, Y., E. J. Shelley, et al. (2013). "Sfrp1 and Sfrp2 are not involved in Wnt/beta-catenin signal silencing during lens induction but are required for maintenance of Wnt/beta-catenin signaling in lens epithelial cells." Dev Biol **384**(2): 181-193.

Surmann-Schmitt, C., N. Widmann, et al. (2009). "Wif-1 is expressed at cartilage-mesenchyme interfaces and impedes Wnt3a-mediated inhibition of chondrogenesis." J Cell Sci **122**(Pt 20): 3627-3637.

Suzuki, H., D. N. Watkins, et al. (2004). "Epigenetic inactivation of SFRP genes allows constitutive WNT signaling in colorectal cancer." Nat Genet **36**(4): 417-422.

Takeuchi, M., T. Sekiguchi, et al. (2002). "Cultivation of aorta-gonad-mesonephros-derived hematopoietic stem cells in the fetal liver microenvironment amplifies long-term repopulating activity and enhances engraftment to the bone marrow." Blood **99**(4): 1190-1196.

Trumpp, A., M. Essers, et al. (2010). "Awakening dormant haematopoietic stem cells." Nat Rev Immunol **10**(3): 201-209.

Valencia, A., J. Roman-Gomez, et al. (2009). "Wnt signaling pathway is epigenetically regulated by methylation of Wnt antagonists in acute myeloid leukemia." Leukemia **23**(9): 1658-1666.

Van Den Berg, D. J., A. K. Sharma, et al. (1998). "Role of members of the Wnt gene family in human hematopoiesis." Blood **92**(9): 3189-3202.

Veeck, J., D. Niederacher, et al. (2006). "Aberrant methylation of the Wnt antagonist SFRP1 in breast cancer is associated with unfavourable prognosis." Oncogene **25**(24): 3479-3488.

Veeman, M. T., J. D. Axelrod, et al. (2003). "A second canon. Functions and mechanisms of beta-catenin-independent Wnt signaling." Dev Cell **5**(3): 367-377.

von Marschall, Z. and L. W. Fisher (2010). "Secreted Frizzled-related protein-2 (sFRP2) augments canonical Wnt3a-induced signaling." Biochem Biophys Res Commun **400**(3): 299-304.

Wang, Y., A. V. Krivtsov, et al. (2010). "The Wnt/beta-catenin pathway is required for the development of leukemia stem cells in AML." Science **327**(5973): 1650-1653.

Warr, N., P. Siggers, et al. (2009). "Sfrp1 and Sfrp2 are required for normal male sexual development in mice." Dev Biol **326**(2): 273-284.

Warrington, J. A., A. Nair, et al. (2000). "Comparison of human adult and fetal expression and identification of 535 housekeeping/maintenance genes." Physiol Genomics **2**(3): 143-147.

Waterstrat, A. and G. Van Zant (2009). "Effects of aging on hematopoietic stem and progenitor cells." Curr Opin Immunol **21**(4): 408-413.

Wilson, A., E. Laurenti, et al. (2008). "Hematopoietic stem cells reversibly switch from dormancy to self-renewal during homeostasis and repair." Cell **135**(6): 1118-1129.

Winkler, I. G., V. Barbier, et al. (2012). "Vascular niche E-selectin regulates hematopoietic stem cell dormancy, self renewal and chemoresistance." Nat Med **18**(11): 1651-1657.

Wodarz, A. and R. Nusse (1998). "Mechanisms of Wnt signaling in development." Annu Rev Cell Dev Biol **14**: 59-88.

Xavier, C. P., M. Melikova, et al. (2014). "Secreted Frizzled-related protein potentiation versus inhibition of Wnt3a/beta-catenin signaling." Cell Signal **26**(1): 94-101.

Xie, Y., T. Yin, et al. (2009). "Detection of functional haematopoietic stem cell niche using real-time imaging." Nature **457**(7225): 97-101.

Xu, D., W. Zhao, et al. (2014). "Expression of Nemo-like kinase after spinal cord injury in rats." J Mol Neurosci **52**(3): 410-418.

Yam, J. W., J. Y. Zheng, et al. (1999). "Identification and characterization of genes whose expressions are altered in rat 6 fibroblasts transformed by mutant p53(val135)." Biochem Biophys Res Commun **266**(2): 472-480.

Yamada, M., J. Ohnishi, et al. (2006). "NARF, an nemo-like kinase (NLK)-associated ring finger protein regulates the ubiquitylation and degradation of T cell factor/lymphoid enhancer factor (TCF/LEF)." J Biol Chem **281**(30): 20749-20760.

Yamamoto, R., Y. Morita, et al. (2013). "Clonal analysis unveils self-renewing lineage-restricted progenitors generated directly from hematopoietic stem cells." Cell **154**(5): 1112-1126.

Yamane, T., T. Kunisada, et al. (2001). "Wnt signaling regulates hemopoiesis through stromal cells." J Immunol **167**(2): 765-772.

Yamazaki, S., H. Ema, et al. (2011). "Nonmyelinating Schwann cells maintain hematopoietic stem cell hibernation in the bone marrow niche." Cell **147**(5): 1146-1158.

Yokota, T., K. Oritani, et al. (2008). "Soluble frizzled-related protein 1 is estrogen inducible in bone marrow stromal cells and suppresses the earliest events in lymphopoiesis." J Immunol **181**(9): 6061-6072.

Zhang, J., C. Niu, et al. (2003). "Identification of the haematopoietic stem cell niche and control of the niche size." Nature **425**(6960): 836-841.

Zhang, P., G. Behre, et al. (1999). "Negative cross-talk between hematopoietic regulators: GATA proteins repress PU.1." Proc Natl Acad Sci U S A **96**(15): 8705-8710.

Zhang, P., X. Zhang, et al. (2000). "PU.1 inhibits GATA-1 function and erythroid differentiation by blocking GATA-1 DNA binding." Blood **96**(8): 2641-2648.

Zhao, C., J. Blum, et al. (2007). "Loss of beta-catenin impairs the renewal of normal and CML stem cells in vivo." Cancer Cell **12**(6): 528-541.

Mouse picture: www.bioquicknews.com